UNIVERSITEIT VAN PRETORIA
UNIVERSITY OF PRETORIA
YUNIBESITHI YA PRETORIA
Faculty of Engineering, Built Environment and Information Technology

Effects of noise and measurement error on load reconstruction of dynamic loads in the frequency domain.

By

J.A. Kruger

Submitted in partial fulfilment of the requirements for the degree

Masters in Engineering (Mechanical Engineering)

in the

Department of Mechanical and Aeronautical Engineering,

Faculty of Engineering, Built Environment, and Information Technology

University of Pretoria

August 2024

Abstract

Load reconstruction involves solving the inverse problem by using measured structural responses to determine the forces acting on a structure. The inverse problem is almost always ill-conditioned making solving the inverse problem more difficult compared to the forward problem. Response measurements will always contain a level of noise even under the best of conditions.

Various methods of performing load reconstruction have been developed in the time and frequency domains. A common problem encountered by all load reconstruction methods are their sensitivity to noise, because of the ill-conditioned nature of the inverse problem. The frequency domain methods have the benefit of limiting the band in which load reconstruction is performed which can eliminate some of the effects of noise. However, frequency domain methods remain sensitive to noise and in certain practical applications noise is present in the same frequency band in which the loads are to be reconstructed. From the literature reviewed, frequency domain methods are less sensitive to noise and have the benefit that they can be performed with very little prior knowledge of the system.

The aim of this research was to establish the sensitivity of several commonly used load reconstruction methods used in engineering applications. In order to accomplish this, literature was reviewed to gain insights into the field of load reconstruction. Mathematical models were created to test the sensitivity of selected load reconstruction methods. These models consisted of a lumped mass analytical model, a rigid body simulation model and an elastic beam model which was replicated experimentally. The feasibility of using finite element modelling in conjunction with experimental data to perform load reconstruction was also briefly evaluated.

It was found that systematic errors posed the greatest risk as in many of the test cases, no clear indications of any error were noticeable. Meaning that there is a great risk of drawing inaccurate conclusions when systematic errors are present in measured data. In terms of stochastic noise, it was found that the Tikhonov methods were the best performing methods. These methods were able to maintain accuracy up to high noise levels. It was also found that it is feasible to make use of finite element analysis in conjunction with experimental data to perform load reconstruction. However, the accuracy of the finite element modelling plays a major role in the accuracy of the load reconstruction.

Acknowledgements

I would like to acknowledge and thank those that provided support, guidance and the opportunity to pursue this project.

- Professor Stephan Heyns, my supervisor for this research project, for his inputs, guidance and support. Without his help this project would not have been possible.
- University of Pretoria Centre for Asset Integrity Management laboratories and in particular Mr George Breitenbach for the training he provided and the use of the instrumentation and laboratory facility.
- Transnet Engineering for allowing me the opportunity to pursue this project and allowing me to use some of their facilities.
- TANDM and Mr Elton Murrison for the use of their equipment.
- Mrs Tania Kruger, my wife for her support, motivation and patience.
- M.r. JP (Joe) Kruger, for the motivation and being an inspiration to us all, may he rest in peace.

Table of Contents

List of Figures

List of Tables

Nomenclature

$CGLS$	Conjugate Gradient Least-Squares
DOF	Degree(s) of Freedom
FEA	Finite Element Analysis
FEM	Finite Element Method
FRF	Frequency Response Function
GCM	Conjugate Gradient Method
GCV	Generalised Cross Validation
IRF	Impulse Response Function
ISF	Inverse Structural Filter
MPM	Markov Parameter Matrix
SNR	Signal-to-Noise Ratio
SVD	Singular Value Decomposition
$SWAT$	Sum of Weighted Accelerations Technique

$[\,]$	Matrix
$\{\,\}$	Vector
a	Exponential Window Constant
C	Damping Coefficient (Ns/m)
F	Force (N)
f	Frequency (Hz)
h	Impulse Response Function (time domain)
H	Frequency Response Function (frequency domain)
K	Stiffness (N/m)
M	Mass (kg)
n	Noise
r	Receptance
s_r	Eigenvalues
T	Matrix condition number
t	Time (s)

w	Window Function
x	Displacement Response (m)
$\dot{x}$	Velocity Response (m/s)
$\ddot{x}$	Acceleration Response (m/s^2)
α	Regularisation Parameter
θ	Eigenvector
ω	Frequency (rad/s^2)
ξ	Damping Ratio

1. Introduction

1.1. Problem Statement

During the design phase of a structure the specific loading at known locations is usually known and considered. However, it is possible that there are other unknown forces (or forces with unknown magnitudes) acting on the structure. These forces could be unknown during the design phase, or the loading can change during the life of the structure. In the case of dynamic loading such as vehicles, the full loading characteristics are often difficult to determine accurately without testing (in operational areas), especially with a completely new design.

The extent of these dynamic forces is generally not fully known during the design phase, especially when no test data of similar structures are available or when no comparable structures exist. In certain cases, the magnitudes of the forces might be known whereas the locations where and the directions in which the forces act are unknown or vice versa. However, the magnitude and locations of these forces are required during the design. Available data is normally used to make assumptions as to what the magnitudes of these forces are. This can lead to over-designing resulting in unnecessary strength which results in higher production costs or failure of the structure due to inaccurate data or assumptions.

Accurate magnitude and location of forces on a structure is required to perform fatigue life predictions. In certain cases, the original design information might no longer be available or may have changed during the life of the structure. It may be necessary to then determine the loads acting on the structure, to determine the safety of the structure or remaining life of a structure.

Measuring the dynamic forces acting on a real structure can quickly become very complex and expensive. Direct measurement methods can be applied in certain cases by means of instruments such as load cells or strain gauges. Direct measurement methods are however not always practical and generally require modification of the structure to attach the measurement equipment, which can influence the dynamics of the structure.

There are many applications where direct measurement methods are not feasible or possible, such as:

- Railway locomotive or wagon component vibration and excitation due to inputs from the rails
- Loading on truck/trailer combinations due to the payload and road surface
- Wind loads on towers and masts (Amiri & Bucher, 2017).
- Forces transmitted from machinery, such as compressors and rotating equipment to foundations and supporting structures (Kriel, 2000).
- Forces exerted on components during manufacturing processes such as machining (Wang, Zhang, Qiao, Cao, & Chen, 2019).
- Engine torque pulses and vibration inducing forces (Patil & Gombi, 2017).

Some of these problems can be overcome by making use of design standards. However, design standards generally take a very conservative approach to loading conditions to cover a broad spectrum of applications. This is because, in most cases it is not feasible to cater for every specific scenario

specifically when developing standards. In certain newly developing fields (or fields that an organisation or country is attempting to enter) there may also not be any applicable design standards available to guide the designer.

During investigations of equipment failures or resolving disputes between equipment designers and end users it may be necessary to determine the loading on a structure to determine a root cause, however manufacturers may be reluctant to disclose design load cases due to the risk of losing trade secrets.

An alternative approach is possible, where the structure's responses are used to determine the loads on the structure, essentially using the structure as its own force transducer (Allen & Carne, 2008). Several such methods have been developed in both the time and frequency domains. However, most of these methods are sensitive to noise in the measured signals, which reduces the accuracy or potentially makes the identification impossible. Noise has a much more significant influence on the inverse problem compared to the forward problem (Sanchez & Benaroya, 2014).

Measurement noise is unavoidable in practical situations. Proper sensor selection and placement, test setup and appropriate use of filters can reduce the effects of noise on measured signals but cannot completely remove noise. Measurements taken on operational structures can be even more susceptible to noise due to electrical, rotating or other noise inducing equipment attached (or in close proximity) to the structure being tested.

Frequency domain methods have received little attention in recent years compared to other methods, due to several reasons such as computational requirements, however there are benefits to frequency domain methods, such as reduced sensitivity to noise compared to time domain methods. Recent work has been more focused on deterministic-stochastic methods (Lourens, et al. 2012).

1.2. Literature Review

1.2.1. Background

Any structure or dynamic system can be described in terms of its degrees of freedom. The minimum number of independent points in space required to fully define the position of the system components at any point in time determines the number of degrees of freedom of a system (Rao, 2011).

In theory almost all engineering structures have in principle infinite degrees of freedom. In certain cases very simple structures can be modelled as rigid body systems with a small number of degrees of freedom, generally in these cases the masses are considered to be rigid and only the connecting elements such as springs deform. However in most engineering applications the elasticity of a structure is important to take into consideration and therefore the elastic behaviour is considered by approximating the continuum systems as discrete with a finite number of discrete degrees of freedom (Allemang & Avitabile, 2022). This is referred to as finite element modelling (FEM) or analysis (FEA). When a structure is considered as consisting of elastic elements, a continuous structure such as a beam is divided into a finite number of elements each with its own mass and stiffness.

The analytical and numerical methods used to analyse structural systems only work if the system parameters (stiffness, damping etc) are known. For real systems, these parameters are often not

known, or well defined, real systems often need to be solved without analytical models and analytical models also need to be verified experimentally (Ewins, 2000).

Loads that are acting on a structure can be either dynamic (fluctuating with time) or static (constant) in nature (or a combination of both), the stresses experienced by a structure are a function of the loads acting on the structure. Knowledge of these loads are critical in the design, analysis and health of the structure. The knowledge of accurate loading on a structure improves the confidence in numerical models which lead to reduced development costs (Patil & Gombi, 2017).

Various direct and indirect methods of determining the loads on a structure have been developed in various domains. However all of the methods require the measurement of either the loads or the responses due to the loads on the structure while in service.

Any measurement signal taken in practice consists of two components, the signal of interest that contains the information about the quantity being measured and noise which consists of extraneous information which degrades the accuracy and precision of the measured signal (Skoog, Holler, & Crouch, 2007).

This chapter aims to provide an overview of the inverse problem and various load reconstruction methods with their respective advantages and disadvantages. Methods of improving the accuracy of results obtained by frequency domain load reconstruction methods are also discussed. From the literature reviewed it is noted that noise has a larger effect on the accuracy of the solution to the inverse problem than the effects it can have on the forward problem or direct measurements.

1.2.2. Direct and Inverse Problem Formulation

This section describes the direct and inverse problems as well as some of the known difficulties and problems of both.

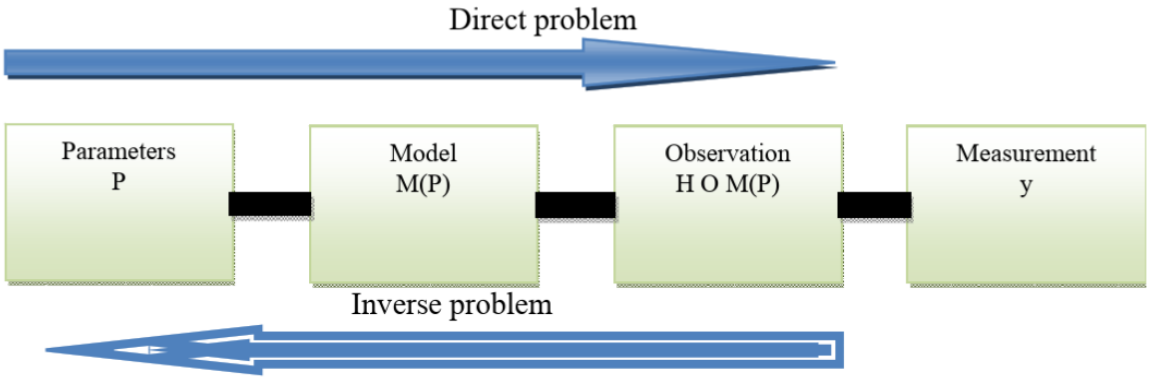

Figure 1.1 Graphical representation of the direct and inverse problems (El Hami & Radi, 2017)

Figure 1.1 above graphically illustrates the relationship between the direct and inverse problems. The direct problem (also known as the forward problem) is the problem of determining the response of a structure from a known input force. Solving the direct problem involves solving differential equations with known parameters to determine the response (El Hami & Radi, 2017). The direct problem is solved by engineers and designers when designing a structure, whether it be by hand or computer aided simulations.

As the name suggests the inverse problem is the inverse of the direct problem (as indicated in Figure 1.1), to determine a structure's parameters or forces acting on the structure from known responses. The inverse problem is normally ill-posed (Allen & Carne, 2008), meaning that the problem violates one or more of the conditions of Hadamard. This means that a small change in the response data can result in large changes in the solution.

For a problem to be well-posed it must meet the following criteria (Uhl, 2007):

- The solution must be unique.
- A globally defined solution for all reasonable data exists.
- The solution depends on the given data (stability criterion).

The inverse problem is not unique to the field of structural engineering and has applications in other fields such as image processing and computational fluid dynamics, however this research focuses on the application of the inverse problem in the field of structural engineering. In the field of structural load identification or reconstruction, the inverse problem involves the determination of unknown forces from generally incomplete and noisy responses in conjunction with the system matrix or transfer function.

In solving the direct problem all the forces acting on a structure are known and located on known positions throughout the structure and the system matrix can be determined analytically or through finite element analysis methods. In many practical applications the locations of the forces are known, but the forces are unknown and the response to the forces are known or can be measured. In which case the aim is to determine the spectra or time histories of the forces acting on the structure from the behaviour of the structure in response to the forces (Sanchez, 2022).

However, in the case of the inverse problem the responses can only be measured at discrete positions which are not necessarily the positions where the forces are acting on the structure, with no response information known between the points of measurement. The other problem is that in most cases there is noise or non-zero vibration responses present throughout the structure. Khoo et al. (2014), noted that if the force locations are known beforehand, the inverse problem can become well-posed. In their work Khoo et al. (2014) also found that pseudo-inverse methods are robust and reliable provided that good measurement locations are selected in advance. It was found that increasing the number of response measurement locations increases the accuracy.

1.2.3. Inverse Load Identification

The solution to the inverse problem is significantly different to that of the forward problem. Solving the forward problem generally involves solving a set of differential equations with known inputs for which there exists well established methods. Due to the inverse problem's sensitivity to noise the problem can easily be influenced by singularities or non-unique solutions.

Methods of solving the inverse problem has received little attention in comparison to the forward problem. It is a relatively small discipline since the focus has generally been more on system identification rather than force identification (Sanchez & Benaroya, 2014).

The biggest problem in solving the inverse problem is the ill-posedness, meaning that there is no single unique solution to the problem, the solutions may be mathematically correct but unrealistic (Rezayat, et al., 2016).

To solve the inverse problem, a known (or approximated) system model is required. Because the system input variables and initial conditions are generally not known in practice, the load identification problem can easily be ill-posed (Uhl, 2007). The basic principle of solving an ill-posed problem is to transform it into a well-posed problem by adding additional data regarding the desired solution. These methods commonly are referred to as regularisation methods which were first developed by Tikhonov for the time domain and are discussed in greater detail in section 1.2.7 (Uhl, 2007).

The methods for solving the inverse load identification can be divided into five main categories:

- Direct Methods
- Optimisation Methods
- Deterministic Methods
- Stochastic Methods
- Artificial Intelligence Methods

Direct methods make direct use of a physical or mathematical model to formulate and solve the inverse problem. These methods do not include any manipulation of the system by filtering or imposing additional constraints, which is performed before load reconstruction is performed. Mathematical analysis is one of the direct methods, where a mathematical model of the structure is developed. Another direct method is the inverse method, where the system matrix (such as the FRF) is inverted and multiplied with the responses but in most practical cases the system matrix is not square and a pseudo-inverse method needs to be applied.

Despite the inherent non-linearities present in a structure, this method is usually limited to linear structures (Sanchez & Benaroya, Review of force reconstruction techniques, 2014). However of approaches of applying direct methods have been developed to deal with non-linear systems, such as extended variations of the conjugate gradient method (CGM) and extended Kalman filters (Chao, Hongxing, & Feng, 2014).

Sanchez & Benaroya (2014) have given a good overview of several mathematical analysis methods that have been used for load identification in different applications. However, as is the case with most of the inverse load identification methods, these methods are also sensitive to noise. Additionally, many of the direct methods require much information about the system which may not always be available in practice.

Optimisation models make use of a looped approach where the input into a forward model is optimised to match the responses to the measured responses (Oosterhuis, Eidhof, van der Hoogt, & de Boer, 2006). These methods can be computationally expensive, especially if the forward model is inaccurate or an incorrect representation of the physical model.

Deterministic methods rely on system model simulation and their results depend greatly on the accuracy of the identified inverse model. The process of identifying the model requires experimentation and measurement of both the inputs and outputs. The experimental results are then used to estimate the model parameters. Highly non-linear systems require the identification of a non-linear inverse model, which is usually inaccurate and difficult to identify (Uhl, 2007).

Stochastic methods rely on finding statistical relationships between the inputs and outputs. In order to determine these relationships, operational measurements of the inputs and outputs on the structure is required. The regression model is one of the most useful models in stochastic inverse load identification (Uhl, 2007). In purely stochastic methods, the unknown force values are considered as deterministic (Lourens, Reynders, De Roeck, Degrande, & Lombaert, 2012).

Artificial intelligence methods can be achieved by using artificial neural network algorithms, fuzzy algorithms or certain machine learning algorithms. One disadvantage of these methods is that they also require direct measurements of the system responses (similarly to stochastic methods), which is difficult or impossible in some cases. However numerical simulation can potentially be used in the training process of these methods (Uhl, 2007). Training these algorithms can require significant computational power depending on the size and complexity of the system.

Two domains are used for inverse force identification (each with several different methods), time and frequency domains. Time domain methods develop force estimates as a function of time, commonly by means of convolution. Frequency domain methods generally utilise the frequency response function which describes the linear relationship between input force and measured responses (Kriel, 2000). Frequency domain methods have advantages in engineering applications in reconstructing random excitation and steady state harmonic excitation whereas time domain methods can be more suited for transient shock excitation identification (Chen, et al., 2021). Reconstruction can be performed in different subspaces, such as the spatial or modal subspace. The benefit of transforming the reconstruction problem to another subspace is that it can truncate the number of unknowns to the number of equations based on the measurement locations (Amiri & Bucher, 2017).

Initially inverse load identification problems were primarily solved in the frequency domain, using the frequency response function method. In more recent times the focus has shifted more towards the time domain with many alternative methods being developed following a deterministic-stochastic combined approach, most of which can trace their origins to control engineering (Lourens, Reynders, De Roeck, Degrande, & Lombaert, 2012).

Due to the ease of use, frequency domain methods are commonly used in the automotive industry to determine loads for use on test-rigs to perform durability testing. Direct methods are applied iteratively in order to deal with nonlinearities (Oosterhuis, Eidhof, van der Hoogt, & de Boer, 2006).

A common problem across all the different methods is the ill-posedness of the inverse problem and the sensitivity to noise in measured data. In order to improve the ill-posedness of the problem various algorithms and regularisation methods have been developed.

Inverse load identification most commonly makes use of accelerometers or strain gauges to measure a structure's responses (Khoo, et al., 2014), however other physical responses such as velocity or displacement can also be used. The choice of response type depends on the method, the algorithm being used and the magnitudes of these responses. Practical factors such as available physical space on the structure, working environment and cost also play a role in the choice of response type. For example, when methods that require matrix inversion are used, responses with low magnitudes are more susceptible to numerical rounding errors as well as errors during the inversion process. However certain methods have been found to be more accurate and stable when acceleration is used instead of displacement, such as time domain integration methods (Uhl, 2007).

1.2.4. Time Domain Methods

There are two ways by which deconvolution can be achieved, by direct discretisation of the convolution integral in the time domain and the other is by using the Fourier or Laplace transform in the frequency domain (Tran & Inoue, 2018), this section will discuss time domain methods and frequency domain methods will be discussed in the following section.

Time domain methods are some of the more recent methods used for load reconstruction and are mainly based on the relationship between the excitation (applied loads) and the structural responses by means of convolution. The responses of the structure are a function of the impulse response function (IRF), and the loads are determined by convolution in the time domain (Patil & Gombi, 2017).

The response of a structure, assuming zero initial conditions, is represented by the convolution integral:

$$x(t) = \int_0^t h\,(t-\tau)F(\tau)d\tau \tag{1.1}$$

where h is the impulse response function of the structure and F the load applied on the structure.

The solution of F does not continuously depend on the data, making it an ill-posed problem. Because structural measurements are discrete measurements, the above equation can be written as a matrix equation (Kammer, 1998):

$$[h]\{F\} = \{X\} \tag{1.2}$$

The above matrix equation is then deconvolved to determine or estimate the input forces from the structural and impulse responses. The deconvolution results in an inverse that does not continuously depend on the responses (Kammer, 1998). The above matrix equation is therefore still ill-posed due to the near singularity of the matrix h. Chang et al. (2019) used a summation to replace the integration, assuming that the time integration range is divided into equally sized time intervals.

The impulse response function of a structure is dependent on the modal properties (eigenvalues, mode shapes, modal mass and damping ratio) and is represented by (Chang, Yan, & Wu, 2019):

$$h(t-\tau) = \sum_{i=1}^{n} \frac{\theta_i \theta_i^T}{M_i \omega_{id}} e_i^{-\xi \omega_i (t-\tau)} \sin\left(\omega_{id}(t-\tau)\right) \tag{1.3}$$

Chang et al. (2019) suggest that in engineering applications power spectrum analysis can be used to obtain the FRF which can then be transformed to the time domain by means of the inverse Fourier transform to obtain h.

In practical applications these problems generally have many inputs and outputs as well as thousands of data points. Methods developed to solve these types of problems in the time domain can therefore become computationally very expensive, which limited the use of these methods in the past, which is one of the reasons why researchers focused more on frequency domain methods.

Because of the ill-conditioned nature of deconvolution, which becomes worse when measurement noise or errors are present in the response data, Tran & Inoue (2018) considered a deconvolution method involving the wavelet transform to reconstruct impact force. The wavelet transform represents a signal as a linear combination of wavelets, often finite in time.

The implementation of this method involves substituting the wavelet expansion into Equation 1.1 as follows:

$$x(t) = \sum_{m=m_0}^{M} \sum_{n=n_0}^{N_m} \widetilde{f_{m,n}^{d}}\, \phi_{m,n}(t) + \sum_{n=n_0}^{N_M} \widetilde{f_{M,n}^{a}} \chi_{M,n}(t) \quad (1.4)$$

where

$$\phi_{m,n}(t) = \int_0^t h(t-\tau)\varphi_{m,n}(\tau)d\tau$$

$$\chi_{M,n}(t) = \int_0^t h(t-\tau)\psi_{M,n}(\tau)d\tau$$

In the above $\varphi_{m,n}$ and $\psi_{M,n}$ is the wavelet and scaling functions and $\phi_{m,n}(t)$ and $\chi_{M,n}(t)$ are the responses to each wavelet force. The matrix consisting of the components of these responses can then be inverted using the generalised Moore-Penrose inverse to determine the force. This method is however also not immune to the effects of measurement noise or error, however generally used regularisation methods perform better with the wavelet decompossition technique compared to the conventional deconvolution method (Tran & Inoue, 2018).

In the case where the loads generate a dynamic reaction on the structure, the modal filter method is recommended (Uhl, 2007). First defined by Meirovitch and later further developed by Zhang, the modal filter is conceptually a reciprocal modal vector that makes it possible to determine the modal response for each separate mode (Uhl, 2007).

Both these methods are applicable if the system or structure is linear. In the case of non-linear (or linear) systems, minimisation of defined objective functions may be utilised. The least squares error between the simulated and experimental responses is commonly used as the objective function. Dynamic programming optimisation is another function commonly used as the objective function (Uhl, 2007). Minimisation or optimisation methods can also be used in the other domains.

The Markov Parameter Method (MPM) described by Kammer (1998), estimates the loads acting on a structure from the responses of the structure due to unit impulse forces, also known as Markov parameters. The Markov parameters of the inverse problem are calculated from the Markov parameters of the forward problem (unit impulse response) using a linear predictive algorithm. The advantage of this method is that the inverse of the Markov parameters only need to be determined once, however this requires a lot of information about the forward system and if the information is not available, experimental measurements are needed to estimate the required parameters. Thereafter any time history of measurement data can be convolved with the inverse Markov parameters to estimate the loads on the structure (Kammer, 1998). Selecting the appropriate sensor locations is critical for this method to ensure a minimum phase system. There should be at least as many sensors as inputs, but the number of inputs may not necessarily be known in practice (Kammer, 1998).

Methods for optimal sensor placements when using the Markov Parameter Method (MPM) have been developed. One method relies on the direct calculation of the condition number of the Markov parameter matrix to determine the optimal sensor configuration. However, this method requires computation for many different sensor combinations, which can become computationally expensive. Another method uses correlation analysis of the Markov parameter matrix. This method performs similarly to the first when the sensor configurations are small but outperforms the first method when the number of sensor combinations become large (Patil & Gombi, 2017).

Another time domain method, known as the Sum of Weighted Accelerations Technique (SWAT) is based on modal filtering and makes use of multiple sensors to estimate the forces acting on a structure by isolating rigid body modal accelerations. It has been extended further to estimate multiple forces simultaneously by also considering elastic modes. The mode shapes are used to create a spatial filter that removes the flexible modes from the responses. The filter is essentially a weighting matrix that isolates the rigid body responses. With the mass properties known, Newton's second law can be applied to obtain an estimate of the resultant force on the centre of mass on the body. In certain cases, unforced response can be used to create a spatial filter, eliminating the need for modal testing (Allen & Carne, 2008).

To avoid ill-conditioning, the SWAT method requires the number of sensors to be at least the same as the number of rigid and elastic modes. However, the exact number of modes of complex structures is not always known. The placement of the sensors is critical to avoid ill-conditioning. The SWAT method does not necessarily determine the actual forces acting on a structure, but rather a set of equivalent forces that would produce the same acceleration of the centre of mass (Allen & Carne, 2008). An extension to the SWAT method was developed that makes use of the elastic modes to identify forces, this makes it possible to identify forces at specific response (measurement) points, provided that the number of forces to be determined is fewer than the number of modes in the band of interest (Allen & Carne, 2008).

Inverting the equations of motion of the system is a newer time domain approach with roots in control engineering. The Inverse Structural Filter (ISF) inverts the discrete time equations of motion of the system. Research has been done into inverting the continuous time equations of motion but due to the difficulty of integrating or differentiating measured time signals, the discrete time approach is preferred (Allen & Carne, 2008). The original ISF method created a stable ISF directly from the measured impulse response, eliminating the need to identify a model for the forward system.

To derive a basic ISF, one starts with the general linear state-space representation of a dynamic system:

$$\{x_{k+1}\} = [A]\{x_k\} + [B]\{u_k\} \qquad (1.5)$$
$$\{y_k\} = [C]\{x_k\} + [D]\{u_k\}$$

The above can be inverted to yield:

$$\{x_{k+1}\} = [\hat{A}]\{x_k\} + [\hat{B}]\{y_k\} \qquad (1.6)$$
$$\{u_k\} = [\hat{C}]\{x_k\} + [\hat{D}]\{y_k\}$$
$$\hat{A} = A - BD^{+}C \quad \hat{B} = BD^{+}$$
$$\hat{C} = -D^{+}C \quad \hat{D} = D^{+}$$

where $(\square)^{+}$ represents the Moore-Penrose pseudo inverse.

The equations can be solved in the same way as the forward system is solved. Allen and Carne (2008) however noted that the system matrix of the inverted system is not the same as that of the forward system, meaning that the inverted system might not be stable even if the forward system is stable. Estimated forces can tend to infinity if any of the ISF's eigenvalues are unstable. They also noted an ISF can be generated from modal parameters determined from a standard modal test. Allen and Carne expanded on the ISF by developing a variation named the Delayed Multi-step ISF (DMISF) that can produce a stable ISF when the original method fails. In essence the DMISF method works by stepping the output forward and neglecting the direct transmission matrix $[D]$. This however results in a time

delay in the identified forces, which depending on the practical application, can be tolerated (Allen & Carne, 2008).

The use of Kalman filters or variations of the Kalman filter is common in newer time domain methods. The Kalman filter has a wide range of applications in engineering, which on a high level regards the responses as observations and noise as Gaussian white noise, to obtain optimal state estimations of a system based on known input forces. The Kalman filter has been rearranged and applied in different formats, among others, to estimate the inputs of both linear and nonlinear systems. In some cases the Kalman filter has been combined with statistical methods, such as Bayesian methods, to also estimate system parameters (Liu, Wang, Qiu, & Chen, 2021).

An algorithm (Tuan's Algorithm) originally developed to solve inverse heat conduction problems was one of the first methods where deterministic stochastic methods were applied. In this case a Kalman filter combined with a recursive least squares estimation was used to determine impulse loads on spring-mass-damper combinations. One important factor to consider with regards to the Kalman filter methods is that it assumes that measured responses contain displacements of all the structure's degrees of freedom, which can be impractical in many situations (Lourens, Reynders, De Roeck, Degrande, & Lombaert, 2012).

This algorithm was further developed and extended to be applied to non-linear systems using an extended Kalman filter. Further development into the use of the Kalman filter yielded a more practical method where all the unmeasured (but required) responses are estimated using a Kalman filter and the forces are then determined with the pseudo-inverse using the complete state vector.

Lourens et al. (2012) proposed an Augmented Kalman Filter (AKF) approach for dynamic load reconstruction using a combined deterministic-stochastic approach. In their work Lourens et al. have shown how combined input and state estimation can be done by including the forces in the system state vector and estimating this vector by means of a normal Kalman filter. Amiri & Bucher (2017) have noted that sensor location and stability are drawbacks and that Tikhonov based methods are more robust. Methods to overcome the stability issues of the AKF method have been developed, such as the introduction of a dummy measurement. The AKF method is computationally more efficient when compared to deconvolution methods (Amiri & Bucher, 2017).

In many of the methods that make use of a Kalman filter (or modified version), the problem is realised as a state-space model, as described by equation 1.5 above, as a means of regularisation. Liu et al. (2021) noted that the state-space method is conditionally stable when the time step is small enough. To reduce the computational requirements without compromising accuracy Liu et al. (2021) transform the problem to the modal subspace.

In their work Liu et al. (2021) incorporate uncertainty factors from multiple sources such as manufacturing and assembly of a structure as well as measurement and process noise into their model. Their modified Kalman filter makes use of covariance matrices to estimate the force acting on the system, however their model is extended to quantify the uncertainties in the system by making use of the Chebyshev orthogonal polynomial approximation method (Liu, Wang, Qiu, & Chen, 2021).

Wang, et al. (2019) proposed and validated the use of the Conjugate Gradient Least Square (CGLS) method based on force identification theory. This is an iterative method used for time domain inverse problem solving. The benefit of this method is that it does not require inversion or the calculation of regularisation parameters.

The CGLS method is derived from the conjugate gradient method which is commonly used in the solving of optimisation and systems of linear equations. The conjugate gradient method has been used successfully to reconstruct forces on single degree of freedom non-linear systems (Chao, Hongxing, & Feng, 2014). According to Wang, et al. (2014) this method on its own is not suitable for the solving of ill-conditioned problems as it requires well-conditioned positive definite problems. Wang, et al. (2019) therefore introduced the least squares method into the conjugate gradient method. The CGLS method works by solving the least squares problem:

$$min\left|\left|HF - X\right|\right|_2 \tag{1.7}$$

where H is the system transfer function.

The conjugate gradient method is applied to the equations:

$$H^T HF = H^T X \tag{1.8}$$

which is the same as:

$$H^T(HF - X) \tag{1.9}$$

It was found that better accuracy could be achieved when H^T is factored out as in Equation 1.9 above.

The basic procedure of the CGLS method as defined by Wang, et al (2019) is as follows:

$$Initialise\ F_0 = 0, r_0 = X - HF_0, d_0 = H^T r_0$$

$$step\ 1:\ \alpha_k = \frac{\left|\left|H^T r_{k-1}\right|\right|_2^2}{\left|\left|Hd_{k-1}\right|\right|_2^2}$$

$$step\ 2: F_k = F_{k-1} + \alpha_k d_{k-1}$$

$$step\ 3: r_k = r_{k-1} - \alpha_k H d_{k-1}$$

$$step\ 4: \beta_k = \frac{\left|\left|H^T r_k\right|\right|_2^2}{\left|\left|Hr_{k-1}\right|\right|_2^2}$$

$$step\ 5: d_k = H^T r_k + \beta_k d_{k-1}$$

$$step\ 6: k = k + 1$$

The above is repeated until convergence is achieved. An acceptable error (δ) can be set to determine if convergence has been achieved such that $\left|\left|HF_k - X\right|\right|_2 < \delta$.

1.2.5. Frequency Domain Methods

Frequency domain methods assume a linear relationship between the measured responses and applied loads as a function of frequency (Patil & Gombi, 2017). The relationship between the inputs and outputs of a system at a frequency (ω) is known as the transfer function or FRF and is represented by:

$$\{X(i\omega)\} = [H(i\omega)]\{F(i\omega)\} \tag{1.10}$$

The FRF can be estimated from experimental measurements (modal testing), reconstructed using a modal model or obtained numerically using methods such as the finite element (this however requires accurate knowledge and modelling of the structure in terms of material as well as any elastic components). The FRF completely defines the dynamic characteristics of the structure and the responses can be measured as any physical quantity such as displacement, velocity or acceleration (Patil & Gombi, 2017).

With a known frequency response function and known responses to unknown loads, Equation 1.10 can be rearranged as shown below. Equation 1.11 forms the basis of frequency domain load reconstruction methods.

$$\{F(\omega)\} = [H(\omega)]^{-1}\{X(\omega)\} \tag{1.11}$$

However, solving the inverse problem is not as simple as the equation above may suggest. If the FRF matrix is square and non-singular, then the solution is quite straight forward, but in reality, this is not the case (Patil & Gombi, 2017).

To determine the forces acting on a structure, the inverse of the frequency response function matrix must be calculated or estimated at each frequency of interest. Numerically this can be an ill-posed problem, at frequencies near the resonances (natural frequencies) the FRF matrix can tend to be dominated by a rank-one component due to a single mode. This could amplify the effects of measurement errors near the resonances, and far away from resonances, the FRF may be well conditioned but dominated by noise in the measurement signals (Allen & Carne, 2008).

Hundhausen et al. (2007) noted that the pseudo-inverse is required to determine the inverse because the FRF matrix is not square. This is due to the fact that the number of response degrees of freedom must be greater than the number of input degrees of freedom to achieve accurate results even though, theoretically, at least the same number of response and input degrees of freedom is required.

An approach to reduce the ill-conditioning of the problem is to over define the problem by measuring the responses at more positions than there are input locations. This is however not always practically possible. First it requires the knowledge of the number of input points or there may be more input locations than there are available locations to measure the responses (Hundhausen, Adams, & Derriso, 2007).

The condition number of the FRF is a means of evaluating the ill-posedness of the reconstruction problem. An FRF matrix with a lower condition number has higher stability and small variations (noise) in the response data is less likely to cause large errors in the reconstruction. For a specific combination of response measurement locations, the average condition number is defined as (Chen, et al., 2021):

$$T_i = \frac{1}{n}\sum_{j=1}^{n} T_j \tag{1.12}$$

where T_j is the condition number at frequency j.

Measuring the response of the structure at the point where the loads that are to be identified are acting can also improve the conditioning of the problem, however this location may not be known or it may not necessarily be practical or possible to measure the response at that exact location. Differing combinations of response measurement locations will result in different condition numbers, which means that the conditioning of the problem can vary. Thus selecting a set of response measurement locations with a good average condition number can improve the accuracy and stability of the reconstruction (Khoo, et al. 2014; Chen, et al. 2021). Because the condition number can amplify the error propagation through the load reconstruction, Jia et al. (2015) proposed the use of a diagonal weighting matrix combined with a total least squares method to reconstruct dynamic loads.

Noise encountered in measurements or measurement errors can greatly affect the accuracy of the load identification. Apart from noise in the response measurements, noise in the system model or FRF can also have a large influence on the load reconstruction (Jia, Yang, Guo, & Wang, 2015). If the FRF matrix is contaminated by measurement noise it can lead to severe errors in the identified loads. Noise in the FRF matrix also reduces the number of significant figures in the matrix resulting in a reduced matrix rank and therefore a reduced number of forces that can be accurately estimated (Kriel, 2000). Some of the effects of measurement noise can be removed by making use of the H_1 FRF estimator (Oosterhuis, Eidhof, van der Hoogt, & de Boer, 2006):

$$H_1(\omega) = \frac{S_{xf}(\omega)}{S_{ff}(\omega)} \tag{1.13}$$

where S_{xf} and S_{ff} is the cross-spectrum and auto-spectrum respectively.

This does take care of uncorrelated noise but does not eliminate the effects of noise in its entirety, the measured response can be seen as the sum of the actual response and the noise, thus Equation 1.11 can be written as:

$$\{F(\omega)\} = [H(\omega)]^{-1}\{X(\omega)\} + [H(\omega)]^{-1}\{N(\omega)\} \tag{1.14}$$

where N is the measured noise.

From the above it can be seen that if the FRF magnitude is small at a certain frequency, the true response will also be small and the result will be dominated by the noise term, the noise will also be amplified due to the small FRF magnitude.

An advantage of the frequency domain methods is that they are less sensitive to noise compared to time domain methods. Noise is easier to deal with in the frequency domain than in the time domain because there are more methods to deal with noise in the frequency domain. Due to the responses generally being within a specific frequency range, some of the high noise level data can be separated out (Dolatabadi, Khanlari, Ashtiany, & Hosseini, 2020).

Apart from ensuring that proper measurement techniques are used during response (or FRF) measurement, there are mathematical methods that can be used in an attempt to improve the

conditioning of the problem, these are referred to as decomposition or regularisation methods which are discussed in section 1.2.7. Dolatabadi et al. (2020) briefly mention another method where an error vector, based on the force and measured responses, is defined and through iteration or optimisation this error vector is minimised.

Frequency domain methods have been shown to be better suited for the reconstruction of random excitation and steady state harmonic excitation (Chen, et al., 2021) and are relatively simple to implement compared to time domain methods (Patil & Gombi, 2017). When combined with system identification methods, frequency domain methods can be applied with very minimal prior knowledge of the structure and its characteristics (Amiri & Bucher, 2017).

A disadvantage of the frequency domain method is that it assumes that the measured data is periodic, which is generally not the case in practical applications (Kammer, 1998). Leakage can occur during the transformation of discrete time domain measurements to the frequency domain which can lead to inaccuracy in the FRF and therefore in the identified loads. The frequency domain method also relies on the assumption that the responses have been measured over a sufficiently long period of time in order to allow for the transformation to the frequency domain by using the discrete Fourier transform (Allen & Carne, 2008).

Another important point to note is that the FRF only describes the system for which it was calculated or estimated. If the system were to change for any reason such as damage or additional components added, the FRF is no longer a valid description of the system and will therefore not yield accurate load identification results. The FRF of a system describes a linear relationship of the inputs to the response of the system and may not be valid if the system is non-linear or exhibits non-linear behaviour in cases such as high velocity impacts (Hundhausen, Adams, & Derriso, 2007).

As mentioned, frequency domain methods are based on the assumption of a linear system, however practical engineering systems are generally non-linear (Chao, Hongxing, & Feng, 2014). In certain situations this assumption may be valid or a non-linear system may be approximated as linear, but this may lead to inaccuracy of the model versus the physical system as well as the force reconstruction.

Chao et al. (2014) discuss a method of load reconstruction of non-linear systems in the frequency domain using a combination of the least squares method and regularisation. Based on the concept of non-linearities as feedback forces, their method of load reconstruction for a multi degree of freedom system makes use of the least squares method combined with regularization to deal with instability. Their method is derived as follows (starting with the general equations of motion):

$$M\ddot{x}(t) + C\dot{x}(t) + Kx(t) = f(t) - \sum_{i=1}^{s} \mu_i L_{ji} q_i(t) \tag{1.15}$$

The non-linear part is described as the sum of s components with $q_i(t)$ as the non-linear function, μ_i the strength of the non-linear element and L_{ji} the location of the non-linear element.

The equation above is then transformed to the frequency domain and the mass, stiffness and damping component is substituted with the frequency response function of the underlying nominal linear system to yield:

$$X = H\left(F - \sum_{i=1}^{s} \mu_i L_{ji} Q_i\right) \tag{1.16}$$

which can be rewritten as:

$$\begin{aligned} X &= HY \\ F &= Y + \left(\sum_{i=1}^{s} \mu_i L_{ji} Q_i\right) \end{aligned} \tag{1.17}$$

This method does require knowledge of the FRF and non-linear parameters beforehand, however they can be estimated. The method was validated numerically (with artificial noise contamination included) as well as experimentally, in both cases very good results were obtained. In both cases the Tikhonov method was used as the regularisation method with the Generalised Cross-Validation (GCV) parameter optimisation method.

Neural networks perform well in solving ill-posed problems using regression and have therefore become more popular in the field of load reconstruction. However neural networks have their shortcomings, in the frequency domain a neural network model has to be established at each frequency independently from each other and can take long to train, making it inefficient (Wang, Chen, Chen, Lai, & He, 2021). Wang et al. (2021) proposed a deep regression adaptation network (DRAN), which makes use of information from adjacent frequencies in order to better train the network, thereby increasing efficiency. They found that the DRAN method performed significantly better compared to conventional neural network models and marginally better than neural network models with model transfer learning and the conventional transfer function method.

1.2.6. Measurement Noise

Theoretically noise is independent from the system, however in practice there are many ways by which the system and noise are coupled. Such a coupling is considered as weak when the noise does not significantly affect the dynamics of the system (Araki, Koo, Martin, & Dankongkakul, 2021).

Measurement noise is the difference between the actual signal and the measured signal. There are two main types of measurement noise, systematic and stochastic (or random). Systematic noise results in predictable errors, every measurement will deviate from the actual value in the same manner, direction or scale for example. Where stochastic noise causes unpredictable errors, each measurement deviates differently from the actual value compared to every other measurement (Bhandari, 2022). Morris (2001), defines random errors as *"perturbations of the measurement either side of the true value".* These perturbations are generally small but can be unpredictably large as well.

According to Bhandari (2022), systematic noise (error) can be worse than stochastic due to results that may seem accurate even though the results may be offset or scaled in some manner. This risks that conclusions can be drawn based on inaccurate results due to data affected by systematic errors.

Systematic noise is more commonly caused by the measurement setup such as instrument calibration, configuration or incorrect sensor transfer functions. Two quantifiable systematic errors are offset and

scale errors. Offset error is where there is a constant offset between the measurement and the actual value, such as an incorrect zero point. Scale error is when the measured values consistently differ from the actual value by a certain factor. This can be caused when the instrument or sensor sensitivity is incorrectly defined, 100mV/g instead of 10mV/g for example (Bhandari, 2022).

Stochastic noise has a blurring effect on the actual signal value (Bhandari, 2022). Stochastic noise can be caused by a number of factors, such as instrumentation, environmental factors (e.g. temperature) and measurement configuration (e.g. sample rate). Improper mounting of sensors can cause noise when for example the sensor moves relative to the structure under test. Electrical interference is another source of stochastic noise which can be due to loose connections, electrical equipment nearby etc. Random errors can be somewhat overcome by taking the same measurement multiple times and extracting values by statistical means such as averaging (Morris, 2001).

There are several sources of noise that may be present in measurements, these sources can be broadly classified into two types, instrumental noise and environmental noise (Skoog, Holler, & Crouch, 2007). Instrumental noise is noise associated with the measurement system, the transducer, signal and data processing elements. Environmental noise is noise emanating from the surrounding area, which can be electrical, vibration etc, environmental noise can also affect the instrumentation.

In vibration measurement one of the most commonly used sensors are piezo electric accelerometers or microelectrical-mechanical (MEMS) capacitive accelerometers. Piezo-electric accelerometers are generally quite small and have high operating frequencies but are not well suited for low frequency (quasi-static) applications and MEMS accelerometers are well suited for lower frequency application (Kutz, 2013). Lang (2018), notes that capacitive accelerometers are superior because of the higher sensitivities possible with capacitive sensors.

An accelerometer is basically a spring mass damper system, and therefore has its own natural frequencies. The frequency operating range of an accelerometer is determined by the sensor's natural frequency (Kutz, 2013).When an accelerometer is operated at (or near) its natural frequency the response is amplified resulting in inaccurate measurements (Lang, 2018). Various environmental factors such as temperature and humidity can influence the accuracy or sensitivity of a sensor, which if not corrected for, can result in measurement errors. Because the inertial mass in an accelerometer is so small, temperature effects can have a significant effect on the noise because the small mass will have large thermal movement relative to its size (Lang, 2018).

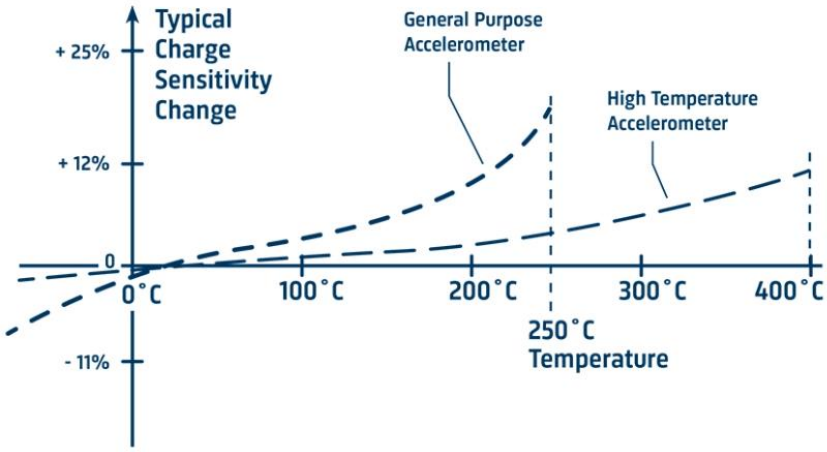

Figure 1.2 Typical accelerometer sensitivity versus temperature (Brüel & Kjaer, 2023)

As shown in Figure 1.2 above, commercial general-purpose accelerometers can generally handle temperature of around 250°C and have temperature sensitivity curves, similar to Figure 1.2, that allow for correction to the change in sensitivity (drift) due to temperature. Piezo electric accelerometers experience temperature transients because of a variation in output due to temperature fluctuations (Brüel & Kjaer, 2023). Another method to counter the effect of temperature changes is the use of a compensating element such as a washer in the accelerometer between the piezoelectric element and the inertial mass that has a thermal expansion coefficient opposite to that of the piezoelectric element, however finding a material with the required properties can be difficult (Kvasnikov & A., 2020).

Other sources of noise in accelerometers include cable noise due to ground loops, tribo-electric noise and electrical noise. If an accelerometer is installed on a surface which is experiencing variations in strain, the strain variations can be picked up by the accelerometer, however accelerometers are designed with stiff bases to reduce these effects. Transverse accelerations can also contribute to noise in acceleration measurements. Piezo-electric accelerometers are sensitive to transverse accelerations, the sensitivity in the transverse directions are generally quite low (around 2% of the main axis sensitivity) but the transverse natural frequency is generally one third of the main axis natural frequency (Brüel & Kjaer, 2023).

Several methods of reducing noise induced errors are available, many of which are common practice during any testing activities. These methods can be divided into hardware and software (numerical) methods (Skoog, Holler, & Crouch, 2007). Hardware methods include proper sensor installation, cable management, grounding, shielding and analogue filtering. Software methods include statistical processing such as averaging and digital filtering. Regular instrument calibration is another method of reducing systematic error (Morris, 2001).

The traditional numerical method of reducing noise is to assume that the noise is faster than the actual signal. With this assumption, there are a number of noise reduction methods. One of the simplest of these is the use of the FFT to deconstruct the signal and reconstructing it with only the low frequency components of the deconstructed signal (Araki, Koo, Martin, & Dankongkakul, 2021).

These methods reduce the effects of noise on measurements, but noise (or error due to noise) cannot be completely eliminated. In most cases the mean strength of the noise is constant and independent of the magnitude of the signal being measured. The signal-to-noise ratio (S/N or SNR) is a useful metric to describe the quality of a measured signal (Skoog, Holler, & Crouch, 2007).

As the term suggests, the SNR is the ratio of the signal power to the noise power and can be defined in serval ways, depending on what type of signal is being analysed, one definition is the reciprocal of the coefficient of variation (or relative standard deviation) (Skoog, Holler, & Crouch, 2007):

$$SNR = \frac{\bar{x}}{s} \tag{1.18}$$

where $\bar{x}$ is the mean and s the standard deviation.

The signal to noise ratio can also be defined by the ratio of the RMS values of the signal to the noise, which is generally used in vibration measurement (Brandt, 2011), alternatively the SNR can be determined by considering the power of the signals (Morris, 2001):

$$SNR = \frac{\overline{x_s}}{\overline{x_n}} \tag{1.19}$$

or:

$$SNR_{db} = 20\,log(\frac{\overline{x_s}}{\overline{x_n}}) \tag{1.20}$$

The smaller the value of the signal to noise ratio is, the more the signal is corrupted by the noise. Skoog et al. (2007) state that in general when the signal to noise ratio becomes less than 2 or 3, the actual signal becomes impossible to detect.

System identification and load reconstruction methods ideally require that the response measurements are done in noise free conditions, but this is not practically possible and according to Dolatabadi et al. (2020) acceleration is generally the only available and economic signal, thus these methods are used with measurements contaminated by noise. Velocity and displacement responses may be obtained from acceleration measurements through integration, however integration of noisy data may lead to further errors such as drift and singularity. Signals may be corrected (improved) through baseline correction methods such as low frequency filtration or the target base algorithm at the cost of loss of accuracy of the signal (Dolatabadi, Khanlari, Ashtiany, & Hosseini, 2020).

Sanchez (2022) performed a mathematical evaluation of the effects of measurement noise in both the forward and inverse problems. By considering the autocorrelation of an error function (calculated displacement versus actual for the forward problem and calculated force versus actual force in the inverse problem) due to measurement noise, he found that in the forward problem low frequency noise can have an effect but the error tends to zero as the frequency increases, thus making the forward problem fairly stable. The opposite is true for the inverse problem, it was found that the error is unbounded and tends to infinity and the measurement noise is amplified infinitely in the inverse problem.

1.2.7. Regularisation

Due to the ill-conditioning of the system matrix in inverse load reconstruction and the effects of noise in measured structural responses, it is very difficult to obtain an accurate solution. Thus additional processing is required to deal with these problems in order to achieve more accurate solutions. A practical solution to this problem is to obtain approximated numerical solutions (Wei, Kaiping, & Ying, 2016). These solutions can be divided into two categories (Sanchez, 2022):

- Regularisation methods
- Probabilistic methods

Several regularisation methods have been developed over the years, some of which include (but are not limited to):

- Data filtering
- Singular Value Decomposition (SVD)
- Generalised Cross Validation (GCV)
- Least Squares Methods
- Tikhonov Regularisation

Regularisation methods are generally either subtractive or additive in nature. Subtractive regularisation methods remove problematic or sensitive information, where additive methods add information or constraints (Sanchez, 2022).

Good measurement practice and filtering (or windowing) of measured signals reduce the likelihood of an ill-posed problem. High frequency noise content in signals is amplified in the inverse problem (Sanchez, 2022), affecting the conditioning of the problem as well as the accuracy of the reconstruction. The simplest method of regularisation is truncation, removing problematic parts of the model or signal and there are a number of different truncation methods. The simplest of these methods is filtering or frequency truncation which involves limiting the frequency range in which the reconstruction is performed (Sanchez, 2022).

The SVD method (also known as the truncated singular decomposition method) involves decomposing the system matrix on a singular value and singular vector, the part relating to the very small (zero) singular value is then cancelled. A more generalised approach is to define a set of values such that allowable singular values are treated as non-zero and removed singular values are treated as zero (Sanchez, 2022). This modified matrix is then used to solve the inverse problem (Uhl, 2007). In systems with low degrees of freedom this can result in a zero FRF matrix.

The GCV method is a simple method which is based on the principle of removing one set of data points and solving the problem using the remaining data. This then provides an estimated solution for all of the variables (including the removed set). The estimated data can be compared to the removed data set to obtain an error on the estimated solution. The calculation is then repeated for all of the data sets in the system and the sum of squares for all of the errors can be used as a measure of how well the model performs. The parameter that is not determined by this method is the smoothing parameter, the smoothing parameter is the parameter that is adjusted to determine the best solution. The value of the smoothing parameter that yields the minimum error is considered the optimal parameter value (Uhl, 2007). A disadvantage of this method is that it can become computationally expensive or time consuming to solve, even for small systems, if the band of interest is wide.

Least squares methods are examples of additive regularisation methods, in general least squares involve minimising the sum of squares of an error. Several methods such as conjugate gradient method or Matlab's *"lsqminnorm"* function make use of the least squares approach when performing regularisation. The common least squares method used in load reconstruction makes use of more response measurement points than excitation forces. Least squares methods are widely used in load reconstruction (or inverse problems) due to the high accuracy and the convenience of the calculation (Chen, et al., 2021). The least squares method is described mathematically as follows:

$$\varepsilon(F) = \left|\left|X - HF\right|\right|_2 \tag{1.21}$$

The aim of the least squares method is to minimise the function $\varepsilon(F)$ in the above equation.

The Tikhonov regularisation method is one of the most regularly used numerical methods to solve the inverse problem (Wei, Kaiping, & Ying, 2016) and one of the most effective for practical applications (Uhl, 2007). The use of Tikhonov's method to regularise least squares problems is also quite common in the field of inverse problems (Sanchez, 2022). Tikhonov's method was developed for application in the time domain, however it can be formulated and applied in the frequency domain. The result is more accurate (and stable) when the Tikhonov method is applied on an inverse load identification problem based on acceleration measurements compared to displacement or velocity (Uhl, 2007).

The basic principle of the Tikhonov method is:

$$min(\left|\left|HF - x\right|\right|^2 + \alpha^2\left|\left|F\right|\right|^2) \tag{1.22}$$

where the regularisation parameter $\alpha > 0$ and constant.

Tikhonov regularisation works by minimising the weighted combination of the solution and residual norms, the second term in Equation 1.22 above is the penalty term which regularises the ill-conditioned problem. The regularisation parameter additionally establishes a balance between minimising $\left|\left|HF - x\right|\right|^2$ and $\alpha^2\left|\left|F\right|\right|^2$. For any fixed value of the regularisation parameter, Tikhonov regularisation always yields a unique solution to Equation 1.22 (Chang, Yan, & Wu, 2019).

The regularisation parameter (α) has the effect of altering the norm of the residual and the solution, a large value of α reduces the norm of the solution and increases the norm of the residual term, which results in better stability, but reduced accuracy and the opposite is true for a small value of the regularisation parameter. Thus, the selection of an appropriate regularisation parameter is crucial to the success of the Tikhonov method (Chen, et al., 2021).

A modified version of the Tikhonov method as described by Equation 1.22 was proposed by Jia, et al. (2022) where a weighted regularisation method was introduced to deal with the ill-posed problem. A weighting matrix is introduced as follows:

$$min(\left|\left|\sqrt{W}HF - \sqrt{W}x\right|\right|^2 + \alpha^2\left|\left|F\right|\right|^2) \tag{1.23}$$

The weighting matrix is a diagonal matrix with each index calculated as follows:

$$w_i = \sqrt{\left(\sum_{j=1}^{2}\left|H_{ij}\right|^2\right)^{-1}} \tag{1.24}$$

With this format of the weighting matrix, good results can be achieved, but it was found that the error in the reconstructed forces were concentrated around the natural frequencies, similar to what was noted by Allen & Carne (2008), however the weighting matrix can be further optimised to improve the result (You, Ruikai, Yanhong, & Haijie, 2022).

1.2.8. Parameter Optimisation

A key component in the regularisation process is the determination and optimisation of the regularisation parameters. Any value of the regularisation parameters may provide an answer, but a parameter that will provide a realistic and accurate answer requires a mathematical approach. Various

methods of determining an optimal regularisation parameter exist. Such as the ridge trace method, quasi optimal criterion, Generalised Cross-Validation (GCV) and the L-curve criterion among others.

The methods for optimal parameter determination can be divided into prior and posterior methods. Posterior methods do not require the noise level of the responses in advance. GCV and L-curve methods are both posterior methods commonly used in engineering for parameter estimation. (Wei, Kaiping, & Ying, 2016).

The GCV function is defined as:

$$GCV(\alpha) = \frac{||x - HF_\alpha||}{Tr(I - H(H_T H + \alpha I)^{-1} H^T)} \tag{1.25}$$

with Tr denoting the trace of the matrix and the optimal regularisation parameter will satisfy the condition:

$$GCV(\alpha_{optimal}) = min\,(GCV(\alpha)) \tag{1.26}$$

One problem with the GCV method is that the curve of the GCV function can sometimes be too flat to properly find the minimum. Additionally, the GCV method may determine a very large regularisation parameter which results in losing a lot of information during the reconstruction or the GCV method may also fail entirely to determine the optimal regularisation parameter (Wei, Kaiping, & Ying, 2016).

The L-curve method makes use of a log-log scale to compare the norm of the regularised solution $||f_\alpha||$ and the residual $||x - Hf_\alpha||$. It makes use of the largest curvature under the log-log scale to determine the optimal regularisation parameter. The L-curve function is defined as follows:

$$L(\alpha) = \frac{\left|log||x - Hf_\alpha||' \theta'' - log||x - Hf_\alpha||'' \theta'\right|}{\left(\left(log||x - Hf_\alpha||'\right)^2 + (\theta')^2\right)^{3/2}} \tag{1.27}$$

The condition that satisfies the determination of the optimum regularisation parameter is:

$$L(\alpha_{opt}) = max(L(\alpha)) \tag{1.28}$$

The L-curve requires a range that includes the optimal regularisation parameter in advance. Large search ranges are possible but require extensive computational effort which is not always practical or available. The L-curve method also does not have an effective method for confirming the optimal regularisation parameter within the search range as the search range is usually small.

According to the research performed by Chen, et al. (2021), the L-curve parameter optimisation method is insensitive to the SNR in the FRF and the measureed responses, the GCV method showed higher reconstruction accuracy but at high noise levels in the FRF the accuracy of the GCV method is low. The L-curve method is therefore recommended in high noise conditions.

Gao (2016) proposed a Quotient Function Method (QFM) which uses a least squares solution solved using the quadratic programming algorithm. The least squares solution on its own is not very accurate and as the value of the regularisation parameter decreases, the accuracy decreases. This is due to the system matrix becoming more ill-conditioned. Gao's method however introduces a quotient function:

$$H(\alpha) = \frac{\left||A^T x - A^T A f_\alpha|\right|}{\alpha^2 ||f_\alpha||} \tag{1.29}$$

with the idea being to find a parameter $\alpha_0 > 0$ that satisfies the following conditions:

$$if\ \alpha \geq \alpha_0\ then\ H(\alpha) = \frac{\left||A^T x - A^T A f_\alpha|\right|}{\alpha^2 ||f_\alpha||} = 1 \tag{1.30}$$

$$if\ \alpha < \alpha_0\ then\ H(\alpha) = \frac{\left||A^T x - A^T A f_\alpha|\right|}{\alpha^2 ||f_\alpha||} \neq 1$$

The parameter $\alpha_0 > 0$ is then selected as the optimal regularisation parameter. Based on numerical as well as experimental data, the QFM has been shown to provide accurate results. This method can be easier to use compared to the GCV and L-Curve methods (Wei, Kaiping, & Ying, 2016).

1.2.9. Applications

Inverse load identification methods essentially transform a structure into its own load transducer without significant changes to the structure's dynamic characteristics. There are several practical applications of these methods.

Design standards generally make use of lab testing, empirical data or a combination of the two to develop guidelines and limits that can be used by engineers during the design of a structure. Accurate load reconstruction data can be used to verify the data used to develop design standards and be used to develop more realistic guidelines and limits (Amiri & Bucher, 2017).

One such application is condition monitoring. If the loads can be identified in real time or near real time, inverse load identification methods can be applied to monitor the health of a structure in operation (Allen & Carne, 2008). Frequency domain methods are not well suited to this specific application when real-time information is required, due to the computational effort required to perform Fourier transforms and matrix inversion at every point in the band of interest, before any reconstruction calculations can be performed.

Since the force amplitudes can provide an indication of the condition of a structure, the knowledge of which can be used to determine areas on a structure that require repair or structural modification to ensure structure integrity (Khoo, et al., 2014).

The validation of analytical or numerical models is another application in which inverse load identification can be useful. If the loading on a structure can be accurately determined or estimated, the result will be improved accuracy of numerical models which in turn would then reduce the time and cost needed to test, leading to a quicker time to market or project completion (Patil & Gombi, 2017).

Accurate identified force data can be used in CAE models to perform trouble shooting, failure analysis or fatigue analysis of a structure. Accurate field data can also be used in the design phase of similar or replacement structures (Khoo, et al., 2014).

Load identification of forces during machining processes such as milling can be used to monitor stability, tool wear, part quality etc. Piezoelectric dynamometers are commonly used to measure these forces, but they are limited in their measuring bandwidth, cost and workpiece geometry (Wang, Zhang, Qiao, Cao, & Chen, 2019). Frequency domain load reconstruction using pseudo-inverse methods was used to accurately determine the forces experienced by a cutting tool during operation (Patil & Gombi, 2018).

Another application discussed by Chen, et al., (2021) is to make use of load reconstruction methods to determine the forces transmitted from equipment mounted to the underside of railway vehicles (due to vibration) to the chassis or floor of the vehicle. The vibration experienced by equipment on a railway vehicle is dependant on a number of factors such as track condition or quality, vehicle loading condition, speed etc. These forces can influence the ride comfort of the vehicle and knowledge of these forces can be usefull in designing mounting systems.

1.3. Scope of Research

The load reconstruction problem is a practical application of the inverse problem in the field on structural dynamics and vibration (Amiri & Bucher, 2017). Load reconstruction can be performed in either the time or frequency domains Initial research focused on frequency domain methods. However, in recent studies the focus has been more on time domain methods (Lourens, Reynders, De Roeck, Degrande, & Lombaert, 2012). This is due to the computational efficiency of frequency domain methods being less compared to many modern time domain methods (Amiri & Bucher, 2017).

Many time domain methods are based on solving the convolution integral (Patil & Gombi, 2017), the solution of the convolution integral can be achieved by summation instead of integration such as what was done by Chang et al. (2019), because of the discrete nature of structural response measurements.

Combined with system identification methods, frequency domain methods can be applied with very minimal prior knowledge of the structure and its characteristics (Amiri & Bucher, 2017). This can be practically very useful in cases where very little information of the structure is available, such as cases where remaining life predictions are to be performed or the original design information of a structure is not available.

Methods in both domains have their respective advantages and disadvantages which are discussed in greater detail in section 1.2. In general time domain methods are more computationally efficient and certain methods are able to provide near real time results, which make them well suited in condition monitoring applications. Time domain methods such as the sum of weighted accelerations technique (SWAT) have an advantage of only needing short duration response measurements to reconstruct the loads (Chao, Hongxing, & Feng, 2014).

A benefit of the frequency domain approach is that it is relatively simple compared to time domain techniques. Time domain techniques often require convolution whereas in the frequency domain multiplication achieves the same result. Frequency domain methods assume a linear relationship between the loads acting on a structure and the responses of a structure (Patil & Gombi, 2017), but real structures are rarely linear. Linear approximations can be used but will not be valid for all situations. Nonlinear structures can still be dealt with in the frequency domain by means of iteration or methods such as what is described by Chao et al. (2014), however this study will focus on linear (or linear approximations) systems or structures.

A common problem encountered in both the domains is the sensitivity to measurement noise. Noise is always present in practice, the intensity of the noise varies and can have a great impact on load reconstruction. Sanchez (2022) performed a mathematical analysis of the effects of noise on both the forward and inverse problems. In this study it was found that in the forward problem low frequency noise can have an effect but is fairly stable with regards to measurement noise, whereas in the inverse problem noise is infinitely amplified. According to Dolatabadi et al. (2020) frequency domain methods are less sensitive to noise compared to time domain methods.

Regularisation methods have been developed to assist in solving the inverse problem and overcome some of the problems associated with the inverse problem and the effects of measurement noise. Commonly used regularisation methods are the Least squares method, SVD (singular value decomposition) and Tikhonov method.

Tikhonov based regularisation methods have been found to be more robust in practice compared to newer methods such as Kalman filters (Amiri & Bucher, 2017). Least-squares methods are also effective in reducing the effects of measurement noise and FRF error under certain conditions (Chang, Yan, & Wu, 2019).

Regularisation methods such as the Tikhonov method make use of a regularisation parameter, the choice of the regularisation parameter has a large influence on the result of the regularisation and by extension the accuracy of the load reconstruction. Methods to determine the optimal regularisation parameter have been developed, two of the most common parameter optimisation methods used with Tikhonov regularisation are the L-curve method and the GCV (Generalised Cross Validation) method. Both of these methods are able to estimate the regularisation parameter without prior knowledge on the measurement noise (Amiri & Bucher, 2017), these two methods are included in the scope of this research because in practice noise levels may not always be known.

A need was therefore identified to review frequency domain methods combined with a few of the commonly used regularisation methods and the effects of measurement noise (or error) on the accuracy of these methods. Much reference to the sensitivity to noise is made in literature, but few studies have investigated the sensitivity to varying levels of noise.

In principle the frequency domain methods are simpler to implement compared to many time domain methods such as the convolution integral and Augmented Kalman Filter (AKF) at the cost of computational efficiency (Amiri & Bucher, 2017).

Frequency domain methods therefore have potential in modern practical applications where the loading on existing structures for which there are no information available (apart from the physical structure itself) are to be evaluated. Measurement noise is always present practise and cannot be avoided, thus methods that can provide accurate results despite the presence of measurement noise can be very useful in practise.

Building on the work by Dolatabadi et al. (2020), Sanchez (2022) and the like, this research focuses on investigating the effects of noise on frequency domain load reconstruction methods and to evaluate the performance of a few commonly used regularisation methods.

The focus is on methods that require minimal information of the structure prior to commencing with the load reconstruction and where the required information can be obtained experimentally. The scope includes numerical studies using cases where only the noise level is varied to investigate the effects of noise, one of these cases is also to be validated experimentally.

1.4. Document Overview

This document consists of the following chapters:

- Chapter 1: Introduction, Literature study and Scope of Research (this chapter)
- Chapter 2: Numerical Modelling
- Chapter 3: Experimental work
- Chapter 4: Results
- Chapter 5: Conclusions

Chapter 2 discusses the analytical and numerical studies that were performed. First, an analytical multi-degree of freedom model is used with impulse and sinusoidal loads applied. The impulse load and the responses are used to estimate the frequency response function of the analytical system. The responses of the system due to the other applied loads are then reconstructed using frequency domain methods. Systematic errors and increasing amounts of randomly generated noise are then added to the response signals to investigate the effects on the quality and accuracy of the reconstruction methods. The purpose of the load reconstruction on analytical models is to verify the functionality of the frequency domain load reconstruction methods being considered during the study.

Following the analytical model, the simulation model responses are used to estimate the FRF (Frequency Response Function), replicating what could be done in practice for an unknown structure and the same procedures as applied in the analytical models are applied. The same methods are applied to a lumped mass simulation (performed in MSC Adams multibody dynamics simulation software), and a finite element model of a cantilever beam. The reasoning behind this approach is to systematically introduce additional factors (such as discretisation and numerical rounding errors) that can have an influence on the load reconstruction methods along with the effects of noise. The feasibility of using finite element software to calculate the FRF is also investigated.

Chapter 3 covers the experimental work performed. A simple cantilever beam experiment was used, first a modal test was performed to determine the FRF. After the modal was performed, loads were applied to the beam by means of a small shaker. The same procedures and load reconstruction methods were applied to the experimental data to evaluate the performance under real world conditions.

Chapter 4 discusses the findings from the test models including the experimental work. The performance of the various methods are compared to one another and differences in performance of the various methods on the models are discussed. Factors that influence (and don't affect) the accuracy of the results are also discussed. An FRF created by the finite element method is used to perform load reconstruction on the experimental model to test the feasibility of using finite element based FRFs to perform load reconstruction.

In chapter 5 conclusions are drawn based on the literature reviewed and the findings obtained in the previous chapters. The chapter also includes recommendations on how to achieve accurate results when using frequency domain load reconstruction methods as well as recommendations for potential future research.

2. Mathematical Modelling

From the literature reviewed it is evident that noise can have a significant impact on the accuracy of load reconstruction. Time domain methods have received more attention in recent years, however, because some of the simplicity compared to time domain methods (Patil & Gombi, 2017) and minimal prior knowledge of the structure required (Amiri & Bucher, 2017), frequency domain methods have been selected as the focus of this study. Several approaches are commonly followed to perform load reconstruction in the frequency domain. In this section a number of these methods are compared to one another using analytical and numerical models.

Three mathematical cases have been considered. Firstly, a pure analytical case for a rigid body *n*-degree of freedom system where the equations of motion for the system are known. Next a simulated rigid body dynamics system where only the forces and responses are known and finally an elastic finite element model where only the forces and responses are known. The analytical model solutions as well as all the calculations for the subsequent cases were computed using Matlab™. An overview of the calculation procedures are presented in section 2.1 of this document.

In each case an FRF is estimated from a simulated impulse load and responses. The estimated FRF is then used to reconstruct another load. Starting from an initial no or low noise level, the noise levels are gradually increased to study the effects the increasing noise has on various load reconstruction methods. Since the originally applied loads are known in all the cases, the reconstructed loads are compared to the original loads in order to determine the accuracy of the reconstruction.

For the purpose of this study the FRFs in all cases are assumed to be obtained in ideal conditions and noise is not added to the response signals used to determine the FRFs.

Several methods can be used to reconstruct loads on a structure. Some of the commonly used methods in engineering applications have been selected. The performance of these methods under noisy and error conditions will be evaluated and compared to one another. Based on the literature reviewed the following methods were found to be the most commonly used methods and have therefore been selected for this study:

- Inverse (or pseudo-inverse)
- Least-Squares
- Singular Value Decomposition (SVD)
- Tikhonov's method with GCV parameter optimisation
- Tikhonov's method with L-Curve parameter optimisation

In each of the above-mentioned scenarios load reconstruction will be attempted with each of these methods. The following sections describe each of the models and their performance under ideal conditions as well as the calculation routines used in all the cases.

In each of the following models the loads are initially reconstructed using the responses in the absence of noise (except for the experimental case where there will be some noise present), this is done to firstly evaluate the performance of each method on each model as well as to evaluate the performance in the absence of noise. Then two types of error/noise are considered, firstly systematic errors which can be caused by the measurement setup or calibration (Bhandari, 2022) and secondly

stochastic error (noise) which is always present in practical measurements. In each case the noise is artificially introduced to only response signals.

Two types of systematic error were considered, the first is an offset error and second is a scaling error. An offset error is replicated by adding a constant value equal to 25% of the mean value of the signal, an error such as this may be encountered when the measurement system is not zeroed correctly before the experiment is conducted or if the temperatures between the setup and the test vary significantly (Lang, 2018). The scaling error is replicated in a similar manner, except that each signal is scaled by a constant factor. This type of error may be encountered if for example sensor sensitivity is incorrectly specified (Bhandari, 2022) or if temperature effects are not compensated for (Brüel & Kjaer, 2023).

Stochastic noise is the next error type that was considered, this was done using predetermined noise levels and the definition of the signal-to-noise ratio given by Morris (2001) to determine mean of the noise signal required. Using this mean, a random signal is generated and added to each response signal using the equation below:

$$X_n = X + n \tag{2.1}$$

where X is the clean signal and n the noise signal.

The above is used in all the cases except for the scaling error case where X is multiplied by n. The table below summarises the various error and noise cases considered in this study.

Table 2.1 Noise & Error Cases Considered

Case	Noise/Error Type	Magnitude
0	None (Baseline)	N/A
1	Systematic – Offset	25% of mean
2	Systematic – Scale	10% increase
3	Stochastic	0.5% Noise
4	Stochastic	1% Noise
5	Stochastic	2% Noise
6	Stochastic	3% Noise
7	Stochastic	4% Noise
8	Stochastic	5% Noise
9	Stochastic	10% Noise

The stochastic noise in Equation 2.1 above is calculated using the equation below:

$$n = (N_p X_{RMS})\big(rand(0,1)\big) \tag{2.2}$$

where N_p is the percentage noise and $rand(0,1)$ is a random number between 0 and 1.

The noise levels in Table 2.1 above were selected based on literature of similar work such as that of Dolatabadi, et al. (2020) and limited to a SNR of 10 as at lower values the signal can become impossible to detect (Skoog, Holler, & Crouch, 2007). It is also assumed that in practice steps would be taken to reduce some of the effects of noise.

2.1. Calculation Procedures

All of the calculations performed during the course of this study were done using Matlab®, the Matlab signal processing toolbox and ModalTools™ a third-party toolbox developed by Axiom EduTech. This section provides an overview of the calculation procedures used in this chapter.

The figure below graphically illustrates the load reconstruction process flow,

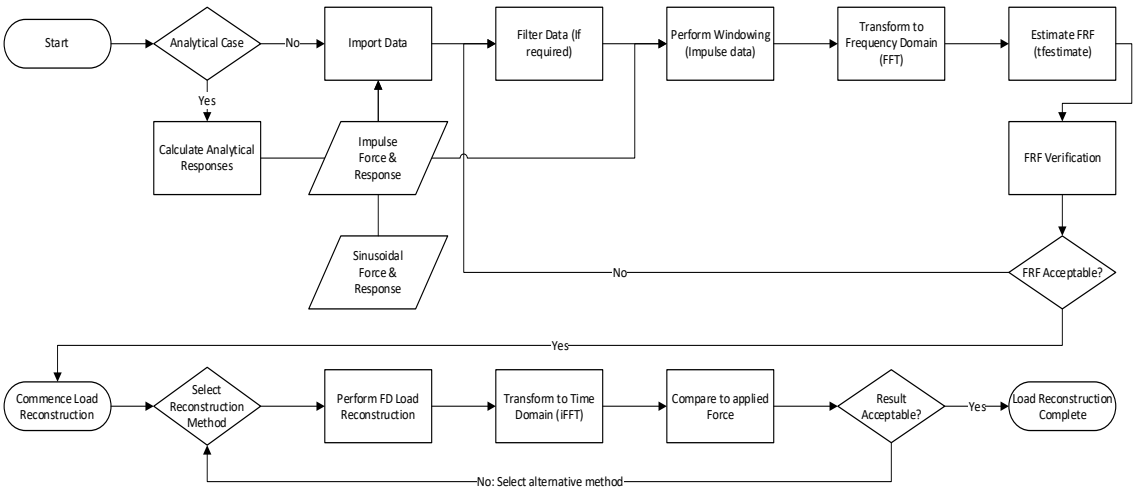

Figure 2.1 Load Reconstruction Process Flow

The procedures for all the load reconstruction test cases are the same, except in the analytical case, as indicated by the branch in Figure 2.1 above, where the responses are calculated instead of imported. In the analytical case all the system parameters are known, therefore the equations of motion can be derived and solved by using known time varying load functions as inputs to determine the responses.

In the other cases the applied forces and responses are imported from either the simulation packages or the experimental results. The first step in the reconstruction process is the windowing of the impulse force and responses. The impulse force is windowed using a force window which is shown schematically in the figure below:

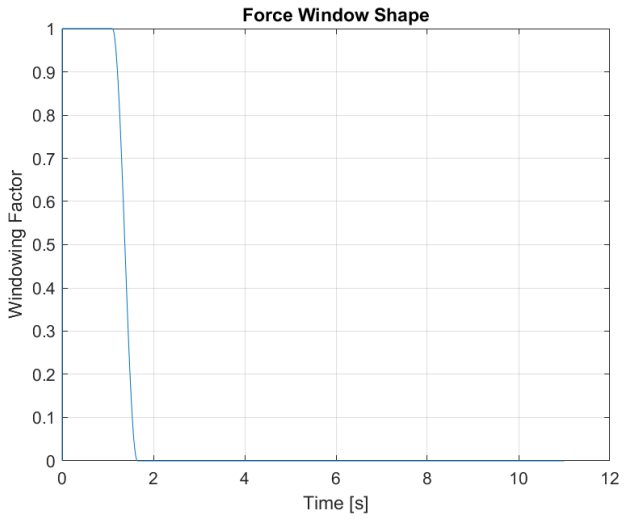

Figure 2.2 Force Window

The purpose of the force window is to ensure that the signal starts and ends at zero in order to minimize leakage effects. Because the signal is not periodic, leakage occurs when the signal is transformed from the time domain to the frequency domain (Crystal Instruments, 2023). Another benefit of the force window is that it removes some of the noise in the signal resulting in a better FRF estimation. In the example given by Figure 2.2, the impulse would occur at 1 second, all the test models were set up such that the impulse occurs at 1 second after the start of the simulation or experiment. The responses are similarly windowed using an exponential window which is illustrated in the figure below:

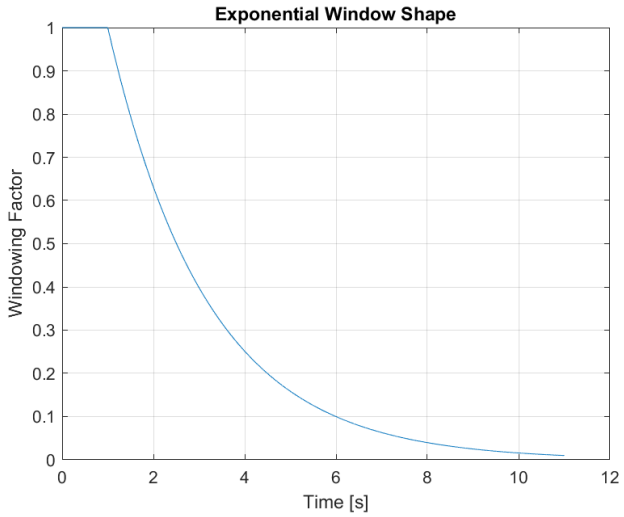

Figure 2.3 Exponential Window

The exponential window forces the response to decay exponentially, resulting in a periodic signal. The general form of the exponential window is given below:

$$w(t) = e^{-at} \tag{2.3}$$

where a is the exponential constant which is adjusted according to the signal (Brandt, 2011).

This window does cause an over estimation of the damping of the structure because it adds additional damping to the response signal but can improve the signal to noise ratio (Brandt, 2011). This additional damping must the compensated for or removed from the signal to correct the FRF for further calculations.

Brandt (2011), has shown that the exponential window only influences the damping and if the window constant is known can be corrected for by:

$$\zeta_c = \zeta_m - \frac{a}{2\pi f_n} \tag{2.4}$$

where ζ_c is the corrected damping and ζ_m is the measured or estimated damping.

After windowing, the time domain signals are transformed to the frequency domain using the fast Fourier transform (FFT). The FFT resolution is determined by calculating the next higher power of 2 based on the length of the signals and the frequency band is taken as half of the measurement sample rate (Nyquist rule).

Once transformed to the frequency domain, the impulse force and responses are used to determine the FRF. This is done by using the Matlab function *"tfestimate"*, this function estimates the transfer

function by dividing the cross-power spectral density of the response and the force by the power spectral density of the force (H_1 estimator). The function has the option to calculate the H_2 estimation but the H_1 was selected because it can remove some of the effects of measurement noise (Oosterhuis, Eidhof, van der Hoogt, & de Boer, 2006). A FRF verification step is included to verify the quality of the estimated FRF, this is done by making use of Equation (1.10) to calculate the response using the known force and estimated FRF and comparing the calculated response to the known response.

Next the load reconstruction methods are applied, the program was set up such that multiple methods of load reconstruction can be used. The methods listed in section 2.0 have all been included into the programming. The first method included is the inverse or pseudo-inverse method, the inverse method is only used in cases where the FRF matrix is square, which is generally only the analytical (analytically calculated) FRF case. In the other cases the Moore-Penrose pseudo-inverse method is used.

The next method included is the least squares method. This method, which is described by Equation (1.21), was selected because according to Chen, et al. (2021) it is a commonly used for high accuracy load reconstruction. The implementation of this method is achieved by making use of the Matlab function, *"lsqminnorm"*. The difference between this method and the pseudo-inverse method is that this method minimises the norm of the solution of the force and uses complete orthogonal decomposition to determine approximation of the FRF matrix with a low rank whereas the pseudo-inverse method uses singular value decomposition to determine a tolerance (Mathworks, 2020).

The SVD method was also included as one of the methods since many methods are based on or make use of singular value decomposition and has been used in solving the inverse problem (Uhl, 2007). In the implementation of this method a tolerance is specified manually and adjusted manually until the error found in the verification step is minimised.

The last method is the Tikhonov method, which is used with two parameter optimisation methods, L-Curve and GCV. The Tikhonov method was included because according to various authors such as Sanchez (2022) and Gao, et al. (2016) it is one of the most used methods in inverse problems and load reconstruction. The L-Curve and GCV parameter optimisation methods were selected because they do not require the noise levels in advance which make them more applicable in practice (Wei, Kaiping, & Ying, 2016). The functions used to perform the parameter optimisation form part of a Matlab toolbox developed by Hansen (2008) for the purpose of regularisation.

Once the load reconstruction has been performed, the results are compared to the known applied forces in each case to determine the accuracy of each method. In practice where the applied forces are not known an alternative verification step is used. In this verification step the reconstructed forces are used with the FRF to calculate the responses and the calculated responses are compared to the measured responses.

2.2. Analytical Model

An analytical model was created to solve the equations of motion for an arbitrary rigid body system with n degrees of freedom. The purpose of this model is to establish the foundation of the method in the absence of noise or measurement error to prove and test the methodologies. With all the system parameters known, the analytical FRF values over a specified frequency range are calculated. The applied impulse force (simulated modal hammer strike) and calculated responses are also used to estimate a FRF similar to what would be done in practical applications. Both the theoretical and

estimated FRFs are then used to reconstruct the applied impulse load as a verification step and then used to reconstruct arbitrary loads.

A two degree of freedom system will be discussed in this section. However, the methodologies discussed can be applied to any linear n-DOF system. Three other models were also considered, namely n = 3, 4 and 7 degree of freedom models. Results from these three models are briefly discussed in section 4. Descriptions and full results for these models are presented in the appendices. These higher degree of freedom models were used to evaluate the performance of more complex models under the same conditions. The free body diagram of the 2 DOF system is shown in Figure 2.4 below:

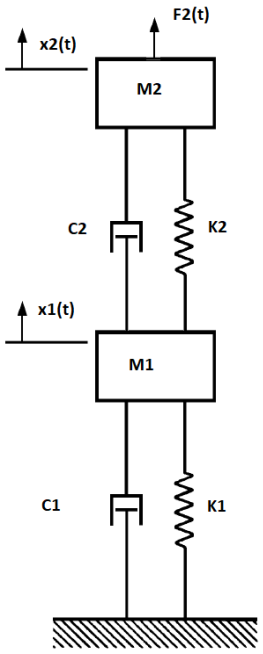

Figure 2.4 Free Body Diagram of Numerical 2-DOF Model

The model parameters of the two degree of freedom model are listed in the table below:

Table 2.2 Analytical 2-DOF System Parameters

Coordinate Point	**1**	**2**
Mass [kg]	6.61	12.18
Stiffness [N/m]	7000	4000
Damping Coefficient [Ns/m]	150	60
Undamped Natural Frequency [Hz]	2.21	6.75
Damping Ratio	0.12	0.39

An impulse load simulating a hit from a modal hammer is applied to the model and the responses are calculated. The impulse load applied to the system is shown in Figure 2.5 below.

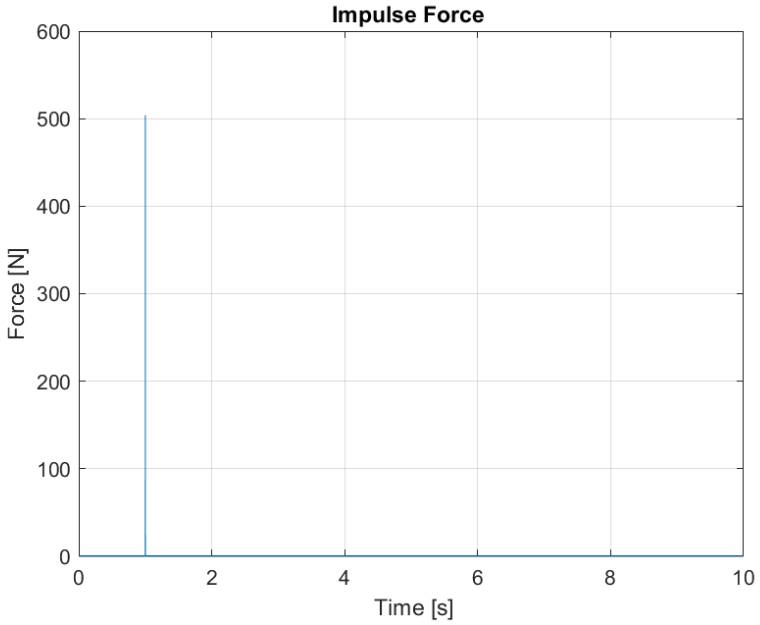

Figure 2.5 Impulse Force Applied to the 2-DOf System

The impulse is applied to the second mass (M_2). The system displacement responses to the impulse are shown below:

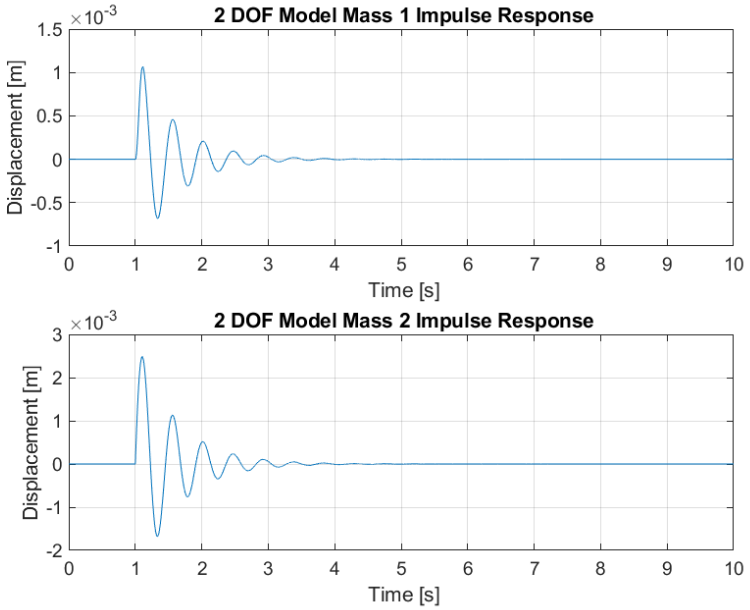

Figure 2.6 Two Degree of Freedom System Impulse Responses

Since all the system information is known in the analytical models, the theoretical damped FRF can be calculated. The modal formulation is used instead of the direct formulation because in most practical applications the spatial matrices (mass, stiffness and damping) is not available. This is achieved by using the equation below (Ewins, 2000):

$$r_{jk}(i\omega) = \sum_{r=1}^{N}\left(\frac{\theta_{rj}\theta_{rk}}{a_r(i\omega - s_r)} + \frac{\theta_{rj}^{*}\theta_{rk}^{*}}{a_r^{*}(i\omega - s_r^{*})}\right) \tag{2.5}$$

where r_{jk} is the receptance matrix value at response location j due to force k. The subscript r denotes the mode number and θ the normalised eigenvectors.

Equation 2.5 above calculates the receptance (displacement FRF) matrix values at each frequency in the band. To calculate the mobility or accelerance the receptance is multiplied by $i\omega$ and $-\omega^2$ respectively.

Using Equation (2.5), all four indices of the theoretical damped FRF of the 2 degree of freedom system are calculated over the frequency band of interest and are shown in Figure 2.7 below (frequency axis is only shown up to 25 Hz for visualisation). The natural frequency at 2.2Hz is clearly noticeable, however the one at 6.7Hz is not as clear due to the high damping.

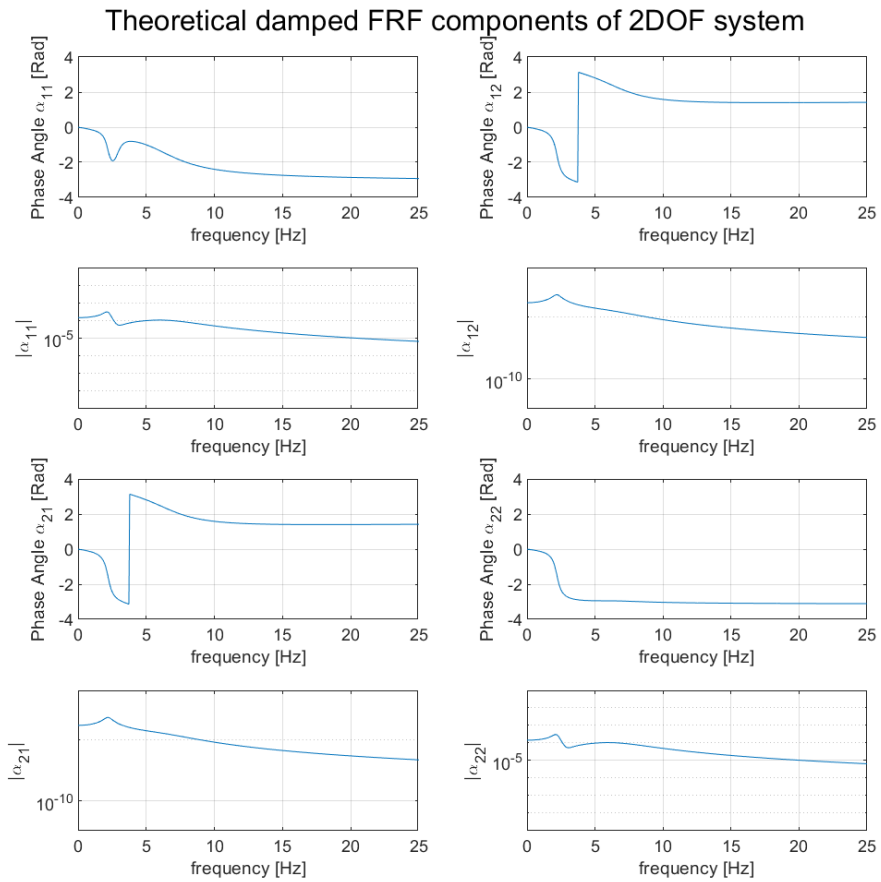

Figure 2.7 Theoretical Damped FRF Magnitudes of the 2 Degree of Freedom system

The analytically calculated FRF is used to verify FRF estimations based on the inputs and responses. The FRF is estimated by determining the relationship between the response and the inputs, however as the force and responses are both ideal cases (both the force and responses are zero at the start and

end in the window of interest), no windowing is performed in this case. The magnitude and phase of the estimated FRF for the 2 DOF system is shown in Figure 2.8 below.

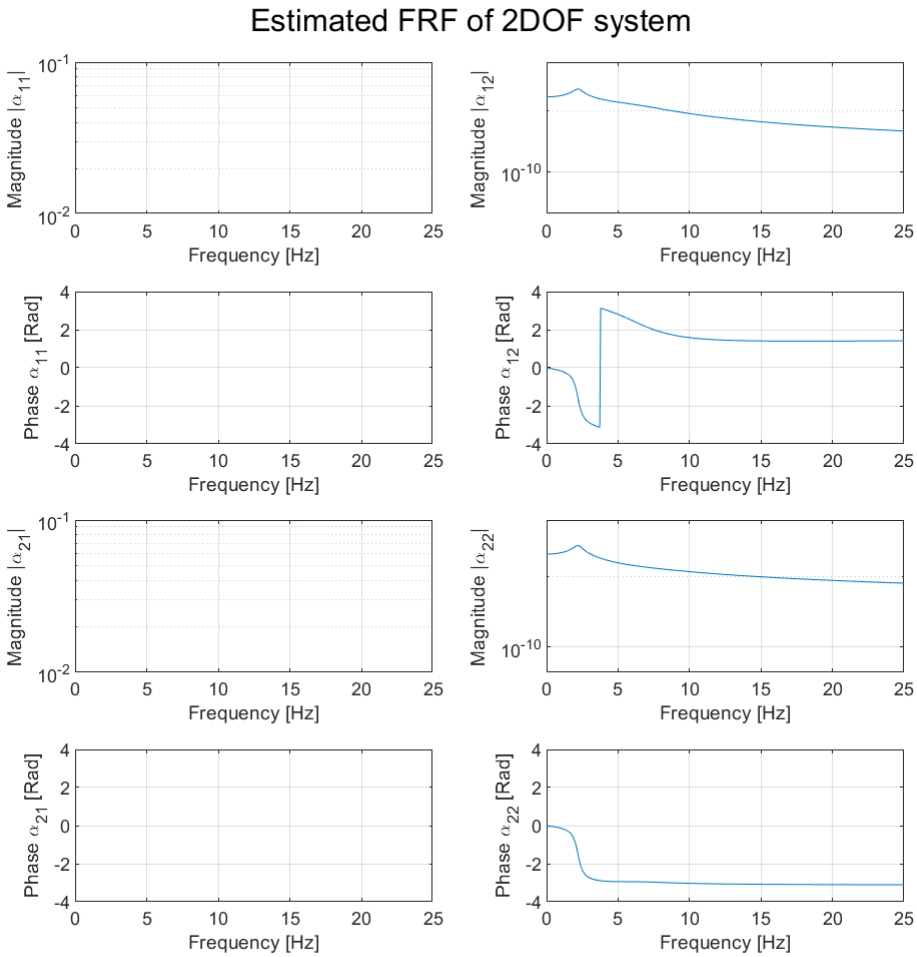

Figure 2.8 Estimated FRF Magnitude for 2DOF System

Since there is only a single force acting on the second mass, only the components of an FRF matrix relating to the force on the second mass can be estimated, as indicated in Figure 2.8. With a FRF estimated from the input and response of the system (using the method as discussed in section 2.1), the estimated FRF can be compared to the analytical FRF as a measure of the accuracy of the estimation, this comparison is shown in the figure below.

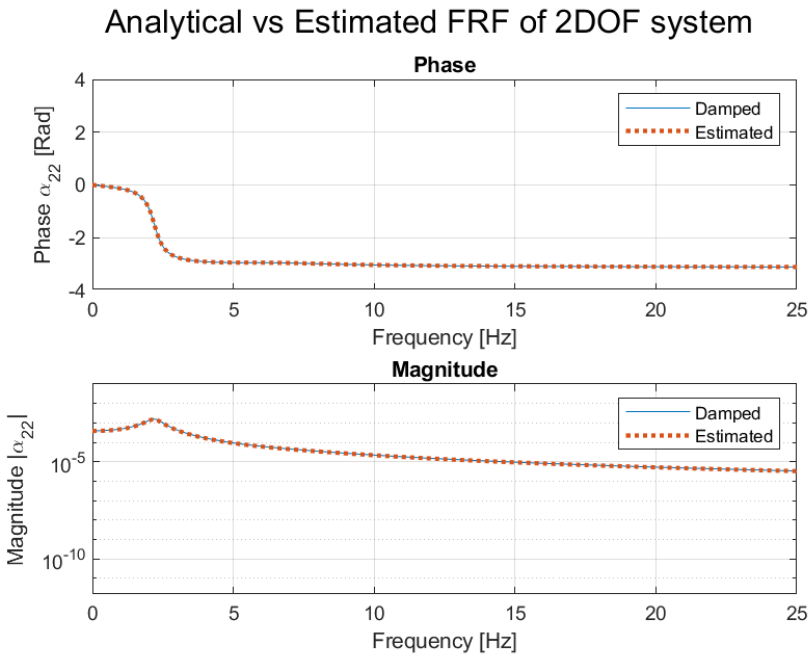

Figure 2.9 Comparison of Analytical and Estimated FRF

Figure 2.9 illustrates that the analytical and estimated FRFs match exactly (in the absence of measurement noise) and verifies that the method used (using the function *"tfestimate"* in Matlab) for estimating the FRF from response measurements is possible.

Next the inverted FRF is used to reconstruct the loads applied to the system, this is done by using Equation (1.11) on which frequency domain load reconstruction methods are based (Patil & Gombi, 2017):

$$\{F\} = [H]^{-1}\{X\} \tag{1.11}$$

The estimated FRF matrix is not square, thus conventional matrix inversion methods cannot be used. Because in this case the number of degrees of freedom are known, it is possible to construct a square (approximate) FRF matrix using the available information. This is however not feasible in practice as the systems are generally not this simple and the exact number of degrees of freedom is not known (especially in the case of complex elastic structures).

The method is the inverse method, using the Moore-Penrose inverse, which is calculated as follows:

$$[H(\omega)]^{+} = ([H(\omega)]^{*}[H(\omega)])^{-1}[H(\omega)]^{*} \tag{2.6}$$

This method requires that the inverse of $([\mathrm{H}(\omega)]^{*}[\mathrm{H}(\omega)])$ exists and is only unique if $[H]$ is of full column rank, i.e., the system is linearly independent (Kriel, 2000). If these conditions are not met, it

does not mean that the matrix cannot be inverted. It means that this method will not be suitable and that alternatives should be considered.

Minimum-norm least-squares is one such alternative approach which is widely used in load reconstruction (Chen, et al., 2021). In this approach a solution is calculated that minimises the equation given by Equation (1.21). In the case where there is more than one solution the minimum norm solution is taken as the solution. This method is discussed in more detail in section 1.2.7 and the implementation thereof in section 2.1. The inverse FRF in this case may be calculated using various pseudo-inverse techniques (including the Moore-Penrose method).

In most of the pseudo-inverse methods an FRF matrix is constructed using the available input and response data. In the case of the two degree of freedom model with one force input, a rectangular FRF matrix with two rows and one column is constructed.

Initially, the direct inverse and least squares methods were used to reconstruct the impulse load. Both methods were able to accurately reconstruct the impulse load on the system. The difference in amplitudes of both estimations is less than 1% of the applied load. The result of the latter method is shown in the figure below.

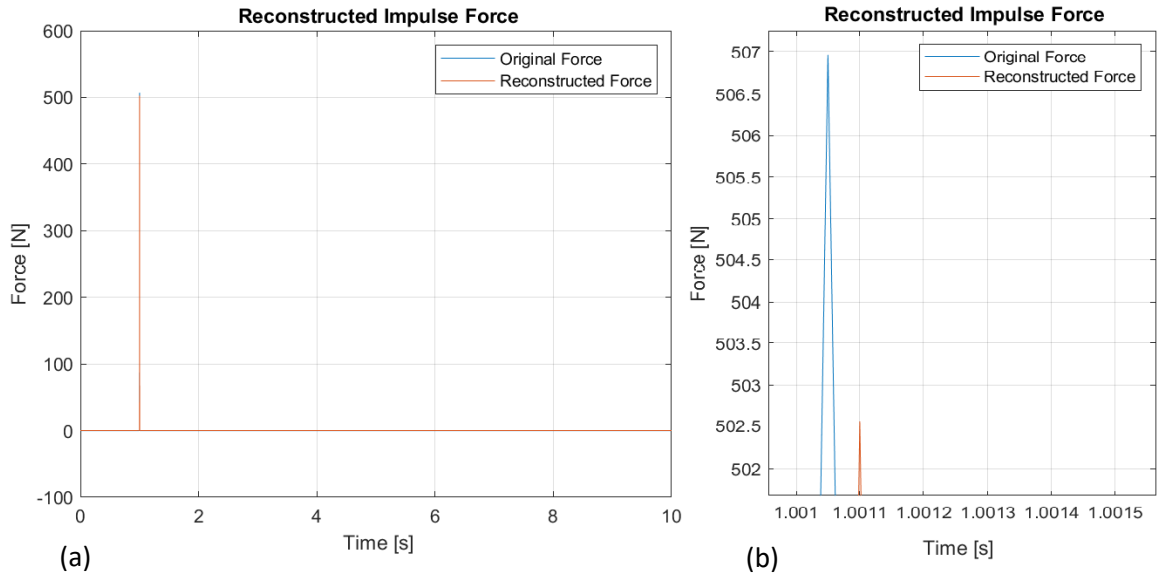

Figure 2.10 Reconstructed Impulse Load of the Analytical System Using Least-Squares Method,

with Figure (a) that gives the overall picture and Figure (b) a zoomed picture

Next, a simple sinusoidal load with a constant frequency is applied to the same system. The equations of motion are solved to be able to test the load reconstruction of the new load using the same FRF and to establish a baseline for the determination of the sensitivity to noise.

To establish a baseline for comparison, the analytical FRF is first inverted and used to reconstruct the applied force. The procedure followed is the same as previously described, except that the standard inverse is used (for the inverse method case) since the analytical FRF is a square matrix.

All the methods considered were able to accurately reconstruct the applied load within 5% or less error. The result of the inverse method is shown in the figure below.

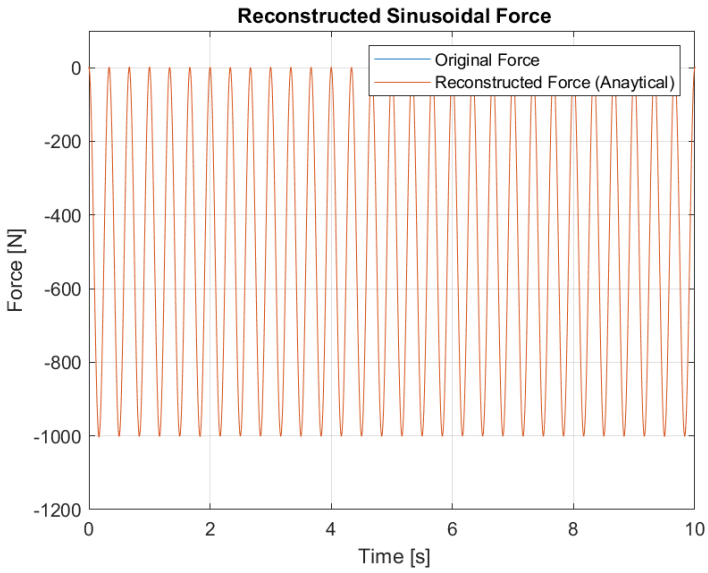

Figure 2.11 Load Reconstructed From Analytical FRF

The above figure shows excellent correlation between the applied and reconstructed load. This confirms that the theory is valid and provides a baseline for the comparisons that follow.

The previously estimated FRF is used to reconstruct the applied sinusoidal load using the responses of the system due to the sinusoidal load as input, using different load reconstruction methods (all initially with no noise).

Reconstruction of the sinusoidal load using the Moore Penrose inverse method did not yield any comparable results even though the FRF matrix is of full column rank and no noise was added to the signals. However, if a Hanning window is applied to the response time signal and the windowed signal is used in the reconstruction a comparable result is obtained. There are however some residual end effects present in the reconstructed force, as shown below:

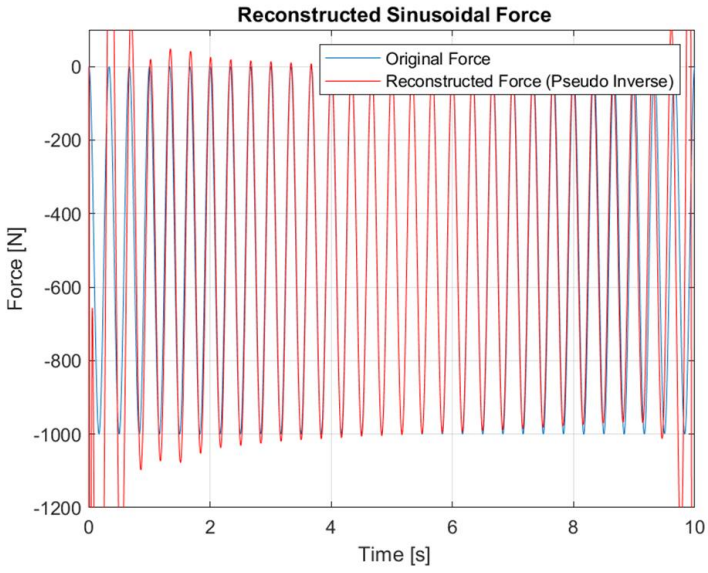

Figure 2.12 Reconstructed Force Using the Pseudo-Inverse Method

The least squares method, using complete orthogonal decomposition (COD) to determine the inverse FRF, was applied next. A fairly accurate result was obtained. It should be noted that the tolerance used during the calculation does influence the accuracy and computational time.

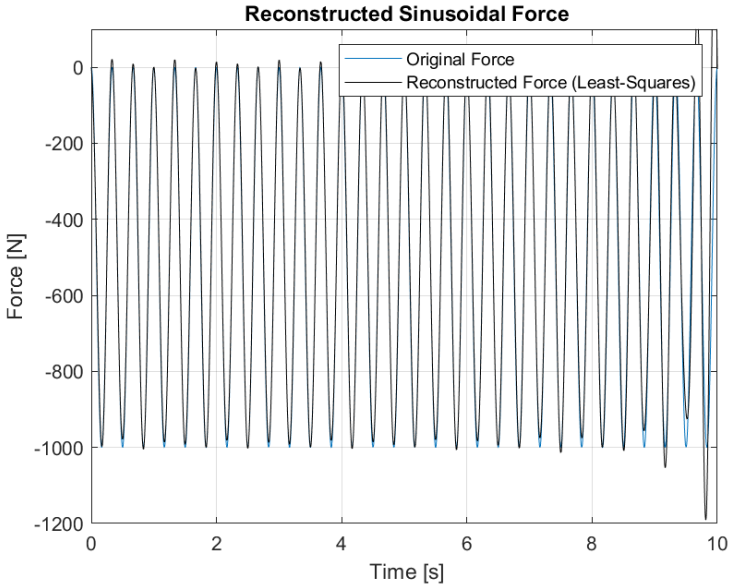

Figure 2.13 Reconstructed Sinusoidal Force of the Analytical System Using Least-Squares

The Classical Tikhonov method was used as an alternative method to the Moore-Penrose inverse and least-squares method. The Tikhonov regularisation parameter optimisation was performed using the L-curve and GCV algorithms. Both parameter optimisation algorithms performed well with the classical Tikhonov method.

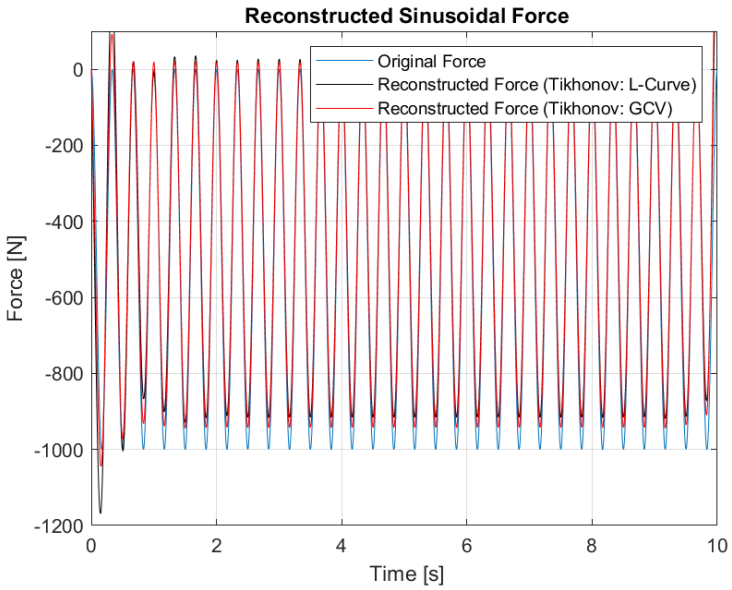

Figure 2.14 Reconstructed Force Using Tikhonov's Method

It should be noted that in the reconstructions performed until this point no windows were applied to the input forces and responses except in the case of the pseudo-inverse. Windowing was not performed on the signals because the assumption was made that the signals are periodic within the

sampling period and are continuous (in the analytical case). Windowing will be included in the subsequent sections as the analysis performed moves more towards real world measurements.

All results discussed thus far have been for case 0, i.e., no noise. When the first case is considered using the analytical FRF, a similar offset is observed in the reconstructed force. However, increased distortion at the start and end of the signal is observed, as shown below.

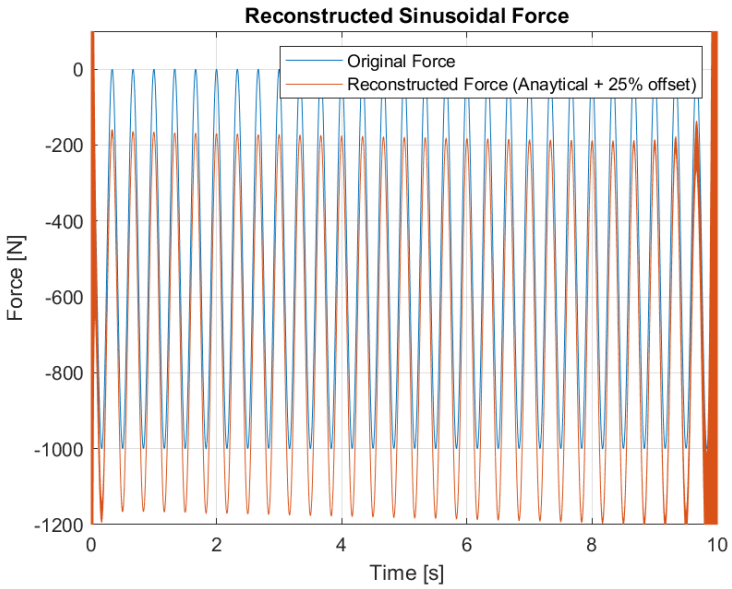

Figure 2.15 Load Reconstruction Result with Systematic Error

It was observed that a positive offset on the response creates a negative offset on the reconstructed load and vice versa, which was expected but no other significant differences. Thus, an offset in only one direction will be considered.

When the response magnitude is scaled down by 10% (case 2) the resulting reconstructed load is also scaled by the same amount. On the analytical case the relationship between the scale factor and the resulting reconstruction appears to be linear, this will be evaluated again for the other models.

The analytical model (using the analytical FRF and displacement responses) fails completely to reconstruct the load when stochastic noise is introduced into the response used for reconstruction, even with a high SNR. Reconstruction using the analytical FRF is much more sensitive to noise compared to reconstruction using an estimated FRF.

The full results of the effects of each of these cases on the accuracy of the reconstruction are provided and discussed in section 4 of this document.

The same procedures for performing load reconstruction will also be used in the following sections using different models, two simulation models and one experimental case with the same cases considered for the effects of noise on the reconstruction.

2.3. Simulated Lumped Mass Model

In this section, a lumped mass dynamics model of a two degree of freedom system was created in Adams®. The simulation results were imported into the same Matlab programs as used in the analytical model for post processing and load reconstruction. The purpose is to test the load reconstruction algorithms using discrete data (simulating measured responses), Adams rounds results data before exporting resulting in clearly defined discrete values. This method also provides the ability to test the algorithms with different physical responses, displacement, velocity or acceleration to evaluate if the choice of response has any significant effect on the load reconstruction.

The physical properties of the model is the same as those described in Figure 2.4 and Table 2.2, simulated with a time duration of 5 seconds and a sampling rate of 20kHz. The sampling rate was increased to reduce the discretisation of the simulation results. The same impulse and sinusoidal loads are applied to this model and 1-dimensional motion and loading is assumed.

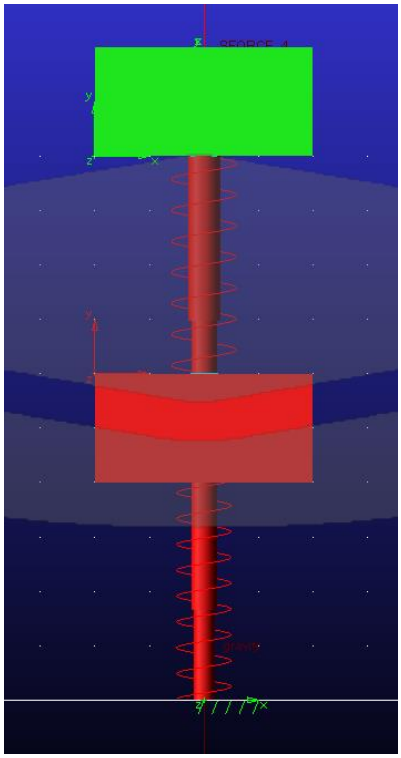

Figure 2.16 Lumped Mass Model Represented in Adams

Similarly to the analytical model previously described, an impulse load is applied and the responses calculated, after which a sinusoidal load is applied and the responses calculated. The aim is to use the impulse load and the responses due to the impulse load to construct a FRF and to use the FRF to reconstruct the sinusoidal load using the same methods as before. The performance of the reconstruction methods with artificial noise using different physical quantities (displacement, velocity and acceleration) will be considered and evaluated.

Once the impulse loads and responses are imported from the simulation, they are windowed using a force window and exponential window respectively, similar to what would be done in practical tests, after which the impulse force and the impulse responses are used to construct an FRF.

It has been observed that the resolution of the results from the Adams simulation is much more course than that of the data of the analytical model. This is due to numerical error and rounding performed by Adams when the results are saved. It is for this reason that a higher sampling rate was used for the Adams simulation.

The impulse and sinusoidal loads used in the Adams simulations are shown in the figure below:

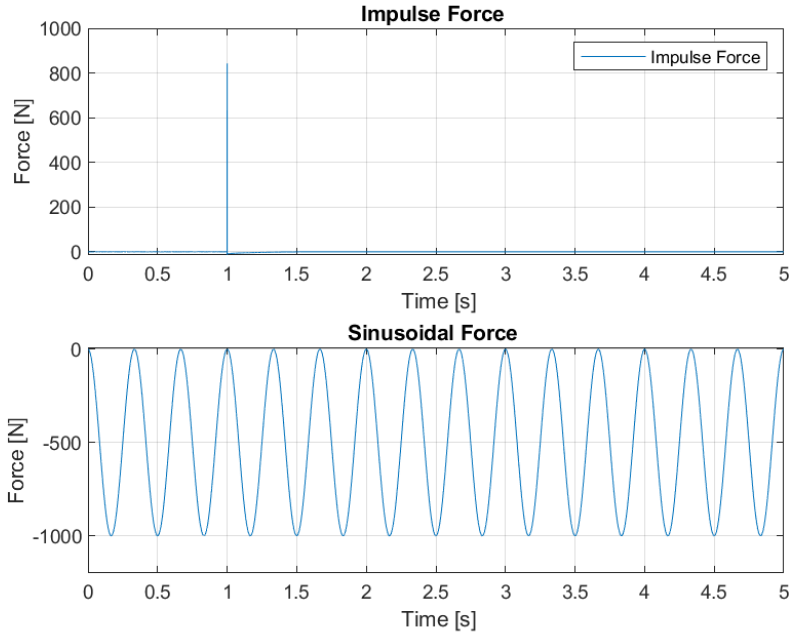

Figure 2.17 Adams Simulation Loads

The simulation responses to the impulse load are shown in the figure below:

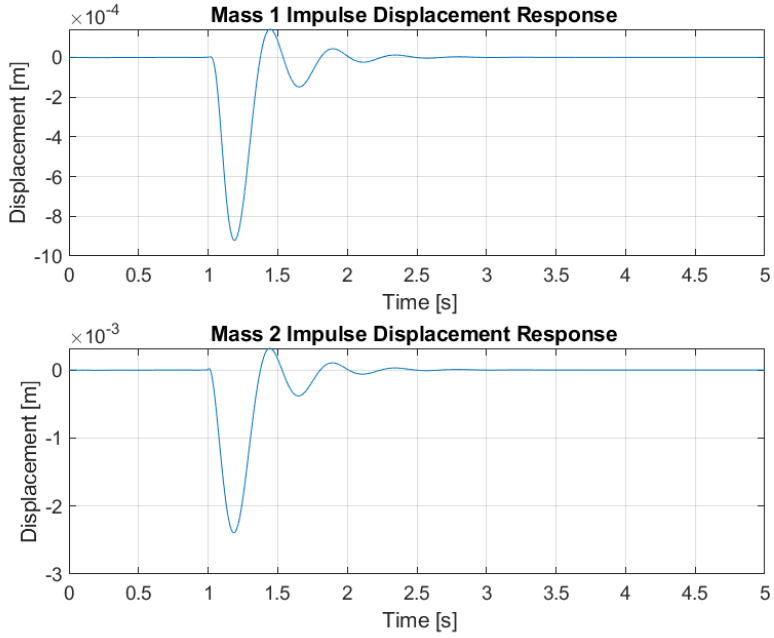

Figure 2.18 Adams Simulation Impulse Load Displacement Responses

The simulation responses to the sinusoidal load are shown in the figure below:

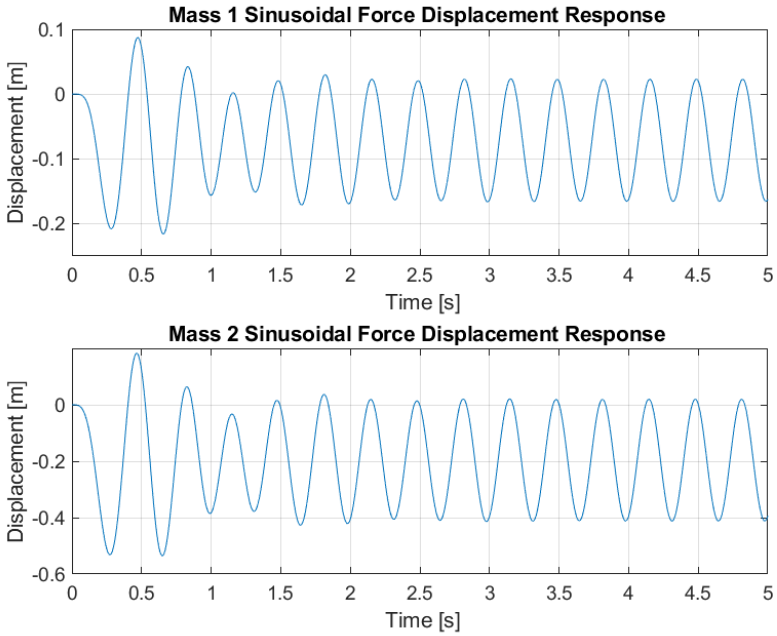

Figure 2.19 Adams Simulation Sinusoidal Load Displacement Responses

The FRF was estimated using the windowed impulse and responses and compared to the analytical FRF calculated in the previous section. The estimated FRF does correlate very well apart from some phase wrapping present above 44Hz. The resonant peak of the estimated FRF correlates very well with that of the analytical FRF except that the estimated FRF shows increased damping compared to the analytical FRF.

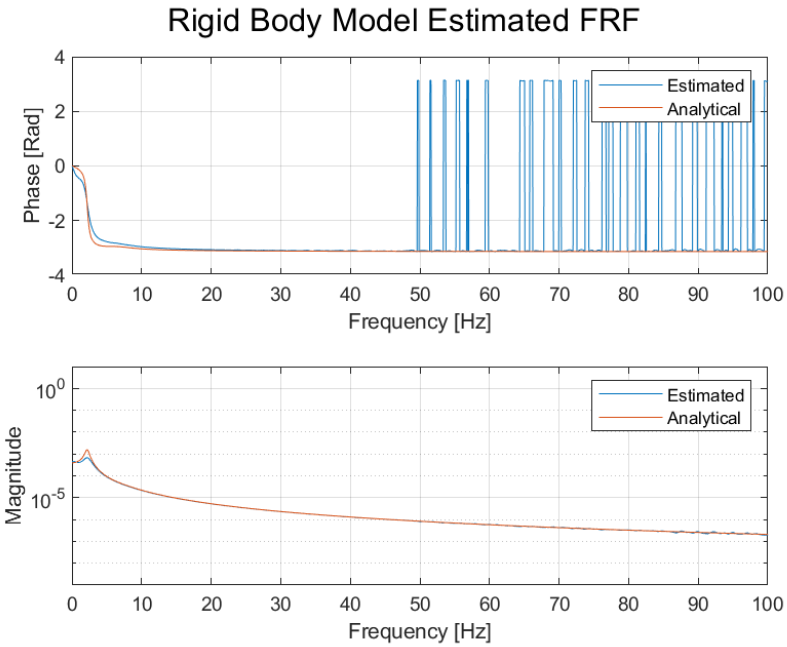

Figure 2.20 Adams Model Estimated FRF vs Analytical FRF

The estimated FRF is then used to perform the load reconstruction, using the same methods as before, starting with the Moore Penrose inverse. This method using the displacement response as the input had similar challenges in the reconstruction as what was seen with the analytical model. However additional windowing did not yield a successful result.

Scaling of the problem did not influence the Moore-Penrose method's ability to reconstruct the load. However, the Moore-Penrose method was able to reconstruct the load when the sampling rate is reduced to 500 Hz, although the quality of the reconstruction is worse compared to the other methods. The result of the reconstruction using the Moore-Penrose method at 500Hz sampling rate is shown in the figure below.

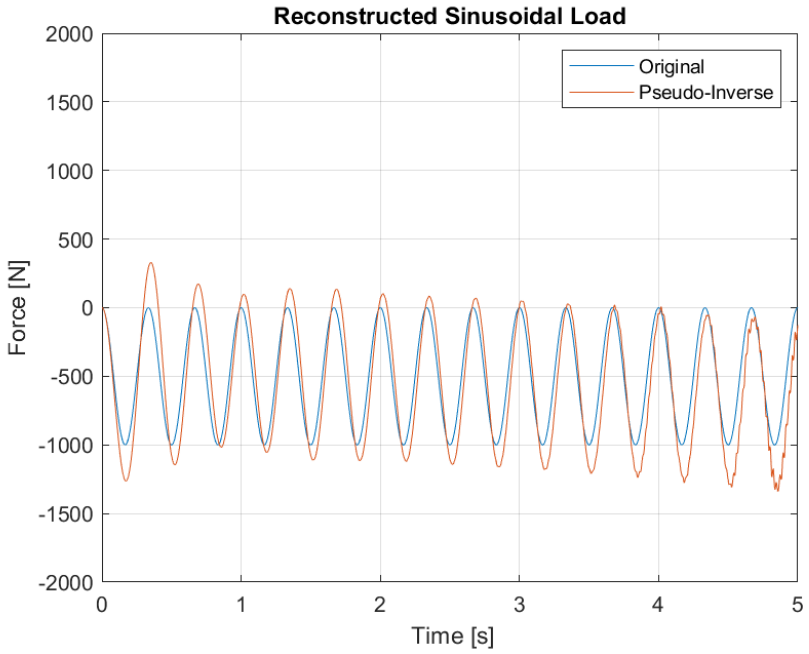

Figure 2.21 Adams Model Sinusoidal Load Reconstruction Using Moore-Penrose Method

The rounding performed by Adams reduces the resolution of the data, which creates discontinuities (steps) in the data. The discontinuities cause similar behaviour as what is experienced with measurement noise, which in turn is amplified at higher frequencies (Sanchez, 2022).

The least squares and Tikhonov methods yielded comparable results. The reason the least squares method is able to achieve a meaningful result is because it utilises a different method of matrix inversion and utilises the minimum norm solution, leading to a more meaningful result.

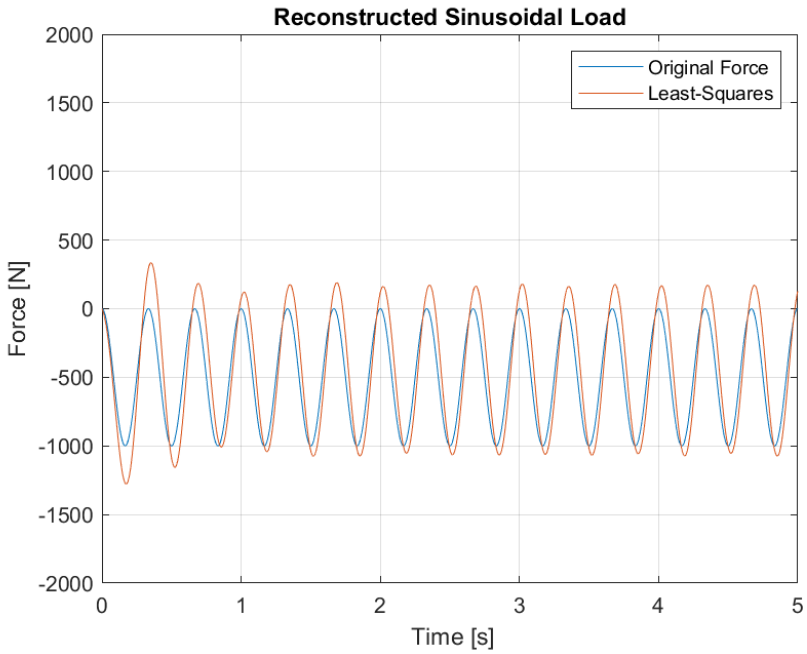

Figure 2.22 Adams Model Sinusoidal Load Reconstruction Using Least-Squares Method

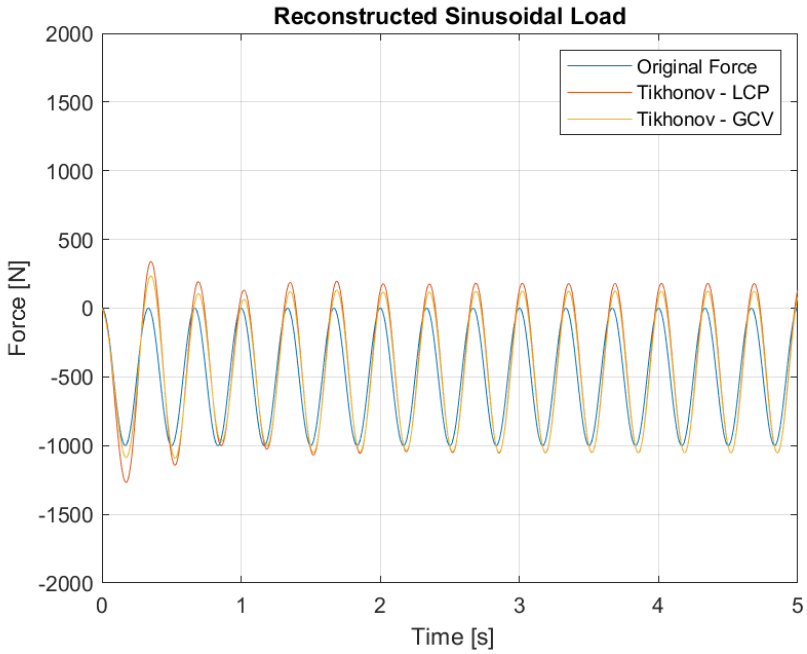

Figure 2.23 Adams model Sinusoidal Load reconstruction Using Tikhonov's method

It was found that velocity or acceleration response data yielded accurate results in the cases where using the displacement responses does not yield meaningful results. The figure below shows the result of load reconstruction using the Moore Penrose inverse method with velocity and acceleration responses as inputs.

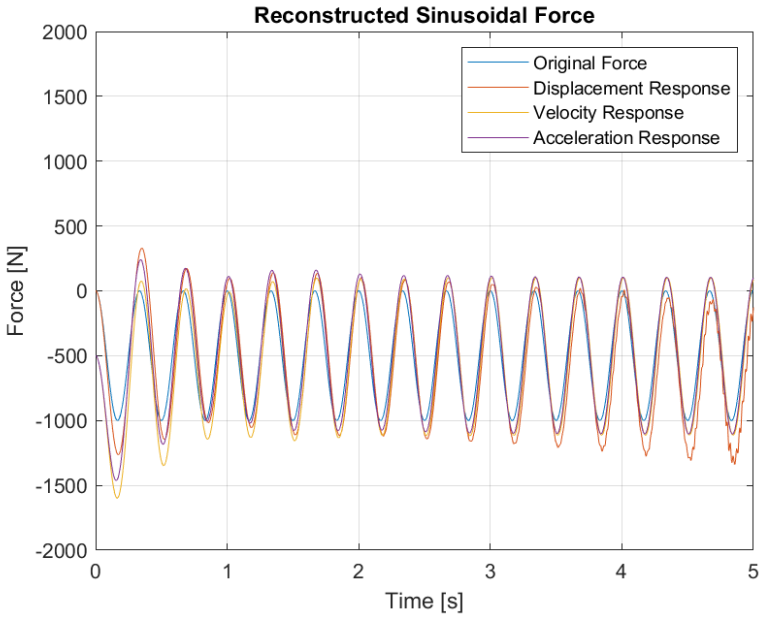

Figure 2.24 Adams Model Load Reconstruction Using Velocity and Acceleration

From the above figure it is noted that both the velocity and acceleration response data yielded accurate results. The reconstructed force using acceleration responses had a slightly higher quality result. All three responses show some deviation at the start of the signal, but the velocity and acceleration responses quickly reach steady conditions.

When the Tikhonov method is used to perform the load reconstruction, the results obtained using any of the physical responses all produce similarly accurate results, as shown below.

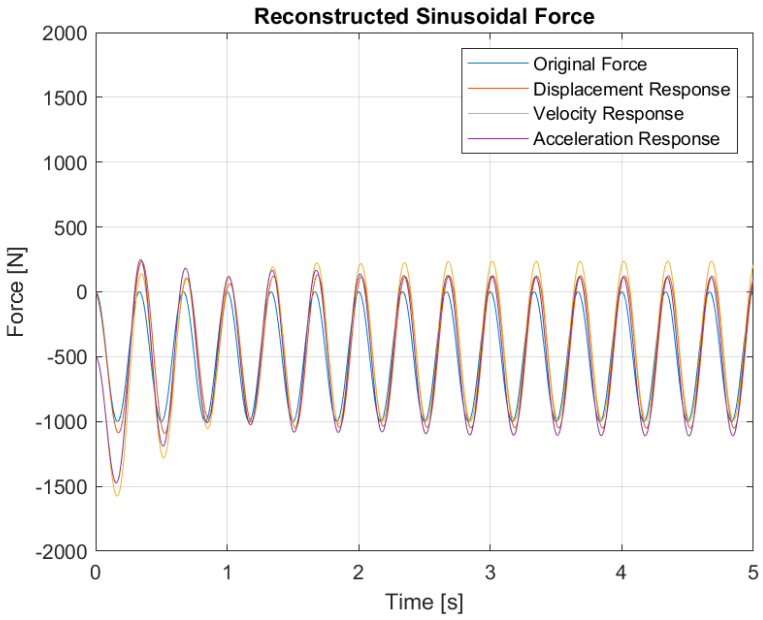

Figure 2.25 Adams Model Load Reconstruction Using Tikhonov Method

This section provided a brief overview of the work performed and the observations for the lumped mass model simulation model case where no noise or error is added to the responses, the results of the study on the effects of noise is discussed in section 4 of this document.

2.4. Simulated Elastic Model

In this section a basic cantilever beam is considered and will also be validated experimentally (discussed in section 3). A cantilever beam (one end fixed and the other free) is modelled using finite element analysis (FEA) with two load cases. The first is a simulated impulse load, simulating a hit with a modal hammer, and the second is a sinusoidal load applied to the beam.

The dimensions of the beam in the finite element model were selected to match those of a beam available for experimental validation. The beam has a free length of 920mm, a width of 40mm and a thickness of 10mm. A schematic representation of the beam is shown below:

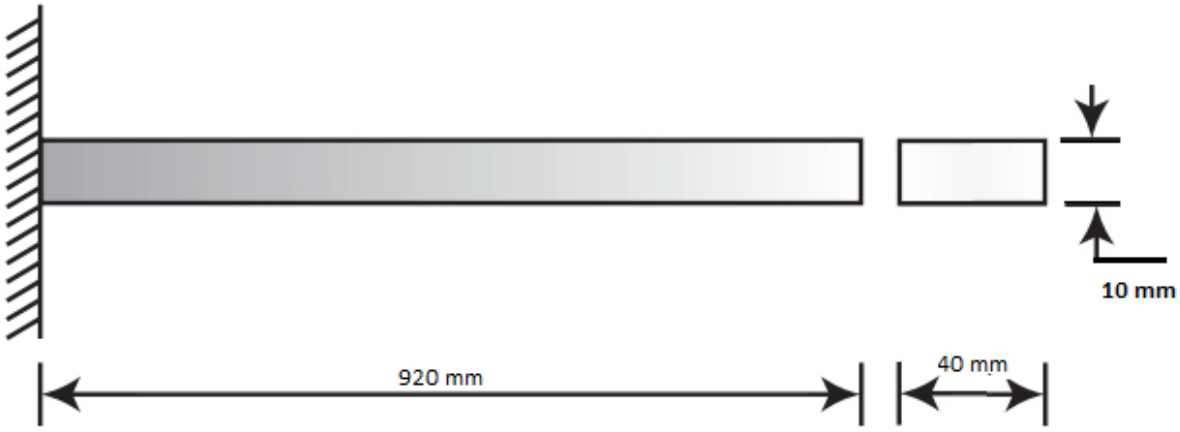

Figure 2.26 Diagram of the Elastic Beam Model

The finite element simulations of the model were performed using Ansys and the analysis type used is a transient analysis. The software package also has the functionality to perform a harmonic analysis from which an FRF can be determined. This calculated FRF will be used as a reference to determine the accuracy of the estimated FRF. The feasibility of using this software calculated FRF was also briefly investigated.

The finite element model is shown in the figure below. Point A on the figure represents the boundary condition and point B the location where the impulse force is applied. The location of the force was selected to match the location of the hammer hit in the experimental case as discussed in section 3 and the responses taken from the same locations as the accelerometer locations in the experimental case.

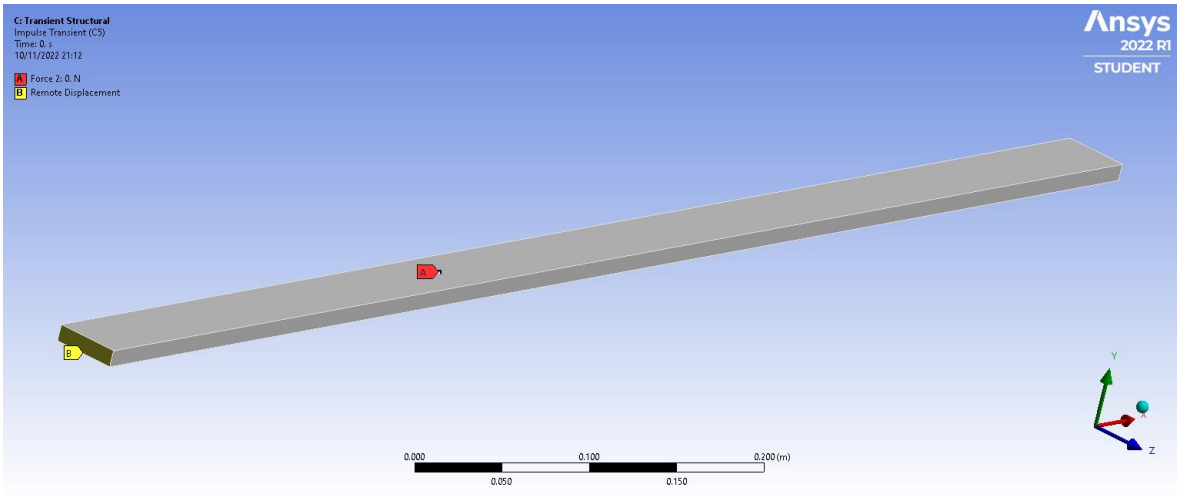

Figure 2.27 Finite Element Beam Model with Boundry Conditions

The simulations that were performed are transient simulations with a total duration of 10 seconds. The responses are extracted at intervals that equate to a 2.4kHz sampling rate. The mesh consisted of Hex elements and was refined such that there are two elements through the thickness, 8 across the width and 184 along the length of the beam (5mm element size).

The software can calculate either the undamped FRF or damping may be added by the user. For this analysis proportional viscous damping of 0.5% was assumed based on experimental data. The calculated FRF is shown below:

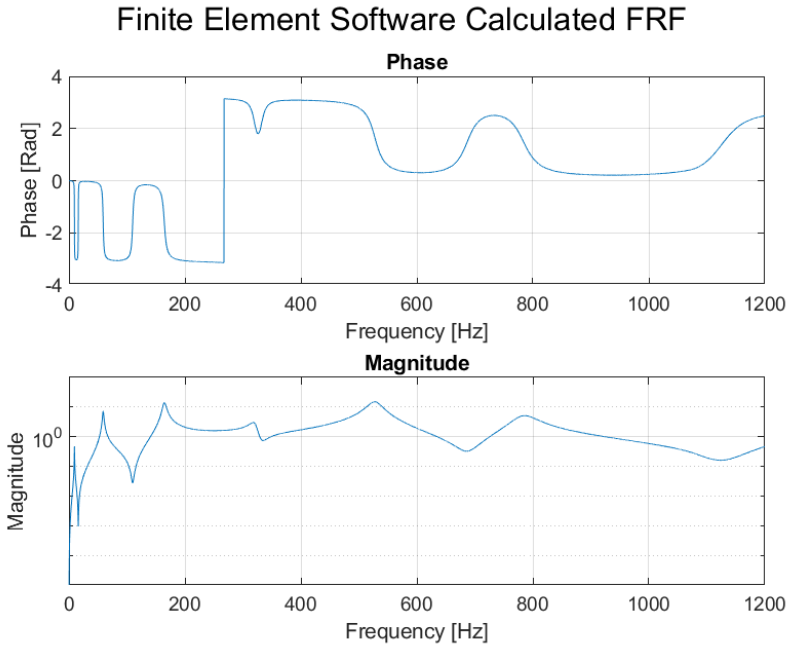

Figure 2.28 FRF Calculated by FEA Software

The modal test procedure is followed using an impulse to estimate the FRF using the impulse force and responses obtained from the FEA. The FRF is then used to reconstruct the applied sinusoidal load from the FEA responses. The estimated FRF is compared to the FRF calculated by the software.

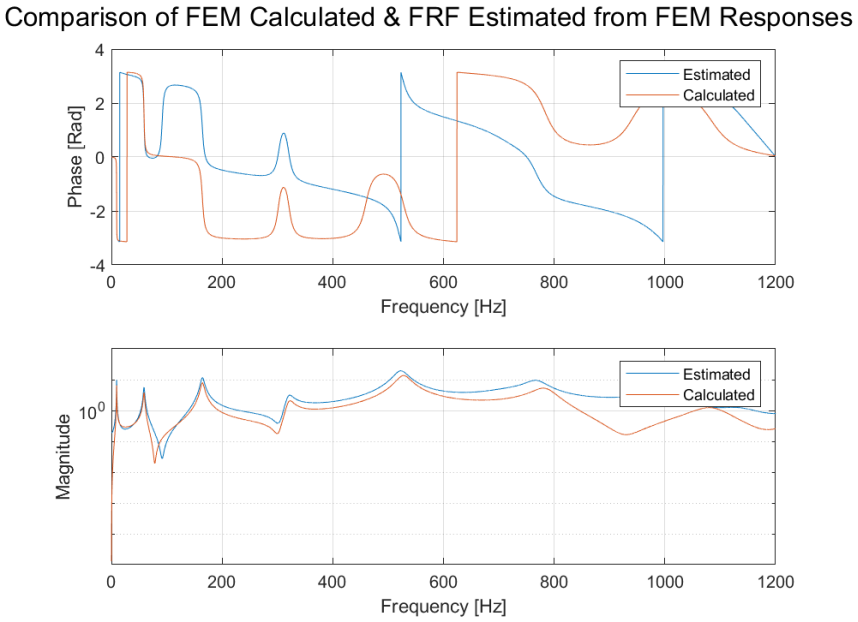

Figure 2.29 Estimated and Calculated Cantilever Beam FRFs

Good correlation is observed until approximately 800Hz, however at higher frequencies the estimated FRF deviates from the calculated FRF. Slightly higher damping is observed in the FRF estimated from the responses, this can be improved through mesh refinement and refinement of the damping parameters in the model. To achieve good correlation between the calculated and estimated FRFs, the finite element model should be setup as accurately as possible, assumptions regarding material properties and boundary conditions have a large effect on the accuracy of both the calculated and estimated FRFs.

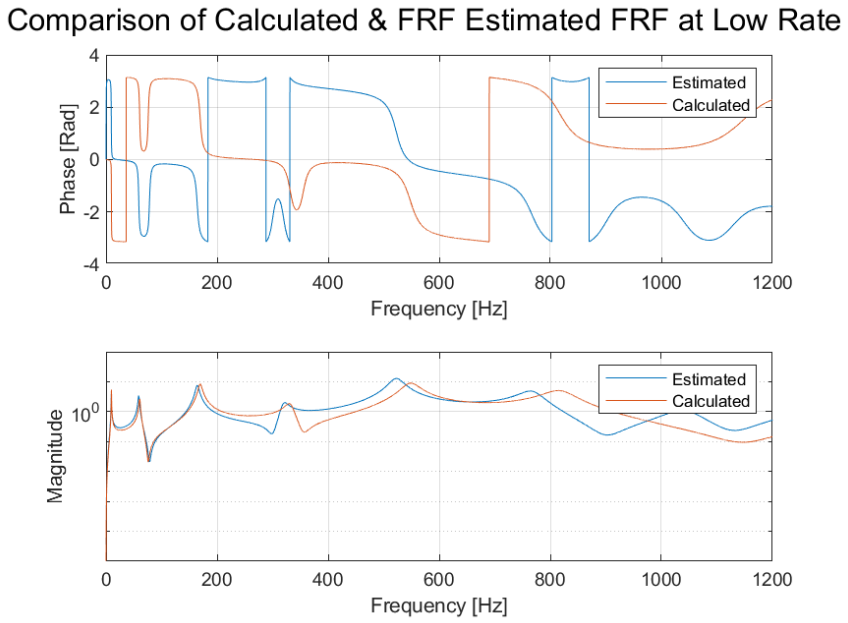

Figure 2.30 FRF Estimated from Low Sampling Rate

The sampling frequency in the transient analysis needs to be set very fine, at least 5 times the maximum frequency of interest. If the frequency of the transient analysis is set too low, the locations of the natural frequencies are not captured correctly. Figure 2.30 above illustrates this point, in the case shown the frequency was set at only double the band of interest, notice that only the first two natural frequencies are estimated correctly.

This indicates that it is possible to utilise finite element software to calculate the FRF of a structure, however very accurate modelling and model information is required to achieve an accurate FRF. Load reconstruction using the software calculated FRF was found to be possible and yielded meaningful results. Making use of the FRF calculated by the finite element software is also less computationally expensive compared to making use of a transient simulation to simulate a modal test.

Load reconstruction of the applied sinusoidal load (initially in the absence of noise) was done using the five methods selected for this study. The Moore Penrose inverse method did yield an acceptable result. The SVD method did not yield any meaningful results. Tikhonov's method using both the L-curve and GCV parameter regularisation methods did produce fairly accurate results. However the least squares method did not yield a very accurate result as shown below:

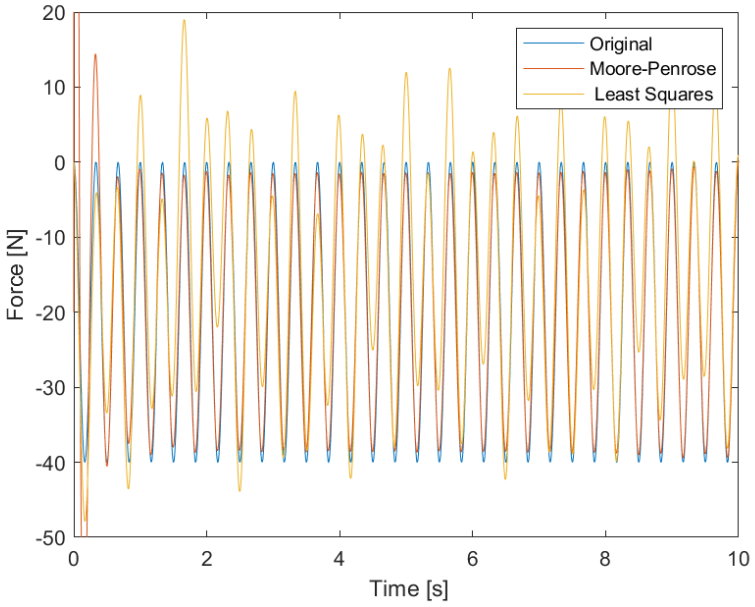

Figure 2.31 Pseudo Inverse Method Result of the Elastic Beam Model

With good reconstructions achieved in the ideal case, the data is then used to evaluate the effects of measurement error and noise on the reconstruction, the results of which are discussed in section 4.

Up until this point all the test cases made use of ideal cases and loads during the reconstructions and did not consider practical situations. In the following section an experimental model of the same cantilever beam is considered.

3. Experimental Work

The cantilever beam case discussed in section 2.4 was replicated experimentally to validate the finite element model as well as to test the methods in a simple real-world case. The experimental setup consisted of a steel beam with a free length of 920mm (40mm wide and 10mm thick) with four accelerometers mounted in various positions throughout the length of the beam, as shown below.

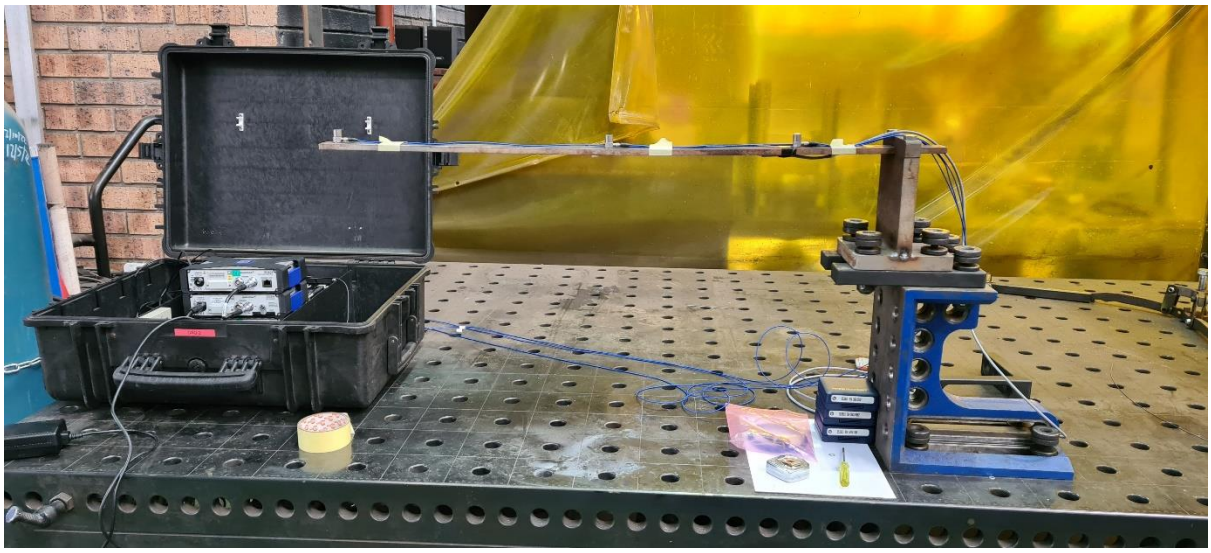

Figure 3.1 Experimental Cantilever Beam Setup

The beam itself was clamped by a rigid steel clamp, which in turn was rigidly attached to the bench. Isolating rubber material was placed between the clamp and the riser blocks to reduce the effects of vibrations from the surroundings.

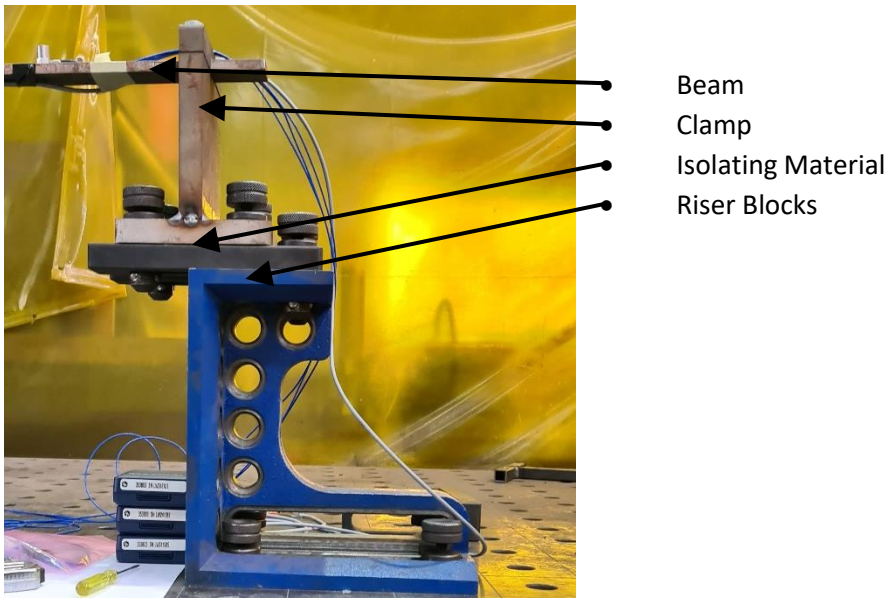

Figure 3.2 Experimental Setup Components

The instrumentation used during the experiments are listed in the table below:

Table 3.1 Instrumentation Used During Experimentation

No	Description	Manufacturer	Model	Installation Position
1	Accelerometer	PCB	3713B1150G	145 mm
2	Accelerometer	PCB	3713B1150G	445 mm
3	Accelerometer	PCB	3713B1150G	895 mm
4	Modal Hammer	Meggit	Endevco 2302-5	N/A
5	Modal Shaker	Modalshop	K2007E01	230 mm
6	Data Logger	HBM	QuantumX MX840B QuantumX CX22BW	N/A

The data was recorded at a sampling rate of 2400Hz with a 1 second pre trigger and a 10 second recording time. This means that once the force exceeded a predefined value the system would start recording including 1 second before the change in force was detected, resulting in a total recording time of 11 seconds. Only an anti-aliasing filter was used during the recording of the data and all further processing was done using Matlab after recording.

The first test conducted was a modal test. Various combinations of hit locations and hammer tips were tested to achieve the best quality FRF possible. The modal hammer was used with a medium hardness tip and the beam was struck approximately one third of its length from the fixed side. It was found that this combination yielded the best results in terms of estimating the FRF. Once the beam was struck with the modal hammer the beam was left to vibrate until the data recording was completed. This was repeated several times to achieve an accurate estimation of the FRF. The impulse force was windowed using a force window and the responses were windowed using an exponential window.

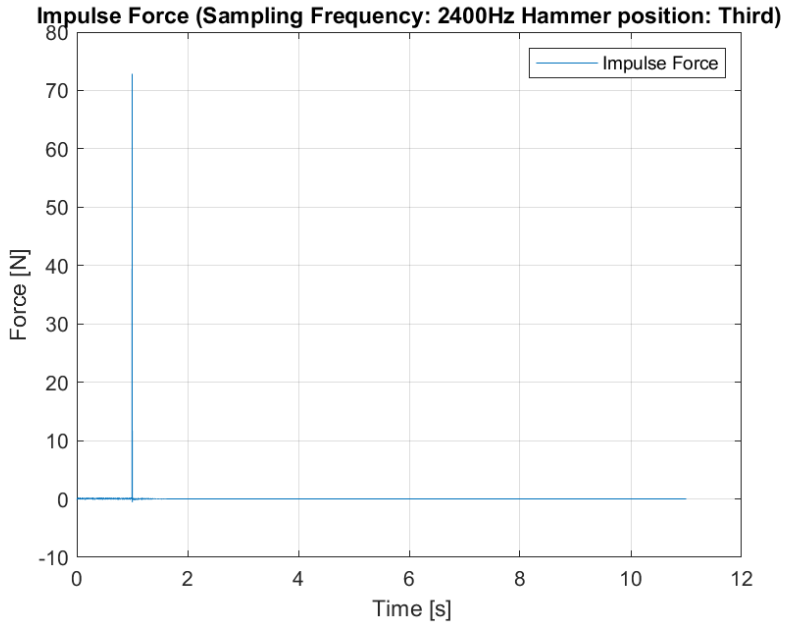

Figure 3.3 Experimental Modal Hammer Impact Force

The figure below shows the windowed acceleration responses to the impulse from the hammer hit shown in the previous figure.

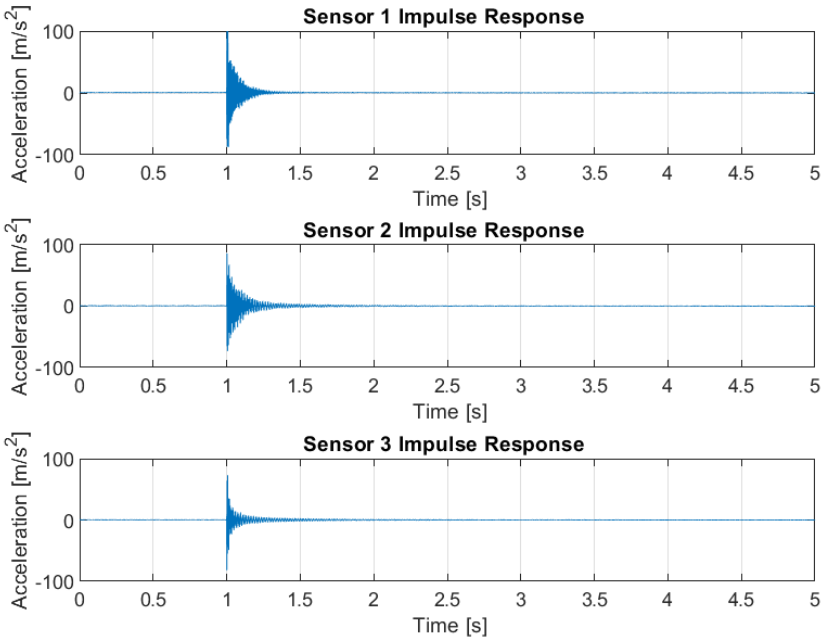

Figure 3.4 Experimental Modal Hammer Responses

Once the modal hammer testing was completed, the modal shaker along with a loadcell was installed on the beam to apply various loads to the beam. The aim was to use the responses due to the loads from the shaker to reconstruct the shaker loads. The modal shaker was rigidly mounted to the bench and connected to the beam by means of a thin steel rod (stringer). The shaker was controlled by a handheld signal generator. The figure below shows the initial transient response of a 15Hz sinusoidal force applied to the beam by the modal shaker, until it reaches steady conditions.

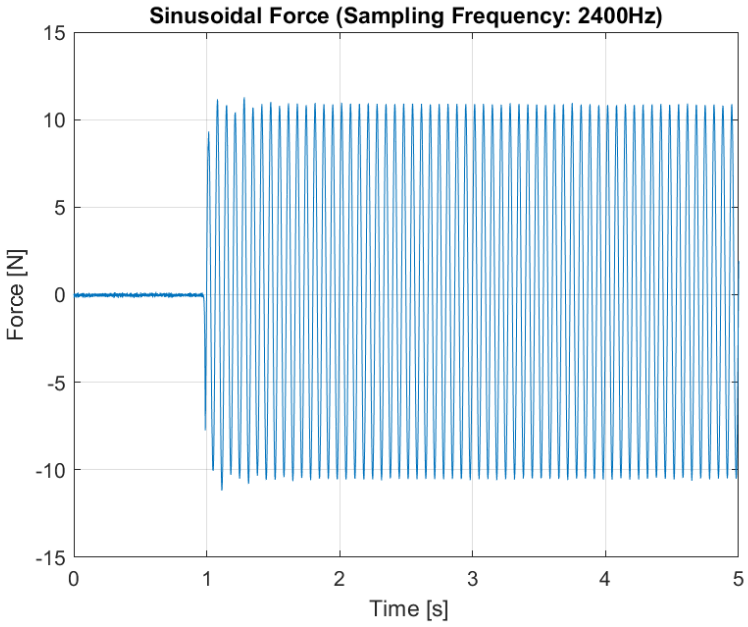

Figure 3.5 Experimental 15Hz Sinusoidal Force

Two approaches were used to obtain a FRF for the purpose of load reconstruction. The first was the same method used during the mathematical cases, estimating the FRF from the impulse and response data using Welch's averaged, modified periodogram method as discussed in section 2.1. Secondly FRF reconstruction methods were used to investigate if a better quality FRF could be obtained.

The FRF reconstruction was performed using Matlab and the ModalTools™ add-on toolbox which provides a number of methods with which the FRF can be reconstructed. The method that was found to yield the best results is the complex exponential method.

The complex exponential method estimates the poles in radians from the time domain impulse response. The poles are then used to estimate the residuals and residues, these parameters are then used to construct the FRF. Curve fitting is performed using the poles, calculated residues and residuals to reconstruct the FRF. The figure below shows the estimated and reconstructed FRF.

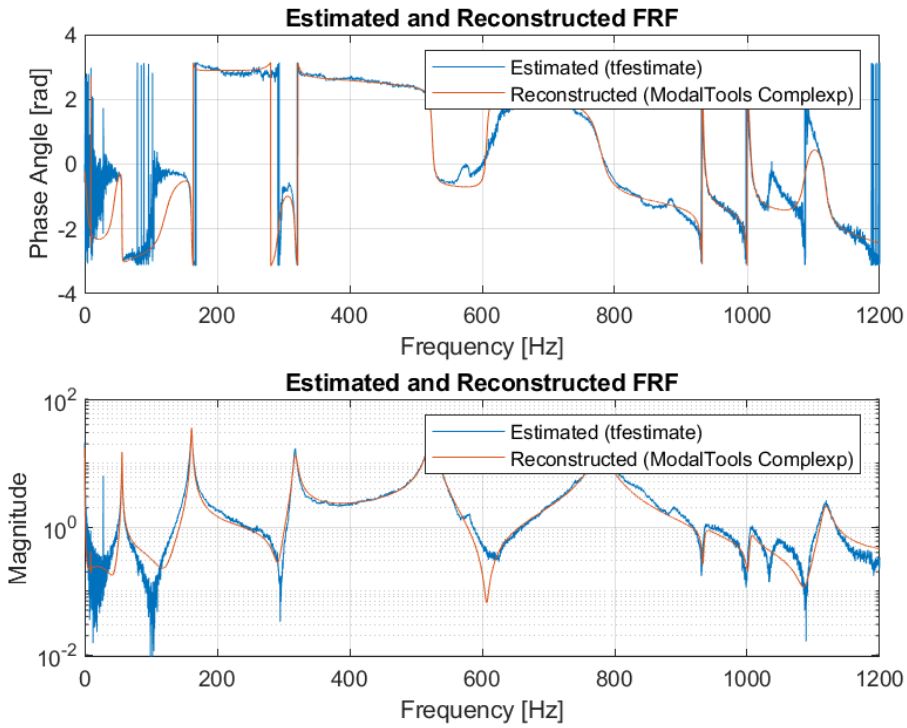

Figure 3.6 Estimated and Reconstructed FRF from experimental data

As seen in the figure above the two FRFs correlate very well, with the reconstructed FRF being significantly smoother than the estimated FRF with more clearly defined peaks and valleys.

Both the estimated and reconstructed FRFs were successfully used to reconstruct the loads applied to the beam by the modal shaker, the results of both as well as their sensitivity to noise and measurement error, are discussed in the following section.

4. Results

This section provides a summary and a discussion of all the results obtained by running each of the models through the test cases described in Table 2.1. The discussion includes a comparison of the performance of each of the models with noise in the response signals.

In each model the reconstructed loads for each error case are compared to the base line result (reconstruction without any artificial error/noise) as well as the applied (known) loads. The baseline cases are compared to the applied loads for the purpose of determining accuracy and each subsequent error case is then compared to the baseline case to determine the effect of the error or noise. Three parameters are considered when determining accuracy, RMS (root mean square), mean and amplitudes of the signals. Accuracy is calculated as a percentage deviation from the baseline value, as shown below:

$$Accuracy = \left(1 - \left|\frac{F_{noise} - F_{baseline}}{F_{baseline}}\right|\right) \times 100\% \quad (4.1)$$

in the equation above F is the RMS or the amplitude of the reconstructed noise and baseline forces.

In this section the results of the comparisons will be presented graphically with the numerical values of the achieved accuracies of each test case for all the models provided in Appendix B of this document.

The comparison of the reconstruction methods for the no noise (base line) case, as shown in Figure 4.1, showed that the Tikhonov method and the least squares method performed the best, with an average accuracy of 94.7% (GCV), 95.2% (L-Curve) and 91.8% respectively across the different test models. Singular value decomposition was the worst performing method with an average accuracy of 42.4%. The figure below graphically summarises the obtained accuracies of the different methods across all the models.

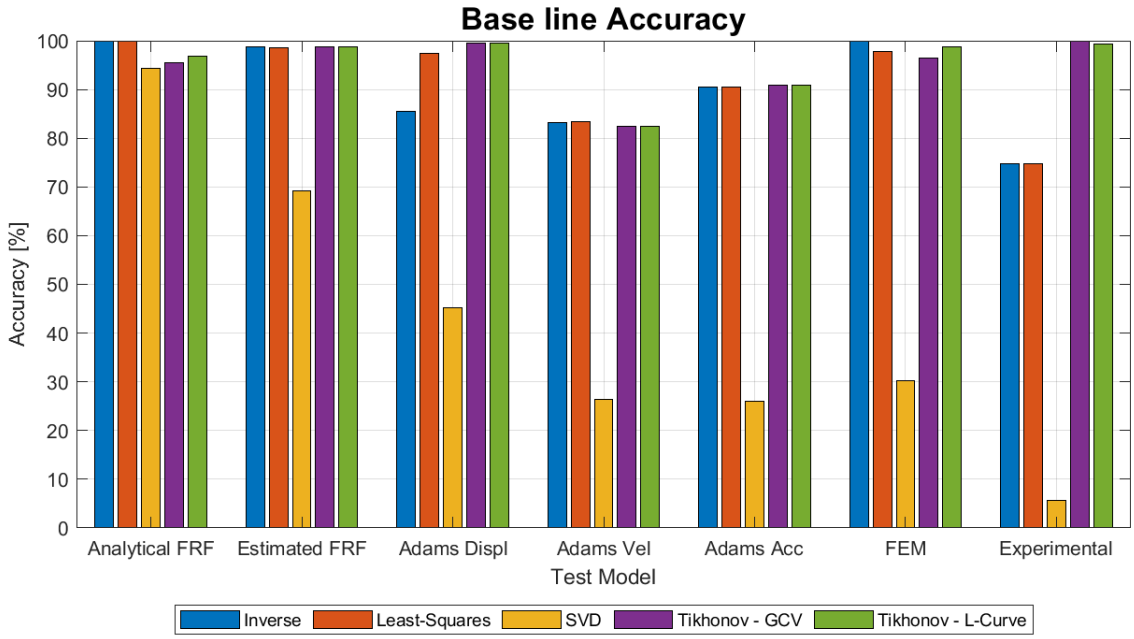

Figure 4.1 Summary of No-Noise (base line) Case Results

The inverse was only able to achieve 100% accuracy in the analytical case, which is expected since the FRF is calculated analytically. The pseudo-inverse method was able to achieve fair accuracies in the simulation models but not in the experimental case, because the experimental case does contain some noise in the responses which reduces the accuracy of the reconstruction (Jia, Yang, Guo, & Wang, 2015).

The SVD method performed the worst with the Adams and experimental models, this can be due to the low number of degrees of freedom resulting in a zero FRF matrix (Uhl, 2007) and noise in the experimental model. It is worth noting that the SVD method was not successful in performing the reconstruction even with the condition number of the FRF being low. Adjustment of the SVD threshold value (point where small values are set to zero) can improve the result but can become an iterative and time-consuming process. In the two degree of freedom cases (or cases were only a small number of responses are considered) the SVD method does not perform well due to too much information being lost in the truncation of the singular values because the SVD is a subtractive regularisation method (Sanchez, 2022).

The least squares method overall performed well, but also showed a reduction in accuracy in the experimental model which may also be attributed to the presence of noise in the experimental responses. Despite the reduction in accuracy in the experimental model overall the least squares method had the one of the best average accuracies across the different models and had the quickest calculation times.

In most cases the GCV and L-Curve parameter optimisation methods used in the Tikhonov method yielded similar results, with the L-Curve method performing slightly better in some cases. Similar to what was observed by Chen et al. (2021), it was observed that the L-Curve method is not very sensitive to increasing noise levels. The GCV method takes considerably more time to solve compared to the L-Curve method in the models considered. When comparing the solving times of the methods considered, all of the methods have longer solving times compared to the inverse method as shown below:

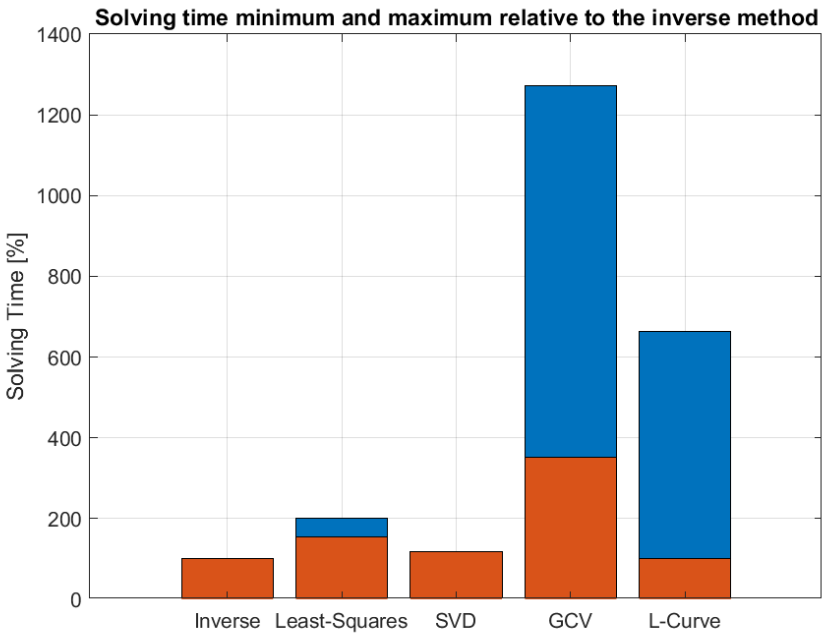

Figure 4.2 Comparison of Minimum and Maximum Computation Times

From the figure above it can be seen that the inverse method and SVD method have similar computational times and the other three methods all have longer times from 200% for the least-squares method up to 1200% in the case of the GCV method. The Tikhonov method on its own can also be fast, but the parameter optimisation methods can significantly increase computational time. The GCV parameter optimisation was found to increase the computational time significantly compared to the L-Curve parameter optimisation method, especially when wide frequency bands were used.

4.1. Systematic Errors

Two types of systematic error were considered, offset error and scaling error. Offset errors appear to have little impact on the amplitude and relative mean value of the reconstructed loads when using the analytical FRF with any of the methods, except for the inverse and SVD methods where a decrease in the amplitude accuracy is observed. The reconstructed load is offset roughly by the same amount compared to the initial response offset. Similar results were obtained when the estimated FRF was used with the analytical models. However, as the complexity of the model increases the accuracy of the reconstruction, due to offset errors, decreases.

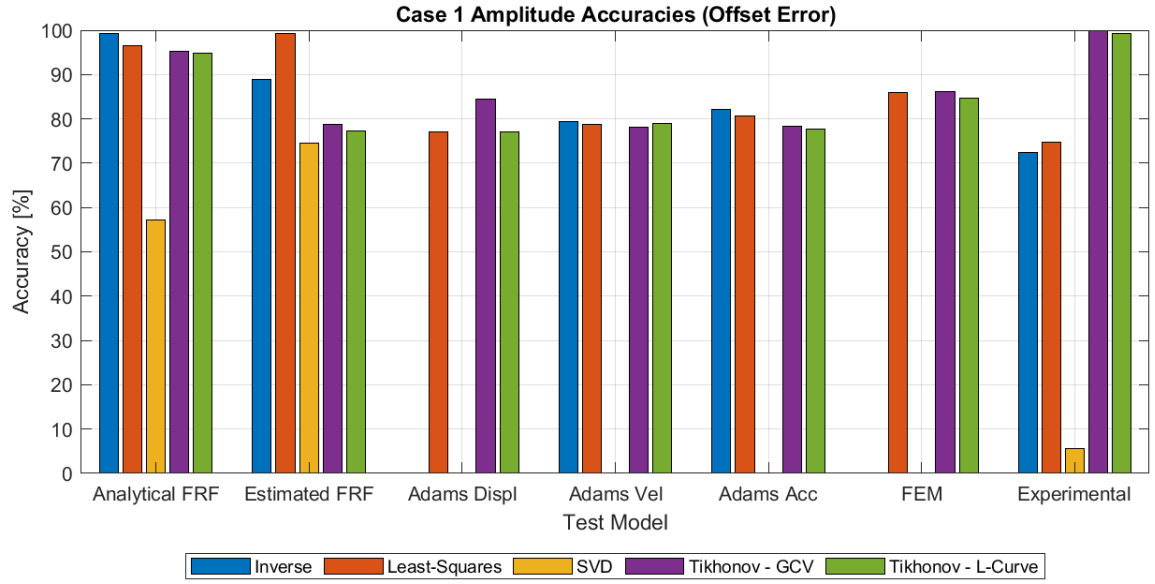

Figure 4.3 Case 1: Summary of Offset Error Results

From the figure above a slight reduction in amplitude accuracy is observed in the rigid body (MSC Adams) simulation model when using displacement responses, however the mean offset error increases when using velocity or acceleration responses. The same behaviour was observed in the finite element model case. In the experimental case, similar behaviour to that of the analytical case was observed even though acceleration responses were used.

The SVD reconstruction was affected more than the other methods, as the amplitude decreased significantly (approximately 40% compared to the base line case) and the mean offset was nearly doubled. In the two simulation cases the SVD method was entirely unable to reconstruct the applied

loads and in the experimental case the accuracy was found to be very low, around 5%. This is due to many of the values in the FRF matrices in these cases being very small values (approaching zero).

Scaling errors showed a consistent reduction in the relative accuracy of the result in all of the test cases. As expected, scaling of the response data yielded a similar effect on the resulting reconstruction. The relationship between the induced scaling error and resulting reconstructed forces appeared linear, which was expected since all the models considered in the study can be considered as linear. The SVD method showed reduced accuracy compared to the other methods and in many cases failed completely to reconstruct the load.

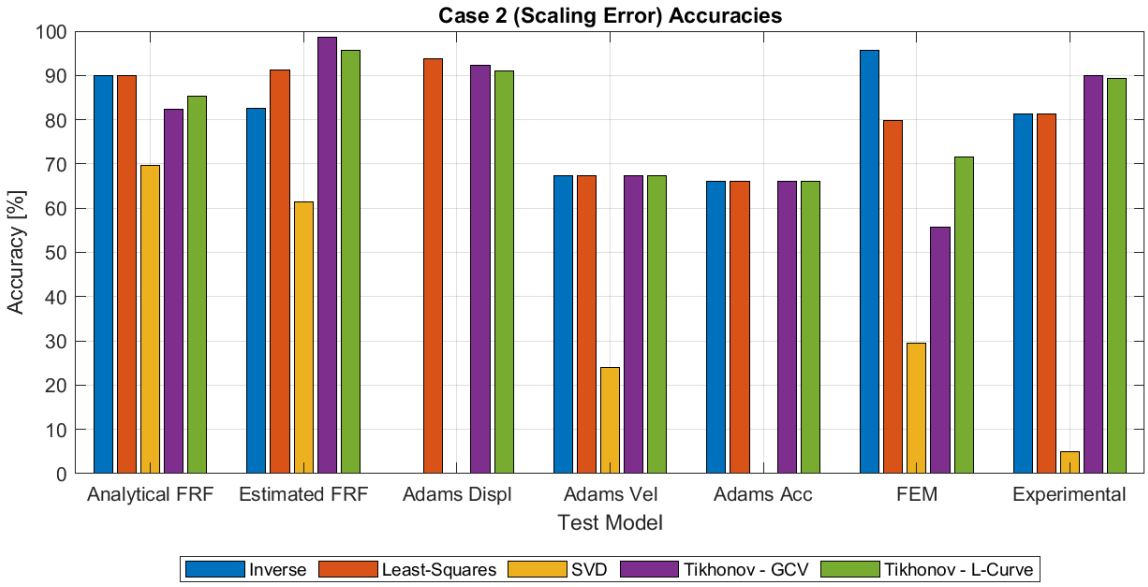

Figure 4.4 Summary of Scaling Error Results

In most cases there were no clear signs in the reconstructed loads that the responses used in the reconstruction were scaled and as shown in Figure 4.4, accuracies of above 90% were obtained. In many of the offset cases, unexpected results were obtained (such as discontinuities and sudden changes in mean value) that could indicate the presence of an error, assuming that at least the form of the signal is known beforehand. If the applied force is of a random nature, offset errors are hard to detect without prior knowledge of at least the range of the applied force.

4.2. Stochastic Errors

The second error type considered in this study is stochastic error or random noise in the signals. As previously discussed, the assumption was made that the FRF was obtained in ideal conditions and for the purpose of this study only the “unknown” responses were subject to noise. The noise that was added to the response signal was generated using random values based on a normal distribution. In all the cases the calculations were repeated multiple times and the averaged results across the multiple runs are provided and discussed.

The inverse FRF matrix is close to singular with very small values in many of the cases and combined with small response values, can result in an even smaller force vector in the frequency domain. The

result becomes very sensitive to any slight change in the response data which results in very large values (and abrupt changes in the force direction) when the force vector was transformed to the time domain (Oosterhuis, Eidhof, van der Hoogt, & de Boer, 2006). This behaviour was observed especially when using the pseudo-inverse and SVD methods.

Another contributing factor is the number of responses considered which was equal to the number of degrees of freedom (Hundhausen, et al. 2007). A lot of information is lost when the singular values are reduced to zero. Models where either more responses were considered or other responses such as velocity were considered, performed slightly better.

When the estimated FRF was used, the pseudo-inverse method was not able to reconstruct any of the loads where additional noise is introduced into the responses. This is also due to the response degrees of freedom that are equal to the input degrees of freedom (Hundhausen et al. 2007). In certain models with more degrees of freedom, the pseudo-inverse method was able to produce results however the accuracy was not very high compared to the other methods used.

The least squares and Tikhonov methods were both able to reconstruct the load at all of the noise levels considered. Overall, the Tikhonov method combined with L-Curve parameter optimisation, was the most accurate method in the simulation and experimental models and the least squares was the most accurate in the numerical models (with the estimated FRF). The GCV and L-Curve parameter optimisation methods yielded very similar results and as was the case in the base line results, the GCV method's solving time was again noticeably longer than that of the L-Curve method.

The least squares method was able to produce the most consistent relative accuracy with increasing signal to noise ratio. The Tikhonov method also performed well but showed an abrupt reduction in relative accuracy at 10% noise and above in certain cases.

Increased distortion of the reconstructed force signal was however observed in all the results. The results obtained by Tikhonov's method showed less distortion compared to the other successful methods but also showed severe distortion at high noise levels. Filtering of the reconstructed load signals was found to reduce the distortion, but filtering has the risk of losing information in cases where the force signal is a random signal. In certain cases, the addition of noise improved the accuracy of the result compared to the base line case. This improved accuracy may be attributed to improved conditioning of the FRF by the addition of noise in regions far from the resonances (Allen & Carne, 2008). In particular the Tikhonov method was observed to reconstruct a load with the same amplitude and mean values of the original force. However, the frequency content of the reconstructed force was found to be significantly different to that of the original force in some instances, primarily due to the random nature of the noise.

The relative changes in accuracy of the reconstruction versus the level of noise for both the analytical FRF and estimated FRF of the 2-degree of freedom model are shown in the figures below.

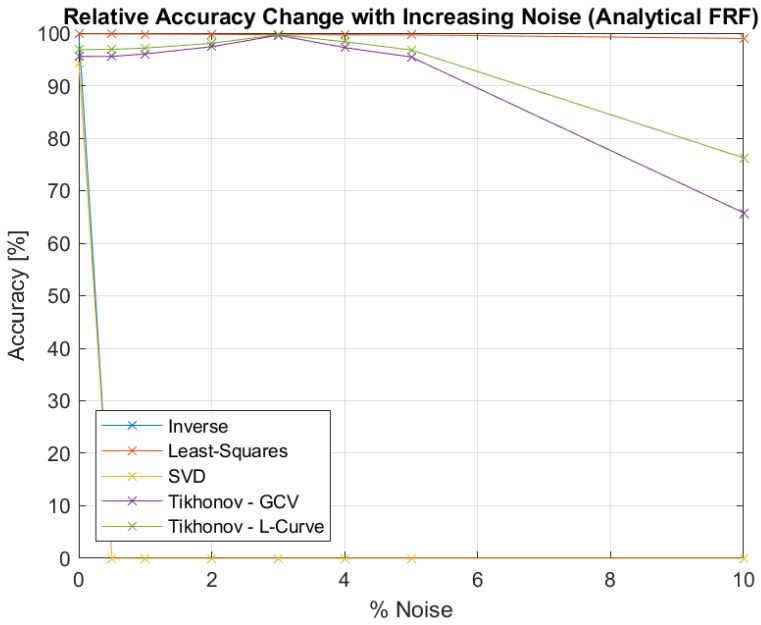

Figure 4.5 Accuracies of Reconstructions using Analytical FRF

When the analytical FRF was used, both the inverse and SVD methods failed to reconstruct the load over the entire range of noise levels, the analytically calculated FRF was found to be very sensitive to the additional noise, the slightest addition of noise caused the inverse and SVD methods to fail when using the analytically calculated FRF. In certain higher degree of freedom models these two methods were able to produce results but with very low accuracy. In the 3 and 4 degree of freedom models these methods were only able to reconstruct the load in the no noise case and in the case of the 7 degrees of freedom model the SVD method had slightly more success until 1% noise at which point the accuracy declined drastically. The accuracy of the least-squares and Tikhonov methods remained reasonably constant as the noise increased. Only at the higher noise levels did the Tikhonov method's accuracy decline.

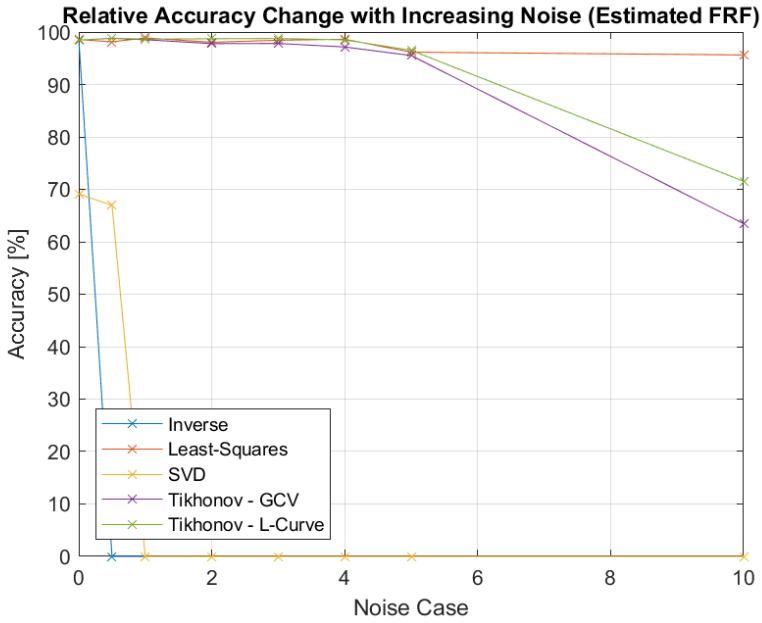

Figure 4.6 Accuracies of Reconstructions using Estimated FRF

When the estimated FRF was used, larger deviations in the accuracies were observed as soon as noise was introduced into the responses. The inverse method was still not able to produce a result at all, apart from the baseline result and a very slight improvement was observed when the SVD method was used. The SVD method was only able to produce a result in the 2 degree of freedom model with a noise level of 0.5% and was able to produce results with an average accuracy of 63% in the 3 degree of freedom analytical model (described in appendix A), but failed entirely again with the higher degree of freedom models.

The least squares method maintained the highest accuracy throughout all the noise cases with the analytical FRF and experienced a slight reduction in accuracy across the range of noise cases compared to the analytical FRF. When the estimated FRF was used in the numerical models, the Least-squares method was the best performing method with more than 95% accuracy across all the noise cases. The Tikhonov methods also performed very well with similar results to the Least-Squares method except that both Tikhonov methods did show a reduction in accuracy from noise levels of 10%.

In the rigid body simulation case, the pseudo-inverse method was only able to reconstruct the loads across all the noise cases when acceleration responses were used and the SVD method was not at all successful when the displacement response was used. The SVD method was able to produce results when velocity or acceleration responses were used (with the appropriate FRF), however the accuracy of these results was low. The accuracy of the SVD was much lower compared to the other methods considered, but less noise was present in the reconstructed load compared to the other methods. The inverse and SVD methods' results are therefore not included in the results shown in the figures below, unless at least a partial result was obtained. The figures that follow show the accuracies achieved in the lumped mass simulation case, using displacement, velocity and acceleration responses to reconstruct the same load.

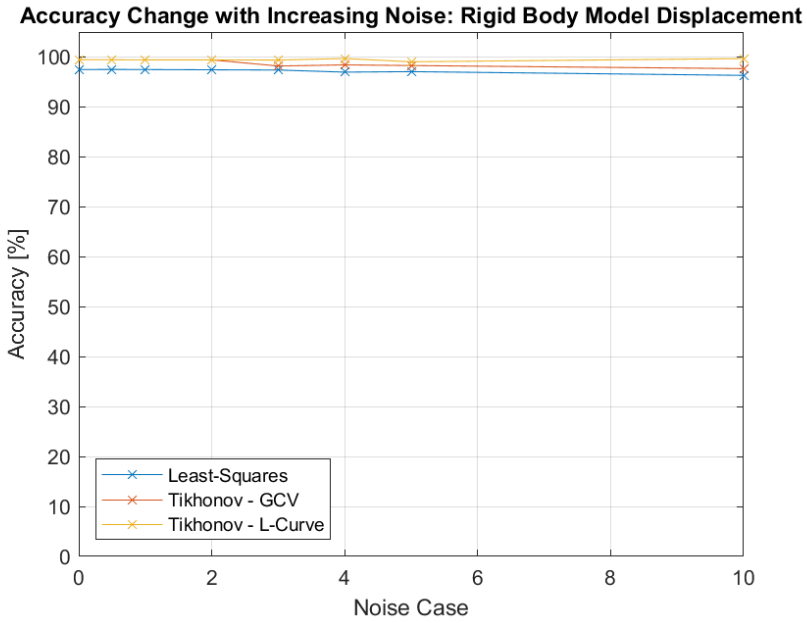

Figure 4.7 Rigid Body Model Results using Displacement Response

The other methods were able to reconstruct the loads regardless of the response type. From the above figure it is observed that the Tikhonov method was the most accurate, but the difference in accuracy between the three methods is quite small.

A slight overall reduction in accuracy was observed when the velocity response was used, compared to when the displacement response was used, as shown in Figure 4.8 below. As mentioned, the inverse method was partially successful in reconstructing the applied load but failed to reconstruct the load from 3% noise and above. The Tikhonov method still yielded the highest accuracy by a small margin and both the Tikhonov and Least-squares methods showed a noticeable reduction in accuracy at 10% noise.

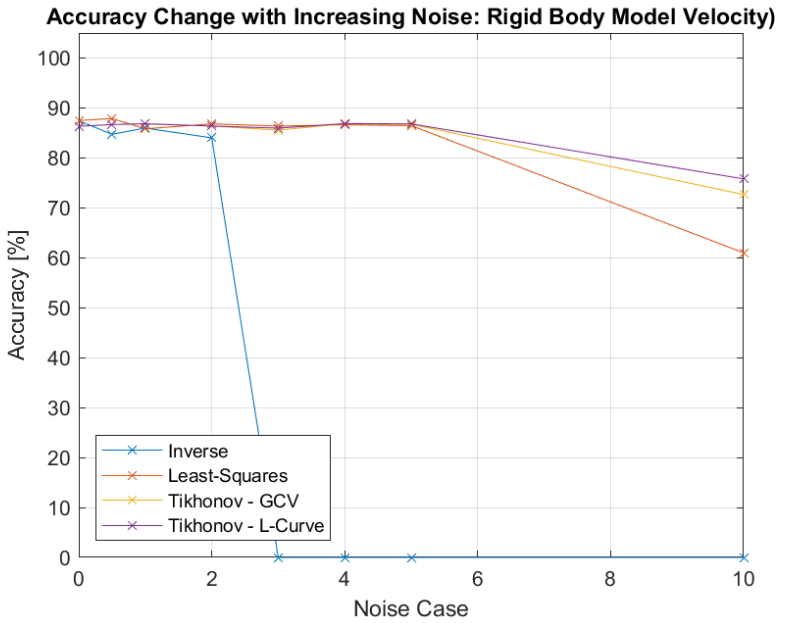

Figure 4.8 Rigid Body Model Results using Velocity Response

The figure below shows the results obtained when the acceleration response was used:

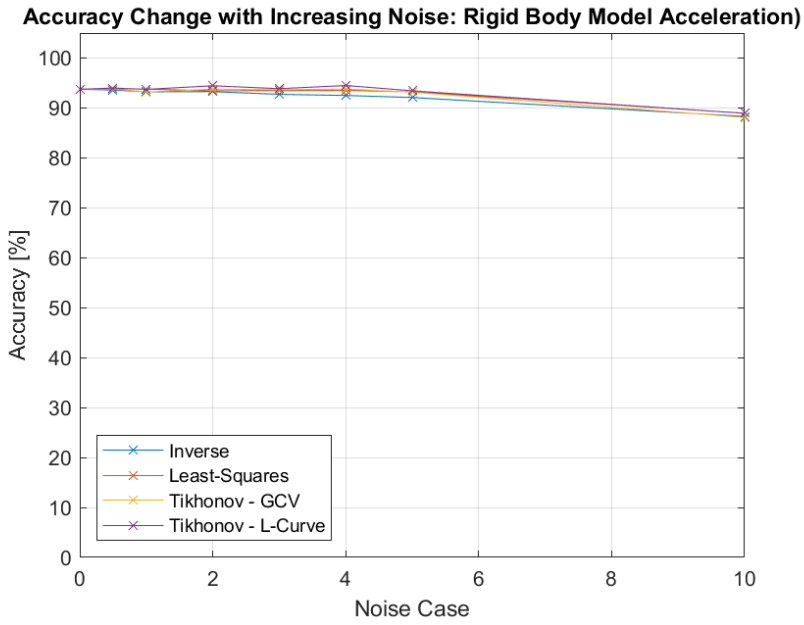

Figure 4.9 Rigid Body Model Results using Acceleration Response

Compared to the results obtained by using the velocity response the accuracy of the results from the acceleration response is higher, but still lower than the results obtained from the displacement response. Apart from the SVD method all the methods were able to reconstruct the load across the noise range with very similar results. The reduction in accuracy at 10% noise is less than what was seen in the velocity response for all the methods and the Tikhonov L-Curve method was the best performing method. The least squares method had the most consistent results across varying noise levels but the Tikhonov method with L-Curve parameter optimisation performed the best overall in terms of accuracy.

The success of the inverse method using acceleration responses may be due to the larger magnitudes in the response compared to the other responses. More information is lost due to rounding performed on the responses with lower magnitudes by MSC Adams, scaling of the responses does not resolve the problem of information being lost. Frequency was also found to have an effect on the accuracy. As frequency increases the measurement noise is amplified reducing the accuracy (Sanchez, 2022), however care should be taken that the frequency is not reduced to such an extent that the behaviour of the system is not correctly captured.

Since the model properties in the numerical and rigid body cases are the same, the results obtained in these two cases can be compared. The performance of each of the methods was similar in both cases and similar results were obtained in both cases. The accuracy obtained from the numerical case was found to be slightly higher compared to that from the lumped mass simulation model, which is expected.

The finite element model is an elastic model (with finite degrees of freedom) which aims to be more representative of practical applications and was created so that its behaviour could be validated experimentally. The same impulse load (modal hammer) that was measured in the experimental case was used as an input to the finite element model.

The FRF calculated by the finite element software (Figure 2.28) and the FRF estimated from the finite element model responses were both used to reconstruct the applied load. The figure below shows the results obtained by using the two FRFs:

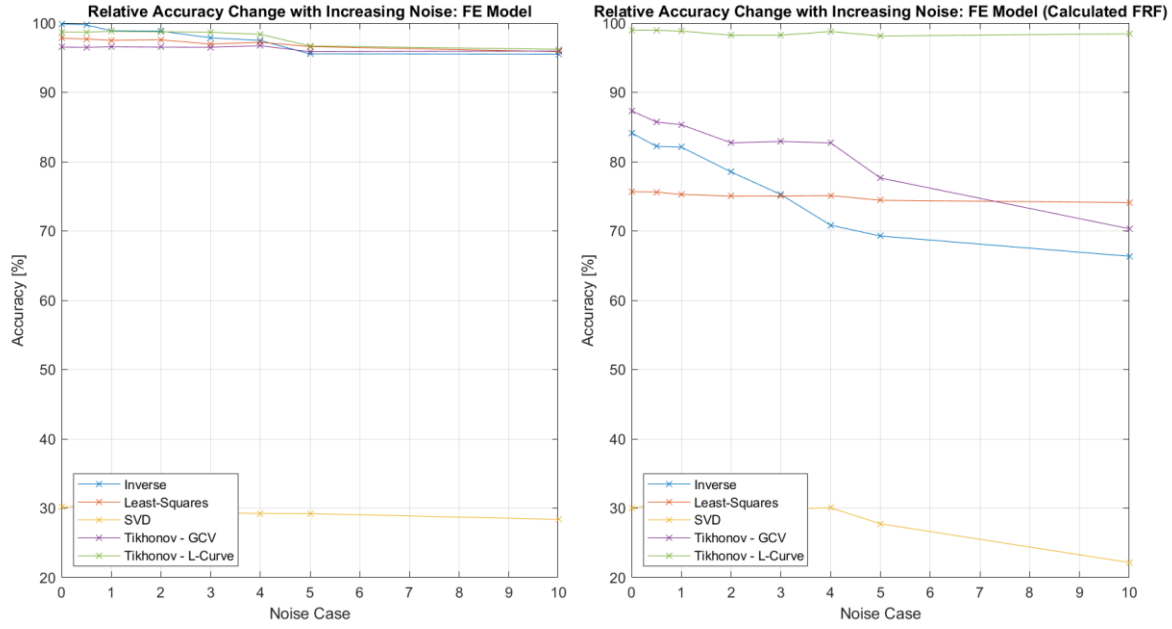

a) b)

Figure 4.10 Finite Element Model Results using Estimated (a) & Calculated FRF (b)

As shown in Figure 4.10a all the methods achieved high accuracy across the noise range, except the SVD method which is due to the SVD being a subtractive method (Sanchez, 2022). In the 0% noise case the inverse method was the most accurate, but once noise was introduced in the responses, the Tikhonov with L-Curve parameter optimisation method, was found to be the most accurate. The Tikhonov method with the GCV parameter optimisation was found to yield the least variation in results as the noise level increased even though the accuracy was slightly less than what was obtained when using L-Curve parameter optimisation.

Since the finite element software has the ability to calculate an FRF (which correlates well with the FRF estimated from the responses), it was investigated if reconstruction could be performed using the calculated FRF instead of estimating the FRF from the responses. Reconstruction was found to be possible using the finite element responses and the finite element calculated responses, all of the methods were able to produce results with similar trends as in the case of using the estimated FRF, these results are shown in figure 4.10b above.

When comparing the accuracies achieved by using the calculated FRF with those achieved using the estimated FRF, all of the methods except the Tikhonov L-Curve method and SVD method showed significant reductions in the achieved accuracies. The inverse and least-squares methods were both about 22% less accurate and the Tikhonov GCV method about 15% less. This is a somewhat unexpected result, this reduction in accuracy may be partially attributed to the variation between the estimated and calculated FRF in the cases where the accuracy is reduced. The Tikhonov L-curve method's performance can be attributed to its insensitivity to error in both the response and the FRF (Chen, et al., 2021). Since the calculated FRF matches the estimated FRF quite well up to approximately 800Hz, the deviations above 800Hz may cause behaviour similar to that of noise.

The finite element model was replicated experimentally (as discussed in section 3) to validate the finite element case and to evaluate the performance of the different methods in a more realistic application.

The responses were measured at the same locations in the finite element model and in the experimental case. The impulse responses between the finite element model and the experimental case correlated quite well, however the magnitudes of the finite element model responses were lower compared to that of the experimental model. These differences were found to be quite small and mainly caused by the boundary conditions in the finite element model causing stiffer behaviour.

The FRF obtained from the finite element model and the FRF obtained from the experimental case are compared in in the figure below:

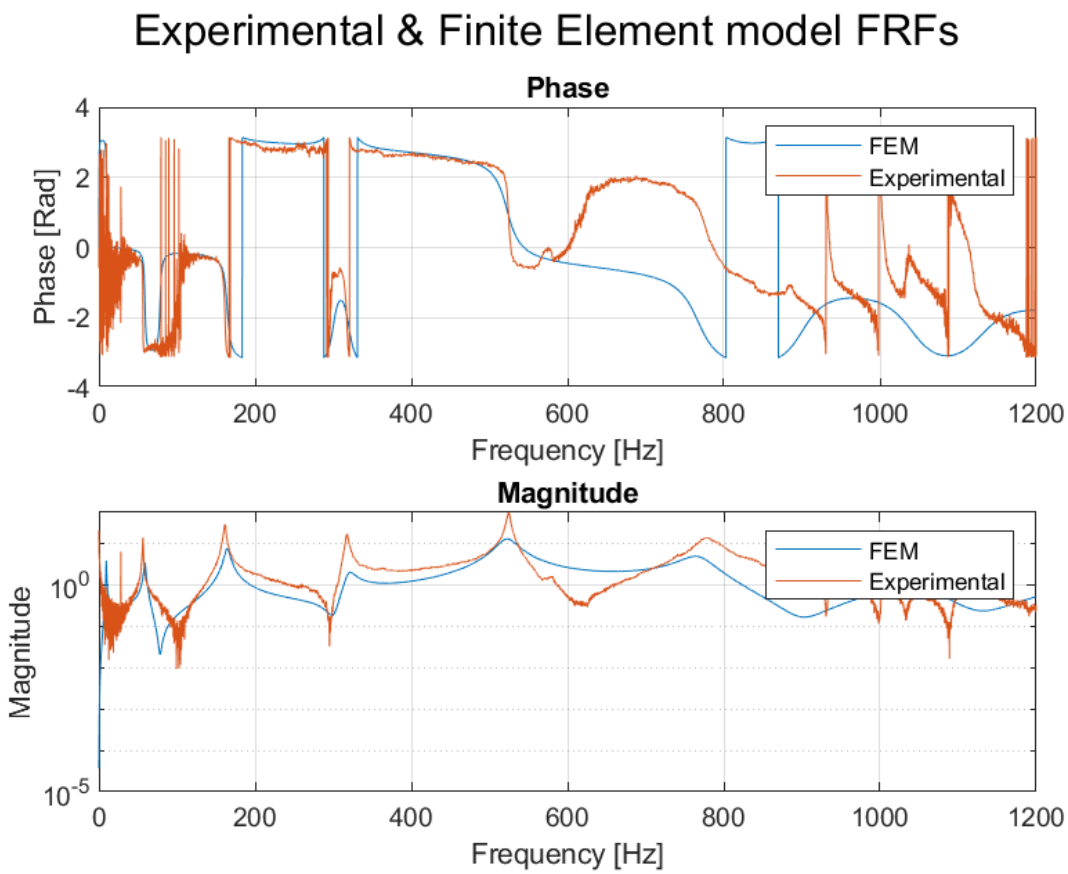

Figure 4.11 Experimental and Finite Element FRF

The experimental and finite element model FRF correlated well up to approximately 800Hz from where deviation is observed. Similar to what was observed in the impulse responses, higher damping is observed in the finite element FRF compared to the experimental FRF. Only the beam itself and not the supporting structures was modelled using finite element analysis, the boundary conditions such as the clamping of the beam was assumed to be rigid, where in the experimental case the clamping may not have been 100% rigid. The clamping of the beam in the experimental case and exclusion of the support structures as well as factors such as assumptions regarding material properties and damping characteristics in the finite element model are all factors that may contribute to the deviations observed.

The results of the reconstructions in the experimental case (using the estimated FRF) are shown in the figure below:

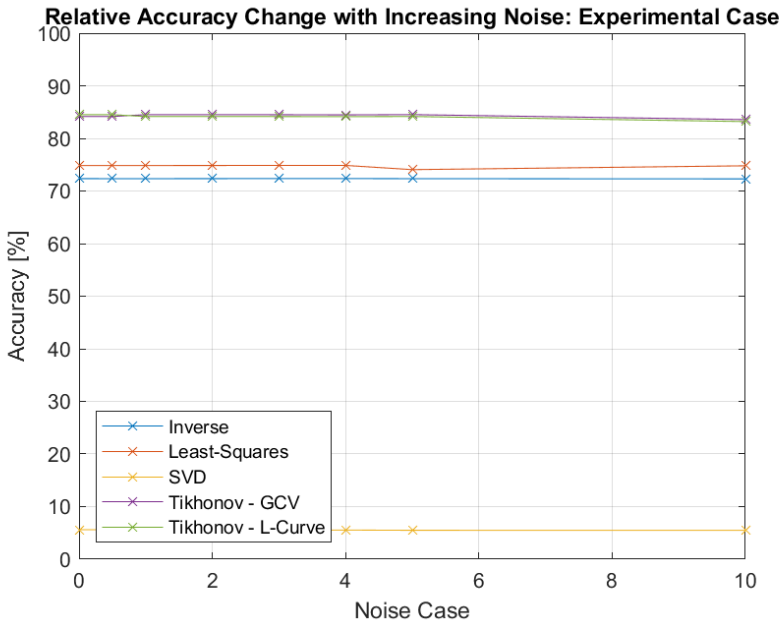

Figure 4.12 Experimental Model Results using Estimated FRF

In the experimental case all the methods were able to reconstruct the load, but again the SVD method was the worst performing method with an average accuracy of 5.6%. This can potentially be improved if more responses are used in the reconstruction. The least-squares method with L-Curve parameter optimisation was the best performing method with an average accuracy of 84%. Despite the poor accuracy of the SVD method all of the methods showed very little sensitivity to noise. When comparing the results shown in Figures 4.10 and 4.13, the accuracy achieved in the experimental case is less than that achieved in the finite element model by between 12% (Tikhonov L-Curve) and 25% (Pseudo-inverse). It was however observed, especially in using the Tikhonov methods, that in the parts of the signal which consisted of only noise (before any force was applied), the noise was greatly amplified.

In the experimental model, an alternative approach of using a reconstructed FRF instead of an estimated FRF was investigated. The FRF was reconstructed using the complex exponential method as previously discussed. The estimated and the reconstructed FRF are compared in the figure below:

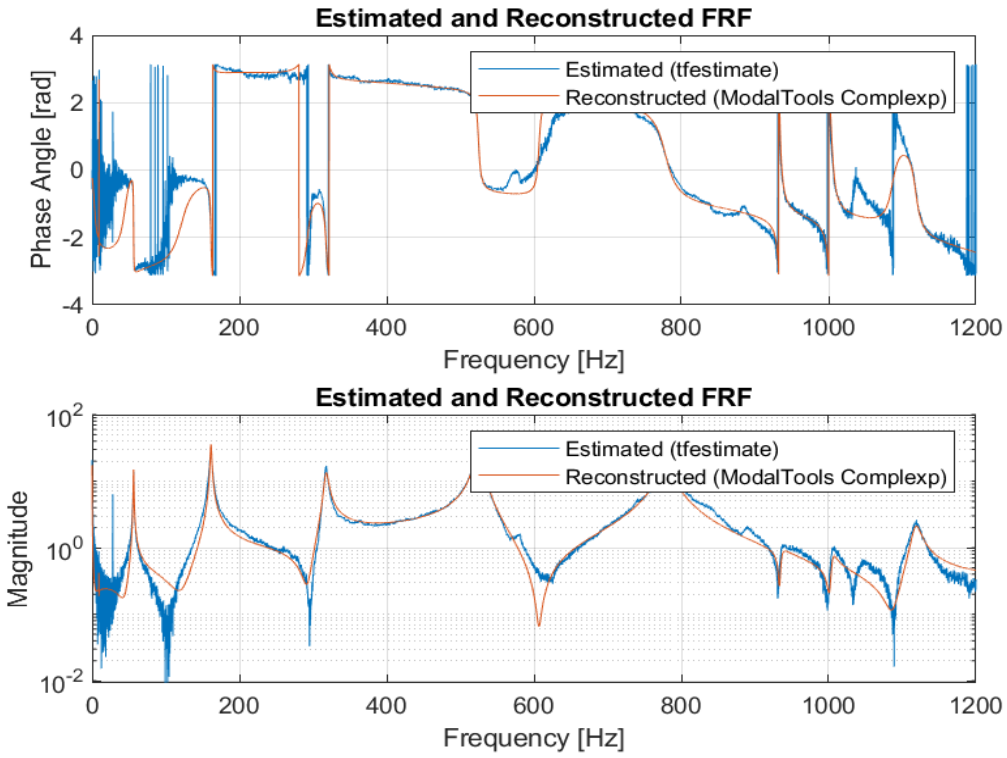

Figure 4.13 Comparison of Estimated and Reconstructed FRFs

It can be seen from the comparison that very good correlation between the estimated and reconstructed FRFs was achieved. The reconstructed FRF was then used to perform the load reconstructions using the experimental responses, the results are shown in Figure 4.14(a) below (the results from Figure 4.12 have been repeated for comparison).

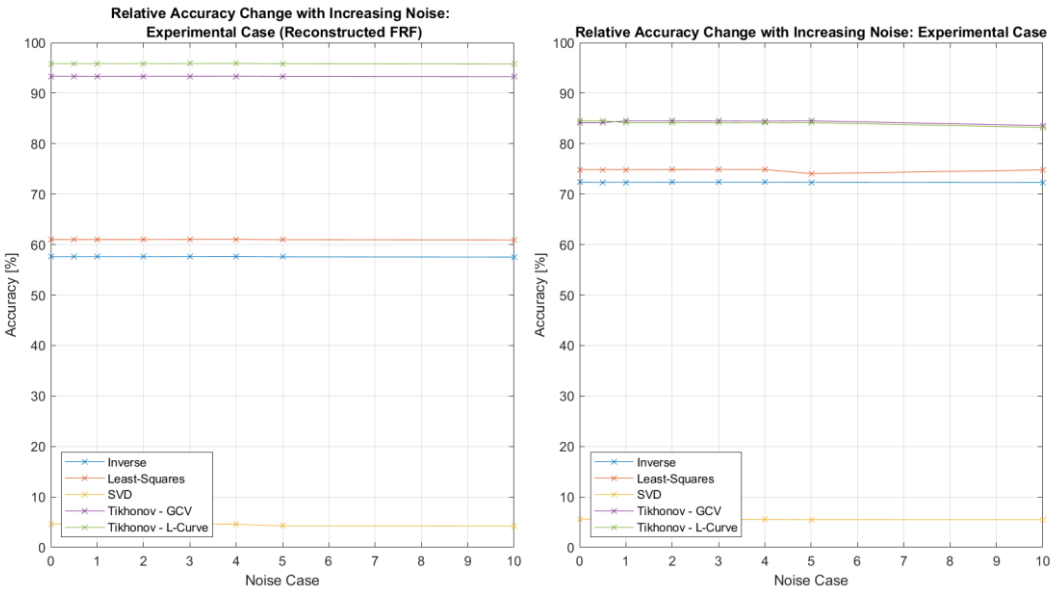

(a) (b)

Figure 4.14 Experimental Model Results using Reconstructed FRF (a) and Using Estimated FRF (b)

The results of the load reconstructions using the reconstructed FRF had similar trends to those of the results obtained using the estimated FRF. The pseudo-inverse and least-squares methods both produced less accurate results compared to when the estimated FRF was used and the Tikhonov method produced more accurate results, approximately 10% change in accuracy in both cases. All the methods showed less variance in the accuracy as the noise increased compared to when the estimated FRF was used.

The most likely cause of the lower accuracy is that the quality (accuracy) of the reconstructed FRF is lower than that of the estimated FRF. The process of reconstructing an FRF is more susceptible to error due to the complex exponential method requiring the user to select points on a graph. The FRF reconstruction calculation and curve fitting methods are performed based on the selected points. Further refinement of the FRF reconstruction may improve these results.

Lastly as part of the investigation of using the finite element calculated FRF, the FRF calculated by the finite element software was used with the experimental responses to reconstruct the applied load. In this case only the Tikhonov method was able to successfully reconstruct the load, the results are shown in Figure 4.15b below.

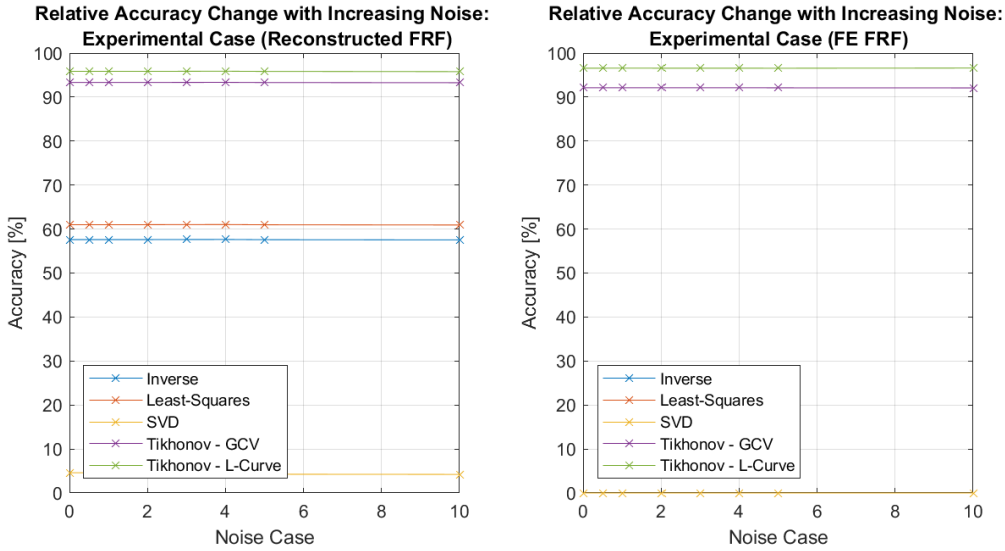

(a) (b)

Figure 4.15 Experimental Model Results using the Reconstructed FRF(a) and the Finite Element FRF (b)

The accuracy obtained when using the finite element software FRF is comparable to the accuracy obtained experimentally. The L-Curve parameter optimisation method performed better with an average accuracy of 96% compared to the 92% of the GCV method. Both methods yielded higher accuracy compared to what was achieved by the same methods using the FRF estimated from the impulse responses. The only part of the reconstruction process that was different in this case, was the FRF, thus the quality of the experimentally obtained FRF may not be high enough.

Further refinement of the finite element model (finer mesh, more accurate material data etc) may improve these results. However, this method will likely not be able to achieve comparable results in more complex or non-linear models, as obtaining accurate properties of the system may not be possible or more expensive than performing an experimental estimation of the FRF. The finite element software also ignores all non-linearities in the FRF calculation process due to the linear assumption of an FRF (Patil & Gombi, 2017).

From all of the cases considered, it can be noted that frequency can have a significant impact on the accuracy of the reconstruction. Firstly, the sample rate of the responses need to be larger than the (expected) frequency of the force to be reconstructed and the natural frequencies of the system also need to be considered. However too large a frequency band may also reduce the accuracy as the high frequency noise has a larger effect on the accuracy (Sanchez, 2022)

5. Conclusion

Research was conducted in the field of load reconstruction with the focus on load reconstruction in the frequency domain. Both time and frequency domain methods, in general, make use of the relationship between the input and the responses of a structure. Frequency domain methods rely on the FRF over the frequency range of interest and matrix inversion methods, where time domain methods rely on convolution (Uhl, 2007). Research in the field of load reconstruction focused mainly on time domain methods because time domain methods have higher efficiency compared to frequency domain methods (Amiri & Bucher, 2017). Where this research frequency domain load reconstruction methods and the effects of noise in responses on these methods were reviewed and evaluated.

According to Amiri & Bucher (2017) frequency domain methods are simple to implement, with minimal prior knowledge of the system or structure required, which forms part of the motivation behind focusing this research on frequency domain methods.

In this research two types of models were considered, firstly lumped mass models and elastic models. In both cases, the forward problem was solved, to have a baseline which could be used for comparison with load reconstructions. The forward problem was solved either analytically or by means of numerical simulation or experimentation where the inputs and responses were recorded. The baseline result along with the input forces (sinusoidal time varying loads) were then used to determine the accuracy of the load reconstruction.

From the simulations and tests conducted it became clear that the quality of the FRF used to perform the load reconstruction is one of the largest contributors to the accuracy of the resulting reconstructed load. Care should therefore be taken to ensure good quality measurements of the forces and responses used to create the FRF as well as the choices of windowing functions and their parameters. Load reconstruction will still be possible with a poor FRF but will provide inaccurate reconstructed loads.

Several load reconstruction methods were considered and their performance were evaluated and compared to each of the four test cases. Based on the results obtained observations were made and conclusions can be drawn.

Similar performance was observed from the methods considered across all the test models used during this study. Due to this consistency in the results, the confidence in the conclusions being drawn is relatively high. However, the assumption of linear behaviour was made in all the cases and methods used in this research and non-linear load reconstruction in frequency domain load reconstruction does not form part of the scope of this work.

The sampling frequency does influence the reconstruction results, thus careful selection of the frequency band in which the reconstruction is to be performed is important. Higher sampling rates increase the likelihood of a reconstruction being possible but does not necessarily improve accuracy and comes with an increased computational requirement. High (above the Nyquist frequency) sampling rates can however also reduce the accuracy of the reconstruction because according to Sanchez (2022) high frequency noise is amplified in the inverse problem. The band in which the FRF is created (calculated, estimated etc) should be wide enough to include all the participating modes of the structure as well as the band in which the forces act. It was for example found in the finite element model, if the impulse responses are measured at twice the frequency band of interest, the resulting

FRF does not represent the structure correctly (Figure 2.30). To achieve a good quality reconstruction, it is necessary to have an indication of the frequency component of the forces in order to be able to select appropriate sampling rates and bandwidths.

The success of frequency domain methods is highly reliant on the accuracy of the frequency response function (FRF). If the FRF is not accurate, even by a slight amount, the reconstruction accuracy decreases significantly or fails entirely.

Two types of noise or error were considered, systematic and stochastic error. The results obtained confirms statements made by Bhandari (2022). It is quite clear that systematic errors can be dangerous when conclusions are drawn based on data affected by this type of error. The result may appear to be correct and accurate where it can be extremely inaccurate.

The effect of a constant offset of the response data on the reconstructed load's amplitude and mean is unpredictable. In simple analytical models, the resulting load is offset by approximately the same amount as the response offset and the amplitude is unaffected. However, in more complex models the amplitude is also affected. This is because these methods are also only suitable for the reconstruction of the dynamic components of a force. This type of error cannot easily be detected as the response values may appear correct. It can be corrected before load reconstruction is performed but only if the offset is known, which in practical applications are unlikely especially if there is little or no prior knowledge of the structure beforehand.

The one distinguishing factor between the results obtained from the scaling error compared to the offset error is an increase in leakage and end effects present with offset error. This may serve as an indication of a potential problem in the reconstruction or data used to perform the reconstruction. Scaling errors can be equally as dangerous and misleading as offset errors.

Based on the work performed, it can be concluded that scaling errors pose a greater risk when drawing conclusions based on measurements and reconstructions affected by scaling errors. Without an indication of the magnitudes of the loads acting on a structure ought to be, there isn't any means by which a scaling error can be detected. It is therefore recommended to ensure that all instrumentation used in response measurement (and FRF measurement or estimation) is properly calibrated and set up correctly to reduce the chance of encountering systematic errors. Care must be taken during the measurement of signals to reduce the possibility of this type of error. Steps to be taken include ensuring the appropriate sensor sensitivities, excitation voltages, stable supply voltages and proper zeroing of signals where appropriate.

When comparing the performance of the five methods used when systematic errors are introduced in the responses, most of the methods performed similarly. The SVD and inverse methods performed worse compared to the other three methods. The performance of these methods may be improved when more response signals are used (Hundhausen, Adams, & Derriso, 2007). More responses would however mean more sensors in practical cases which may not be practical in terms of cost, number of available channels or physical space.

With stochastic noise, again the inverse and SVD methods performed very poorly, the SVD method generally produced reconstructed loads with significantly lower accuracies or failed completely. The inverse method is able to produce meaningful results in some cases, but a slight (1%) increase in noise may cause it to fail entirely. A slightly improved performance was noted when acceleration responses were used compared to displacement responses, however displacement and velocity measurement is impractical in most applications (Khoo, et al., 2014). Similarly to the systematic errors, the performance of these methods may improve with more responses used. The singular value matrix

indices can easily all become zero in which case no result can be obtained. Refinement of the SVD cut off value can improve the accuracy of the result. A simple approach to achieve this would be to systematically increase this value until consistent results are achieved. This does however not guarantee an accurate result. Instead, the Tikhonov method with regularisation parameter algorithms can be employed which is less iterative and was found to produce more accurate results.

The Least-Squares and Tikhonov methods were the best performing methods. These methods produced more accurate results with the same number of responses compared to the inverse and SVD methods. These methods also produced consistent results with increasing noise levels and generally only started deviating at noise levels of 10% and higher. As the SNR decreases, the signal almost becomes undistinguishable from the noise. It is therefore understandable that load reconstruction at high noise levels will be difficult to achieve.

Based on the results obtained it can be concluded that the Tikhonov method combined with the L-Curve parameter optimisation algorithm is the best performing method, because it performed the best between all the methods investigated. It was found to be the best performing with systematic and stochastic errors. The GCV parameter optimisation algorithm yielded similar results (slightly lower on average) as the L-curve method but is slower computationally, especially when load reconstruction was performed across a wide frequency spectrum.

It can be concluded that stochastic noise does not have a significant effect on the accuracy of the frequency domain methods confirming what is stated in literature by authors such as Dolatabadi, et al. (2020) and Sanchez (2022). From all of the methods investigated it was found that the inverse method is the most sensitive to noise in the responses and the Tikhonov (in particular with L-Curve parameter optimisation) was the least sensitive.

The inverse and SVD methods were found to be the fastest methods but also the least reliable. The least squares method was found to be slightly slower than the inverse method but faster than the Tikhonov method combined with parameter optimisation and yielded very accurate results but was not always able to produce a result. It is recommended as a first pass method due to its speed, but if it is unable to produce a result the Tikhonov method should be used (the Tikhonov method can also be used as a means of validating the results achieved by the least-squares method). Potential future work could include the investigation into alternative parameter optimisation methods, the improvement of existing methods or the development of new methods that are less computationally expensive without compromising the accuracy.

The feasibility of using an FRF calculated by finite element software was investigated. The aim was to determine the feasibility of using a finite element based FRF instead of modal testing. The Tikhonov method was able to reconstruct loads applied to a cantilever beam using an FRF calculated from a finite element model and measured acceleration response data. The accuracy of the load reconstruction using a software calculated FRF is comparable to the accuracy obtainable using an experimentally obtained FRF. The benefit is therefore that it has the potential to make load reconstruction easier (assuming accurate finite element modelling is done) and reduces costs. It is recommended that this is further investigated in future work in order to gain more insight into the possibilities and limitations of creating FRFs from finite element models for use in practical load reconstruction problems.

However, accurate modelling and model parameters such as material properties are required, which is not always practical for large structures. This approach would be more suited for cases where additional (or unexpected) loads need to be determined on a newly designed structure where most

of the structure's properties are known. Compared to physical testing, this approach is more cost effective.

The aim of this study was to investigate the effects of different types of noise on frequency domain load reconstruction methods, which was achieved. This work can be extended in future to include other frequency domain methods or include time domain methods. Similar studies could potentially be undertaken to investigate load reconstruction in non-linear systems, since this study was limited to linear systems. Another area for potential future work may include studies on accurate calculation of FRFs using simulation software (such as FEM) that can be used with measured data to reconstruct loads on a structure.

References

Allemang, R., & Avitabile, P. (2022). *Handbook of experimental structural dynamics.* Springer New York.

Allen, M. S., & Carne, T. G. (2008). Delayed, multi-step inverse strucural filter for robust force identification. *Mechanical Systems and Signal Processing, Volume 22*, 1036-1054.

Amiri, A., & Bucher, C. (2017). A procedure for in situ wind load reconstruction from structural response only based on field test data. *Journal of Wind Engineering and Industrial Aerodynamics 167*, 75-86.

Araki, S., Koo, J., Martin, R., & Dankongkakul, B. (2021). A grid-based nonlinear approach to noise reduction and deconvolution for coupled systems. *Physica D: Nonlinear Phenomena, 417*.

Bhandari, P. (2022, January 4). *Random and systematic error | Differences, sources & examples*. Retrieved from Sribbr: https://www.scribbr.com/methodology/random-vs-systematic-error/

Brandt, A. (2011). *Noise and vibration analysis : Signal analysis and experimental procedures.* Wiley.

Brül & Kjaer. (2023, February 23). *Measuring vibration*. Retrieved from Brül & Kjaer: https://www.bksv.com/en/knowledge/blog/vibration/environmental-effects-on-measurements

Chang, X., Yan, Y., & Wu, Y. (2019). Study on solving the ill-posed problem of force load reconstruction. *Journal of sound and vibration 440*, 186-201.

Chao, M., Hongxing, H., & Feng, X. (2014). The identification of external forces for a nonlinear vibration system in frequency domain. *Journal of mechanical engineering science, vol. 228(9)*, 1531-1539.

Chen, J., Zhou, J., Gong, D., Sun, W., Sun, Y., You, T., & Ji, Y. (2021). Identification of excitation force for under-chassis equipment of railway vehicles in frequency domain. *Journal of vibration engineering & technologies 9*, 701-714.

Crystal Instruments. (2023, March 07). *Basics of modal testing and analysis*. Retrieved from Crystal Instruments: https://www.crystalinstruments.com/basics-of-modal-testing-and-analysis

Dolatabadi, P., Khanlari, K., Ashtiany, M., & Hosseini, M. (2020). System identification method by using inverse solution of equations of motion in time domain and noisy condition. *Physica A: Statistical Mechanics and its Applications, 538*.

El Hami, A., & Radi, B. (2017). *Dynamics of large Structures and inverse problems.* John Wiley & Sons.

Ewins, D. (2000). *Modal Testing: Theory, Practice and Application (Second Edition).* Research Studies Press.

Hamarik, U., Palm, R., & Raus, T. (2012). A family of rules for parameter choice in Tikhonov regularization of ill-posed problems with inexact noise level. *Journal of Computational and Applied Mathematics, 236(8)*, 2146-2157.

Hansen, C. (2008). Regularization Tools. Technical University of Denmark.

Hundhausen, R. J., Adams, D. E., & Derriso, M. (2007). Impact loads identification in standoff metallic thermal protection system panels. *Journal of Intelligent Material Systems and Structures, Vol.18(6)*, 531-541.

Jia, Y., Yang, Z., Guo, N., & Wang, L. (2015). Random dynamic load identification based on error analysis and weighted total least squares method. *Journal of sound and vibration, 358*, 111-123.

Kammer, D. C. (1998). Input force reconstruction using a time domain technique. *Journal of Vibration and Acoustics, 120(4)*, 868-874 .

Khoo, S., Ismail, Z., Kong, K., Ong, Z., Noroozi, S., Chong, W., & Rahman, A. (2014). Impact force identification with pseudo-inverse method on a lightweight structure for under-determined, even-determined and over-determined cases. *International Journal of Impact Engineering, 63*, 52-62.

Kriel, T. E. (2000). *Assessment of frequency domain force identification procedures.* Pretoria: University of Pretoria.

Kutz, M. (2013). *Handbook of measurement in science and engineering volume 1.* John Wiley & Sons.

Kvasnikov, V., & A., P. (2020). Removal of temperature drift of zero of piezoelectric accelerometer. *Technology Audit and Production Reserves, 1 (1 (51))*, 41–44.

Lang, W. (2018). *Sensors and Measurement Systems.* River Publishers.

Liu, Y., Wang, L., Qiu, Z., & Chen, X. (2021). A dynamic force reconstruction method based on modified Kalman filter using acceleration responses under multi-source uncertain samples. *Mechanical systems and signal processing, Vol. 159*.

Lourens, E., Reynders, E., De Roeck, G., Degrande, G., & Lombaert, G. (2012). An augmented Kalman filter for force identification in structural dynamics. *Mechanical Systems and Signal Processing, Vol. 27*, 446-460.

Mathworks. (2020). *Matlab Documentation.* Mathworks.

Morris, A. S. (2001). *Measurement and Instrumentation Principles.* Elsevier Science & Technology.

Oosterhuis, E., Eidhof, W., van der Hoogt, P., & de Boer, A. (2006). Force prediction via the inverse FRF using experimental and numerical data from a demonstrator with tuneable nonlinearities. *13th International congress on sound and vibration, Vol. 3*, (pp. 1807-1814).

Patil, R. A., & Gombi, S. L. (2017). Review on determination of forces using inverse techniques. *International Journal of Emerging Technology and Advanced Engineering, Vol.7(6)*, 120-125.

Patil, R., & Gombi, S. (2018). Experimental study of cutting force on a cutting tool during machining using inverse problem analysis. *Journal of the Brazillian society of mechanical sciences and engineering, Vol. 40(10)*, 1-8.

Rao, S. (2011). *Mechanical Vibrations 5th Edition.* Prentice Hall.

Rezayat, A., Nassiri, V., De Pauw, B., Ertveldt, J., Vanlanduit, S., & P., G. (2016). Identification of dynamic forces using group-sparsity in frequency domain. *Mechanical systems and signal processing, 70-71*, 756-768.

Sanchez, J. (2022). Mathematical examination of force reconstruction and the deconvolution problem. *Results in Engineering 14*.

Sanchez, J., & Benaroya, H. (2014). Review of force reconstruction techniques. *Journal of Sound and Vibration, 333*, 2999-3018.

Skoog, D. A., Holler, F. J., & Crouch, S. R. (2007). *Principles of Instrumentation Analysis.* Belmont: Brooks/Cole.

Tran, H., & Inoue, H. (2018). Development of wavelet deconvolution technique for impact force acting on a load-cell. *International journal of impact engineering, 122*, 137-147.

Uhl, T. (2007). The inverse identification problem and its technical application. *Archive of Applied Mechanics 77(5)*, 325-337.

Wang, C., Chen, D., Chen, J., Lai, X., & He, T. (2021). Deep regression adaptation networks with model-based transfer learning for dynamic load identification in the frequency domain. *Engineering applications of artificial intelligence, 102*.

Wang, C., Zhang, X., Qiao, B., Cao, H., & Chen, X. (2019). Dynamic force identification in peripheral milling based on CGLS using filtered acceleration signals and averaged transfer functions. *Journal of Manufacturing Science and Engineering, Vol. 141*.

Wei, G., Kaiping, Y., & Ying, W. (2016). A New method for optimal regularization parameter determination in the inverse problem of load identification. *Shock and Vibration*.

You, J., Ruikai, L., Yanhong, F., & Haijie, H. (2022). A novel inverse time-frequency domain approach to identify random forces. *Mathematics, 10(2331)*.

Appendices

Appendix A: Higher Degree of Freedom Analytical Models

This section describes the higher degree of freedom analytical models considered as part of this study. These models were included to evaluate the performance of the load reconstruction methods when applied to slightly more complex models. The procedure followed is the same as what is discussed in section 2.2. Three additional models were considered: 3, 4 and 7 degrees of freedom, the figures and tables below describe these models and in each case only one force is applied to one of the masses.

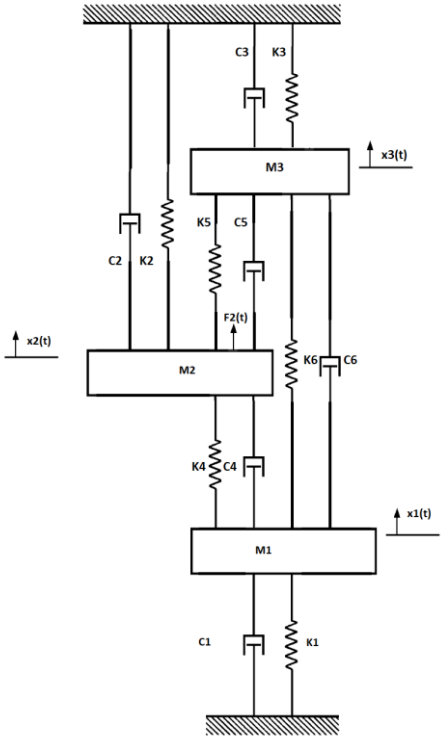

Figure A.1 Analytical 3 Degree of Freedom Model

Table A.1 3-DOF Model Properties

Coordinate Point	1	2	3	4	5	6
Mass [kg]	1	2	3	N/A	N/A	N/A
Stiffness [N/m]	3000	3000	3000	3000	3000	3000
Damping Coefficient [Ns/m]	10	10	10	20	20	20
Undamped Natural Frequency [Hz]	6.01	11.29	15.95	N/A	N/A	N/A
Damping Ratio	0.28	0.2	0.07	N/A	N/A	N/A

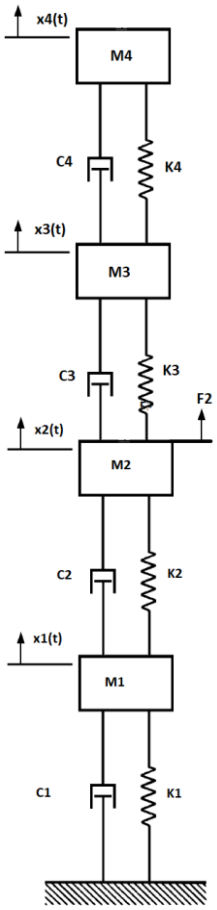

Figure A.2 Analytical 4 Degree of Freedom Model

Table A.2 4-DOF Model Properties

Coordinate Point	1	2	3	4
Mass [kg]	3	8	50	18
Stiffness [N/m]	24 000	480 000	144 000	540 000
Damping Coefficient [Ns/m]	4	12	12	8
Undamped Natural Frequency [Hz]	2.56	20.47	32.61	76.48
Damping Ratio	0.0072	0.0018	0.0058	0.0012

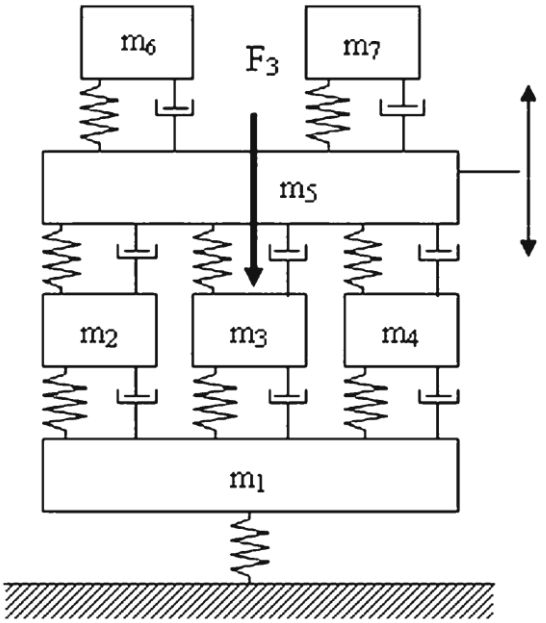

Figure A.3 Analytical 7 Degree of Freedom Model (adapted from (Uhl, 2007))

Table A.3 7-DOF Model Properties

Coordinate Point	1	2	3	4	5	6	7	8	9
Mass [kg]	8	1	15	21	4	28	62		
Stiffness [kN/m]	80	15	15	15	14.8	15	15	28	28
Damping Coefficient [Ns/m]	12	5	5	5	5	5	5	9	9
Undamped Natural Frequency [Hz]	30.34	23.38	18.63	6.78	1.80	5.56	4.25	N/A	N/A
Damping Ratio	0.032	0.023	0.013	0.007	0.055	0.0042	0.0017	N/A	N/A

Appendix B: Complete Tabulated Results

This section provides the tabulated results of all of the test cases across all of the models considered as part of this study.

Table A.4 Analytical 2-DOF Model Results

Case	Inverse	Least-Squares	SVD	Tikhonov: GCV	Tikhonov: L-Curve
0	99.99%	99.83%	94.36%	95.58%	96.84%
1	99.18% Amplitude 30% Mean offset	96.6% Amplitude 25.9% Mean offset	57.2% Amplitude 48% Mean offset	95.25% Amplitude 23% Mean offset	94.85% Amplitude 23% Mean offset
2	90.00%	90.00%	69.57%	85.25%	85.26%
3	-	99.83%	-	95.55%	96.91%
4	-	99.81%	-	96.04%	97.15%
5	-	99.77%	-	97.41%	98.05%
6	-	99.68%	-	99.59%	99.70%
7	-	99.66%	-	97.24%	98.36%
8	-	99.65%	-	95.45%	96.79%
9	-	99.63%	-	92.44%	94.74%

TableA.5 Analytical 3-DOF Model

Case	Inverse	Least-Squares	SVD	Tikhonov: GCV	Tikhonov: L-Curve
0	100%	99.99%	84.54%	84.36%	88.72%
1	99.37% Amplitude 32% Mean offset	99.6% Amplitude 32% Mean offset	57.2% Amplitude 48% Mean offset	89.26% Amplitude 16% Mean offset	84.47% Amplitude 11.6% Mean offset
2	90.00%	79.03%	66.09%	73.29%	72.62%
3	-	99.99%	-	84.41%	88.74%
4	-	99.10%	-	84.58%	88.79%
5	-	99.70%	-	85.20%	88.93%
6	-	99.60%	-	84.24%	88.19%
7	-	99.16%	-	83.74%	87.83%
8	-	99.16%	-	83.45%	87.51%
	-	90.38%	-	82.80%	85.59%

TableA.6 Analytical 4-DOF Model

Case	Inverse	Least-Squares	SVD	Tikhonov: GCV	Tikhonov: L-Curve
0	94.64%	86.55%	98.65%	65.90%	91.75%
1	99.90% Amplitude 1% Mean offset	21.0% Amplitude 63.6% Mean offset	-	24.0% Amplitude 52.2% Mean offset	44.58% Amplitude 45.1% Mean offset
2	90.32%	80.49%	-	52.23%	81.4%
3	-	86.55%	-	62.23%	91.74%
4	-	86.53%	-	61.76%	91.70%
5	-	86.55%	-	61.53%	91.56%
6	-	86.45%	-	61.44%	91.30%
7	-	86.44%	-	60.04%	90.96%
8	-	86.40%	-	54.19%	90.50%
	-	86.05%	-	53.87%	86.96%

TableA.7 Analytical 7-DOF Model

Case	Inverse	Least-Squares	SVD	Tikhonov: GCV	Tikhonov: L-Curve
0	100%	96.55%	98.65%	58.35%	89.54%
1	99.15% Amplitude 25% Mean offset	96.2% Amplitude 20.2% Mean offset	79.9% Amplitude 21.2% Mean offset	87.4% Amplitude 12.6% Mean offset	49.37% Amplitude 15.1% Mean offset
2	90.00%	86.90%	91.21%	47.59%	78.52%
3	-	96.55%	82.89%	58.44%	89.55%
4	-	96.55%	45.52%	58.42%	89.57%
5	-	96.54%	-	58.51%	89.64%
6	-	96.52%	-	58.48%	89.58%
7	-	96.46%	-	58.39%	89.36%
8	-	96.20%	-	58.00%	88.99%
9	-	95.59%	-	41.96%	82.16%

TableA.8 Analytical 2-DOF Model Results using Estimated FRF

Test Case	Inverse	Least-Squares	SVD	Tikhonov - GCV	Tikhonov – L-Curve
0	98.69%	98.57%	69%	98.47%	98.47%
1	88.88% Amplitude 33.5% Mean offset	99.2% Amplitude 200% Mean offset	74.5% Amplitude 15% Mean offset	78.66% Amplitude 35% Mean offset	77.3% Amplitude 30% Mean offset
2	82.58%	91.19%	61.43%	98.59%	95.59%
3	-	98.13%	66.96%	98.80%	98.93%
4	-	98.88%	-	98.53%	98.64%
5	-	98.05%	-	97.79%	98.72%
6	-	99.43%	-	97.82%	98.76%
7	-	98.62%	-	97.15%	98.50%
8	-	96.16%	-	95.52%	96.51%
9	-	97.84%	-	63.46%	71.54%

Table A.9 Analytical 3-DOF Model Results using Estimated FRF

Test Case	Inverse	Least-Squares	SVD	Tikhonov - GCV	Tikhonov – L-Curve
0	99.05%	99.11%	68.26%	91.20%	91.20%
1	87.84% Amplitude 36.6% Mean offset	98.51% Amplitude 13.9% Mean offset	67.71% Amplitude 9.17% Mean offset	95.75% Amplitude 166% Mean offset	95.9% Amplitude 167% Mean offset
2	90.47%	90.45%	60.45%	84.78%	84.78%
3	-	98.91%	67.72%	93.92%	93.92%
4	-	98.05%	68.12%	93.45%	93.45%
5	-	98.09%	62.11%	92.87%	94.02%
6	-	97.84%	62.06%	88.15%	93.65%
7	-	97.15%	62.10%	88.17%	93.11%
8	-	97.10%	61.87%	88.02%	93.08%
9	-	96.69%	61.23%	68.87%	86.68%

Table A.10 Analytical 4-DOF Model Results using Estimated FRF

Test Case	Inverse	Least-Squares	SVD	Tikhonov - GCV	Tikhonov – L-Curve
0	-	96.23%	49.97%	94.34%	95.43%
1	-	91.7% Amplitude 12.2% Mean offset	-	95.75% Amplitude 14% Mean offset	95.9% Amplitude 14% Mean offset
2	-	83.20%	-	86.26%	83.26%
3	-	94.26%	41.62%	94.24%	95.16%
4	-	94.06%	41.44%	94.54%	95.24%
5	-	94.19%	-	94.64%	95.06%
6	-	94.17%	-	93.31%	94.34%
7	-	94.25%	-	92.68%	93.75%
8	-	93.97%	-	86.35%	90.79%
9	-	93.96%	-	82.81%	87.83%

Table A.11 Analytical 7-DOF Model Results using Estimated FRF

Test Case	Inverse	Least-Squares	SVD	Tikhonov - GCV	Tikhonov – L-Curve
0	74.23%	91.82%	16.52%	90.81%	90.81%
1	57% Amplitude 240% Mean offset	44.1% Amplitude 31.1% Mean offset	6.1% Amplitude 76.7% Mean offset	38.6% Amplitude 29% Mean offset	40.5% Amplitude 33% Mean offset
2	43.96%	51.40%	14.59%	44.48%	44.42%
3	71.19%	92.61%	16.53%	94.10%	94.10%
4	68.77%	92.89%	16.42%	95.28%	95.38%
5	63.95%	90.70%	16.90%	91.98%	91.98%
6	62.88%	90.78%	16.21%	80.21%	91.70%
7	-	90.72%	16.13%	79.66%	91.34%
8	-	89.22%	16.02%	77.80%	90.77%
9	-	84.47%	12.79%	72.36%	85.46%

Table A.12 Rigid Body Simulation Model Results - Displacement Responses

Test Case	Inverse	Least-Squares	SVD	Tikhonov - GCV	Tikhonov – L-Curve
0	85.60%	95.91%	45.23%	99.47%	99.47%
1	-	77.0% Amplitude 23% Mean offset	-	84.4% Amplitude 15% Mean offset	77.08% Amplitude 22.9% Mean offset
2	-	87.51%	-	89.45%	89.45%
3	-	97.49%	-	99.42%	99.42%
4	-	97.44%	-	99.42%	99.42%
5	-	97.39%	-	98.20%	99.39%
6	-	96.97%	-	98.42%	99.69%
7	-	97.07%	-	98.29%	99.04%
8	-	96.32%	-	97.67%	99.68%
9	-	97.51%	-	99.45%	99.45%

Table A.13 Rigid Body Simulation Model Results - Velocity Responses

Test Case	Inverse	Least-Squares	SVD	Tikhonov - GCV	Tikhonov – L-Curve
0	87.42%	87.48%	26.39%	86.32%	86.32%
1	79.46% Amplitude 184% Mean offset	78.65% Amplitude 184% Mean offset	-	78.03% Amplitude 184% Mean offset	79.03% Amplitude 185% Mean offset
2	67.36%	67.35%	24.08%	67.36%	67.38%
3	84.73%	87.88%	-	86.68%	86.68%
4	85.97%	85.83%	-	86.79%	86.84%
5	84.01%	86.80%	-	86.38%	86.38%
6	-	86.37%	-	85.55%	85.96%
7	-	86.63%	-	86.84%	86.87%
8	-	86.46%	-	86.74%	86.81%
9	-	60.99%	-	72.66%	75.79%

Table A.14 Rigid Body Simulation Model Results - Acceleration Responses

Test Case	Inverse	Least-Squares	SVD	Tikhonov - GCV	Tikhonov – L-Curve
0	93.75%	93.77%	25.95%	93.72%	93.73%
1	82.1% Amplitude 210% Mean offset	80.7% Amplitude 220% Mean offset	-	78.3% Amplitude 220% Mean offset	77.6% Amplitude 210% Mean offset
2	66.14%	66.14%	19.1%	66.13%	66.14%
3	93.59%	93.88%	25.95%	93.81%	93.99%
4	93.23%	93.77%	25.90%	93.20%	93.72%
5	93.27%	93.44%	25.39%	93.76%	94.44%
6	92.72%	93.47%	24.88%	93.64%	93.86%
7	92.50%	93.52%	24.29%	93.78%	94.49%
8	92.09%	93.21%	23.20%	93.16%	93.43%
9	88.30%	88.94%	22.90%	88.11%	88.92%

Table A.15 Finite Element Model Results - Acceleration Responses

Test Case	Inverse	Least-Squares	SVD	Tikhonov - GCV	Tikhonov – L-Curve
0	99.88%	97.83%	30.24%	96.52%	98.68%
1	-	85.85% Amplitude 150% Mean offset	-	86.25% Amplitude 170% Mean offset	84.74% Amplitude 120% Mean offset
2	95.71%	89.84%	23.42%	87.72%	83.47%
3	99.73%	97.68%	30.19%	96.50%	98.68%
4	98.89%	97.51%	30.20%	96.56%	98.81%
5	98.83%	97.58%	30.18%	96.52%	98.73%
6	97.87%	96.96%	29.31%	96.50%	98.66%
7	97.48%	97.23%	29.24%	96.72%	98.38%
8	95.55%	96.60%	29.22%	95.87%	96.68%
9	95.50%	95.87%	28.38%	95.96%	96.21%

Table A.16 Finite Element Model Results - Acceleration Responses (Using FEM FRF)

Test Case	Inverse	Least-Squares	SVD	Tikhonov - GCV	Tikhonov – L-Curve
0	84.15%	75.68%	30.00%	87.34%	98.97%
1	-	86.28% Amplitude 150% Mean offset	-	-	92.5% Amplitude 617% Mean offset
2	74.85%	64.06%	22.94%	70.99%	81.36%
3	82.20%	75.61%	30.54%	85.72%	98.95%
4	82.10%	75.26%	30.05%	85.33%	98.84%
5	78.51%	75.04%	29.62%	82.72%	98.24%
6	75.26%	75.06%	29.81%	82.91%	98.25%
7	70.83%	75.11%	30.07%	82.71%	98.77%
8	69.27%	74.43%	27.75%	77.64%	98.14%
9	66.35%	74.09%	22.16%	70.32%	98.44%

Table A.17 Experimental Model Results - Acceleration Response (Estimated FRF)

Test Case	Inverse	Least-Squares	SVD	Tikhonov - GCV	Tikhonov – L-Curve
0	72.35%	74.84%	5.60%	84.16%	84.51%
1	72.31% Amplitude 46.9% Mean Offset	74.82% Amplitude 46.9% Mean Offset	5.60% Amplitude 95% Mean Offset	99.93% Amplitude 48% Mean offset	99.33% Amplitude 48% Mean offset
2	67.35%	67.30%	5.00%	80.04%	79.38%
3	72.34%	74.84%	5.60%	84.16%	84.51%
4	72.34%	74.84%	5.59%	84.51%	84.16%
5	72.35%	74.85%	5.59%	84.51%	84.16%
6	72.36%	74.86%	5.55%	84.50%	84.15%
7	72.36%	74.86%	5.54%	84.47%	84.13%
8	72.34%	74.06%	5.50%	84.52%	84.16%
9	72.30%	74.79%	5.49%	83.57%	83.20%

Table A.18 Experimental Model Results - Acceleration Response (Reconstructed FRF)

Test Case	Inverse	Least-Squares	SVD	Tikhonov - GCV	Tikhonov – L-Curve
0	57.60%	60.99%	4.6%	93.33%	95.85%
1	57.57% Amplitude 115% Mean Offset	60.95% Amplitude 115% Mean Offset	4.6% Amplitude 93% Mean Offset	95.82% Amplitude 110% Mean offset	93.30% Amplitude 109% Mean offset
2	54.89%	54.88%	4.14%	87.36%	84.00%
3	57.60%	60.99%	4.60%	93.33%	95.86%
4	57.60%	60.99%	4.60%	93.32%	95.85%
5	57.60%	60.99%	4.60%	93.33%	95.85%
6	57.62%	61.01%	4.60%	93.34%	95.87%
7	57.63%	61.02%	4.59%	93.35%	95.88%
8	57.58%	60.97%	4.26%	93.31%	95.84%
9	57.53%	60.92%	4.22%	93.27%	95.79%

Table A.19 Experimental Model Results - Acceleration Response (Software Calculated FRF)

Test Case	Inverse	Least-Squares	SVD	Tikhonov - GCV	Tikhonov – L-Curve
0	-	-	-	92.13%	96.57%
1	-	-	-	88.16% Amplitude 41.5% Mean offset	92.94% Amplitude 21.1% Mean offset
2	-	-	-	80.92%	84.34%
3	-	-	-	92.13%	96.57%
4	-	-	-	92.12%	96.58%
5	-	-	-	92.13%	96.57%
6	-	-	-	92.13%	96.57%
7	-	-	-	92.13%	96.57%
8	-	-	-	92.11%	96.56%
9	-	-	-	92.09%	96.60%